

DESIGN AND EVALUATION OF A NOVEL PULSATILE BIOREACTOR FOR
BIOLOGICALLY ACTIVE HEART VALVES

by

Daniel Kenneth Hildebrand

BS, University of Pittsburgh, 2001

Submitted to the Graduate Faculty of

School of Engineering in partial fulfillment

of the requirements for the degree of

Master of Science in Bioengineering

University of Pittsburgh

2003

UNIVERSITY OF PITTSBURGH

SCHOOL OF ENGINEERING

This thesis was presented

by

Daniel Kenneth Hildebrand

It was defended on

December 2, 2003

and approved by

James F. Antaki, Ph. D., Associate Professor
Department of Bioengineering, University of Pittsburgh
Department of Biomedical Engineering, Carnegie Mellon University

Sanjeev G. Shroff, Ph. D., Professor and Gerald McGinnis Chair
Department of Bioengineering

Thesis Advisor: Michael Sacks, Ph. D., Associate Professor
Department of Bioengineering

ABSTRACT

DESIGN AND EVALUATION OF A NOVEL PULSATILE BIOREACTOR FOR BIOLOGICALLY ACTIVE HEART VALVES

Daniel Kenneth Hildebrand, MS

University of Pittsburgh, 2003

Biologically active replacement heart valves (tissue engineered, recellularized xenograft) offer enhanced function compared to current valve therapies by possessing the capacity for remodeling and growth to meet the hemodynamic needs of the patient and eliminating the need for chronic medication. However, many fundamental questions remain as to how these valves will function in vivo, and new in vitro tools need to be created to address these questions. Traditional in vitro heart valve testing devices (mock flow loops) are designed to subject valves to physiologic and pathologic hemodynamic conditions. These devices offer a heart valve designer a useful tool with which to evaluate the mechanical functioning of their device in a variety of well-controlled hemodynamic situations. Unfortunately, these devices have not been designed for testing valves built of biologically active materials which require proper nutrient and waste exchange, pH, temperature, and freedom from attacks by microbial organisms in order to function. Pulsatile bioreactors have been developed to provide the aforementioned biological requirements to developing tissue engineered valves [1, 2], but these systems offer very limited hemodynamic control in comparison to mock flow loops. Therefore, in order to better understand

the role of hemodynamics in the function of biologically active heart valves (BAHV), and to thereby create better BAHV designs, a new type of pulsatile bioreactor should be created that also incorporates more of the hemodynamic control found in mock circulatory loops. This thesis details the both the development of such a device and evaluating its functionality.

TABLE OF CONTENTS

PREFACE	xiv
1.0 INTRODUCTION	1
1.1 The Heart	2
1.2 Native Heart Valves	4
1.2.1 Structure and Composition	4
1.2.2 Environment, Stresses, and Motions	5
1.3 Heart Valve Disease	6
1.4 Heart Valve Therapies	8
1.4.1 Allographs and Autographs	8
1.4.2 Mechanical Valves	9
1.4.3 Bioprosthetic Valves	10
1.1.4 Tissue Engineered Heart Valves	10
1.4.4.1 Xenograft Scaffolds	11
1.4.4.2 Polymeric Scaffolds	13
1.4.4.3 Cell Sources & Types	14
1.4.4.4 Scaffold Materials	16
1.4.4.5 Seeding, Pre-implantation Culture, and Mechanical Stimulation	17
1.4.4.6 Recent Studies	18

1.5 Mock Circulatory Loop Design	19
1.5.1 Modeling the Cardiovascular System: Windkessel Theory	20
1.5.1.1 Resistance & Impedance	21
1.5.1.2 Compliance	23
1.5.1.3 Features in Pressure and Flow Waveforms	24
1.5.2 Hemodynamic Control Systems	25
1.5.3 Actuation Methods	27
1.6 Heart Valve Bioreactor Design	28
1.7 Study Aims	30
2.0 METHODS	31
2.1 Device Design Process	32
2.2.1 Device Requirements	34
2.1.2 Hardware Design & System Overview	36
2.1.2.1 Pneumatic System	38
2.1.2.2 Atrium	40
2.1.2.3 Ventricle	41
2.1.2.4 Outflow Valve Holders	42
2.1.2.5 Compliance Chamber	44
2.1.2.6 Variable Resistor	45
2.1.2.7 Sensors	49
2.1.2.8 Incubator	49
2.1.2.9 Computer Interfacing	49
2.1.3 Software Design	50

2.1.3.1 Driving Waveform	50
2.1.3.2 Mean Pressure and Flow Control Code	53
2.1.2.4 Data Acquisition	56
2.1.3 Tissue Engineered Heart Valve Design	57
2.1.3.1 Scaffold Design.....	57
2.1.3.2 Cell Expansion and Scaffold Seeding.....	59
2.2 Hydrodynamic Testing.....	60
2.2.1 System Calibration, Response, and Stability	61
2.2.2 Control and Flexibility	61
2.2.3 Waveforms	61
2.3 Tests of Biological Relevance	62
2.3.1 Sterility.....	62
2.3.2 Measuring Dissolved Gases and pH	62
2.3.3 TEHV Ramped Flow Study	64
2.3.4 Tissue Analysis	65
3.0 RESULTS	66
3.1 Hydrodynamic Studies.....	66
3.1.1 System Response & Stability.....	66
3.1.2 System Control and Flexibility	67
3.1.3 Waveforms	71
3.2 TEHV Feasibility Studies	74
3.2.1 System Sterility	74
3.2.2 Gas Concentrations and pH	75

3.2.3 TEHV Ramped Flow Study	77
3.2.3.1 Pressure and Flow Control	77
3.2.3.2 Tissue Analysis	79
4.0 DISCUSSION	81
4.1 Study Findings	81
4.1.1 Hydrodynamic Performance	81
4.1.2 Biological Performance	82
4.2 Limitations	85
4.2.1 Non-compliant Sinus	85
4.2.2 Manual Atrial Head Pressure Adjustment	85
4.2.3 TEHV Design	86
4.3 Future Modifications and Potential Applications	86
4.4 Summary	87
Appendix A. Mechanical Drawings	89
Appendix B. Device Control Code – LabView	90
Appendix C. Input-Impedance Code - MatLab	91
Appendix D. Device Software Manual	92
BIBLIOGRAPHY	93

LIST OF TABLES

Table 1	Table summarizing previous pulsatile bioreactor studies. Note the cells, scaffold materials, and the coupled mean pressure and flow rate changes. Other relevant study parameters such as pressure and flow waveforms and heart rate were not reported.	19
Table 2	Table of the design requirements for the pulsatile BAHV bioreactor	35
Table 3	Summary of tests performed during the evaluation phase of the study	80

LIST OF FIGURES

Figure 1	Diagram of the heart: tricuspid valve, a; pulmonic valve, b; mitral valve, c; aortic valve, d.....	3
Figure 2	Pressure and flow waveforms of the aortic or pulmonary circulations: ventricular contraction starts & inflow valve closes, 1; Isovolumic contraction, 1-2; outflow valve opens, 2; ejection, 2-3; outflow valve closes, 3; isovolumic relaxation, 3-4; inflow valve opens, 4; ventricular filling, 4-1.	4
Figure 3	Picture of an aortic heart valve leaflet. Increasing gray intensity corresponds to increasing thickness. Note the very large bundles of tissue, primarily collagen, oriented circumferentially (parallel to the free edge).....	5
Figure 4	Number of heart valve procedures in the United States 1979-2000 (AHA)	7
Figure 5	LifeNet Allograft (St. Jude Medical).....	9
Figure 6	On-X bileaflet pyrolytic carbon mechanical aortic valve (MCRI Inc.).....	9
Figure 7	Porcine aortic valve (Edwards Lifesciences)	10
Figure 8	Theoretical lifecycle of a decellularized xenograft	12
Figure 9	Process diagram of the steps used in constructing a TEHV. Note the dynamic incubation is a step that is not used by all investigators.	14
Figure 10	Transdifferentiation of cell types associated in TEHV (adapted from Fig. 37.1 in [26]). Cell types that have been used in seeding scaffolds are those in white.	15
Figure 11	Equivalent electrical circuit of a 3 element Windkessel system: characteristic resistance, R_c ; peripheral resistance, R_p ; and compliance, C	21
Figure 12	Plots of human aortic pressure and flow data with forward and backward components as well as aortic input impedance spectrum (magnitude and phase). Note dichrotic notch shown as a slight secondary pressure pulsation after the main pressure pulse. Raw pressure and flow data was provided by Dr. Sanjeev Shroff of the University of Pittsburgh and was analyzed with the Matlab script in Appendix C.	25
Figure 13	Diagram of design and evaluation processes.....	31

Figure 14 CAD assembly of an overhead view of the pulsatile bioreactor: atrium, I; ventricle, II, compliance chamber, III, variable resistor, IV; pressure sensors, a; flow sensor, b; stepper motor, c.	36
Figure 15 Picture of the pulsatile bioreactor in operation within the incubator: atrium, I; ventricle, II, compliance chamber, III, variable resistor, IV; pressure sensors, a; flow sensor, b; stepper motor, c.	37
Figure 16 Schematic of the entire system	38
Figure 17 Schematic of the pneumatic system	40
Figure 18 Picture of the atrium	41
Figure 19 Diagram of the ventricle	42
Figure 20 Tissue engineered heart valve holder assembly showing the stent and base	43
Figure 21 Diagram showing the method for suturing the TEHV scaffold into the stent. Note the holes within the stent are curved the same as the needle allowing for easy suturing since the needle never has to be manipulated within the inflow aspect of the scaffold	43
Figure 22 Diagram of the compliance chamber: the compliance is proportional to the amount of air trapped within the chamber	45
Figure 23 Diagram of the variable resistor. Flow is restricted depending on the position of the spiral plate in relation to the tube network. Adapted from a design used in [41].	46
Figure 24 Number of open tubes vs. angle of spiral plate in the resistor	48
Figure 25 Resistance vs. angle of the spiral plate in the resistor. Resistance was calculated by measuring mean pressure and flow across the resistor.	48
Figure 26 Plots of varying the waveform parameters n_1 (a), n_2 (b), and α_1 (c) in the normalized air valve function, f_{act} , which controls the driving ventricular pressure waveform. Standard parameter values: $t_p \text{ max} = 30\%$ period, $n_1=2.00$, $n_2=30.0$, $\alpha_1=0.07$	52
Figure 27 Screenshot of flow loop software showing the waveform control interface	53
Figure 28 Diagram of the control system for mean pressure, P , and mean flow, Q . Errors from the target values, ΔP and ΔQ , are functions of the magnitude of the pneumatic waveform, V , and resistance, R	54
Figure 29 Partial screen capture of the flow loop software showing the mean pressure and flow vs. time protocol where: initial and final mean pressure, P_a and P_b ; initial and final mean flow rate, Q_a and Q_b ; initial phase, Phase 1; ramping phase, Phase 2; and final phase, Phase 3	56

Figure 30 Screenshot of the flow loop software showing acquired waveforms and displaying various measured parameters	57
Figure 31 Diagram showing the geometry (in mm) of a single TEHV leaflet in the TEHV#2 design. TEHV #1 featured the same height and width dimensions without the parabolic cutout.....	58
Figure 32 Tissue engineered heart valve, TEHV#2, after rotisserie incubation.....	60
Figure 33 Picture showing the acid-base indicating ability of phenol red which is present in the culture medium. Note physiological pH is approximately 7.4. pH levels have to change at least 0.5 pH units before a noticeable change in pH can be detected.	64
Figure 34 Sectioning diagram for performing collagen analysis. 3 sections per leaflet were used for evaluation: near the free edge, belly region, and a basal region sewn to the stent. 65	
Figure 35 Results of the system response test: mean pressure and mean flow were stepped from 3.0 lpm at 30 mmHg to 3.5 lpm at 40 mmHg. Note the critically damped behavior of the mean pressure solution	67
Figure 36 Histograms of the mean pressure and flow rate errors from the input (command) for the high flow ramped pressure and flow studies with a bioprosthetic valve. Both passed the Kolmogorov-Smirnov test [67] for following a normal distribution.....	68
Figure 37 High flow hydrodynamic control tests: ramped mean pressure test (a), ramped mean flow test (b), ramped mean pressure and mean flow test (c). All tests are run at 60 bpm	69
Figure 38 Low flow hydrodynamic control tests: ramped mean pressure test (a), ramped mean flow test (b), ramped mean pressure and mean flow test (c). All tests were run at 60 bpm.....	70
Figure 39 Acquired physiologic waveforms at 60 bpm: pressure (mmHg) and volumetric flow (lpm).....	72
Figure 40 Analysis of the aortic waveform produced by the pulsatile bioreactor: measured, forward, and backward pressure and flow waveform components, a & b; impedance spectrum, c; phase angle, d. The black line in the impedance magnitude plot shows the average of the 8 th -12 th harmonics.	73
Figure 41 Analysis of the pulmonary waveform produced by the pulsatile bioreactor: measured, forward, and backward pressure and flow waveform components, a & b; impedance spectrum, c; phase angle, d. The black line in the impedance magnitude plot shows the average of the 8 th -12 th harmonics.	74
Figure 42 Dissolved oxygen tensions as a function of flow rate and incubator oxygen % in water	76

Figure 43 Dissolved gas concentrations and pH as a function of mean flow rate in culture medium. Incubator conditions were standard 37C, 21% O ₂ , and 5% CO ₂	77
Figure 44 Measured pressure and flow waveforms for TEHV#2	78
Figure 45 Mean pressure and flow data for the ramped flow TEHV study until system went on standby due to leaflet tear	79
Figure 46 Collagen concentration as a function of location in the leaflet (n=3). There was found to be a significant difference between the amount of collagen within the free edge and at the portion attached to the stent (p<0.01).....	79

PREFACE

I have been at the University of Pittsburgh since the fall of 1997 as a freshman and have been working at the Tissue Mechanics Lab since January 1998. Five years is a long time, and the work contained in this thesis serves as both a fitting testament to what I have learned in those years as well as symbolizing the end of a very long chapter in my life. We are all influenced over time both consciously and unconsciously by all people and all things that surround us. As such, making a true list of all those that have helped and inspired me to complete the work herein would simply be impossible.

Consciously, there are a number of people who have been directly connected to myself and the project over the last few years whom I would like to thank: David Smith and Claire Gloeckner who both took me under their wings five years ago and passed on to me much of their knowledge and experience. Dr. Jon Wu and George Engelmayr whose assistance with the project was invaluable. Jon Grashow, Thanh Lam, Brent Sugimoto and Wei Sun for loads of for making working here fun. Jill Ulrich for constant and inspired comic relief. Dr. Michael Sacks for paying the bills. Just kidding. Thanks to Dr. Sacks for helping to develop my analytic and synthetic skills and also for allowing me the freedom to run with my ideas.

Thanks to all my family and friends. Especially my parents, Connie and Bill Hildebrand, for their love and support. My brother David for holding down the west coast for me until I get there. My special lady friend Joanna Manders for being the best

1.0 INTRODUCTION

In the year 2000, approximately 87,000 heart valve operations were performed [3]. Replacement heart valves can generally be divided into two classes: those that are built of biologically active materials and those that are built of non-living materials. With the exception of allografts, commercial heart valve therapies are this latter type and are further subdivided by the materials used in their manufacturing. Mechanical valves are built from materials whose source is not biological, while bioprosthetic valve are built from materials that were at one time biologically active such as chemically treated bovine pericardium and porcine tissues. More recently, another approach that has been gaining interest is to use materials with living cells [4-7]. These valves theoretically offer enhanced function when compared to current commercial therapies since they could possibly remodel and grow to meet the needs of the patient [6]. However, this technology is still in its infancy and many fundamental questions remain as to how these valves will function in vivo, including optimization of scaffold materials that will best balance mechanical properties and degradation rate, what cell source(s) will produce the best tissue, and how do hemodynamic variations affect these valves [6].

In order to help address these questions concerning the function of biologically active heart valves, new tools must be created. Traditional in vitro heart valve mock circulatory flow loops are designed to subject the valves to physiologic and/or pathologic hemodynamic pressure and flow conditions. These devices offer a heart valve designer a useful tool with which to evaluate the mechanical functioning of their device in a variety of well-controlled hemodynamic

situations. Additionally, many of these tests are required for regulatory clearance before clinical and commercial use [8]. Unfortunately, these devices have been designed to test replacement mechanical or bioprosthetic valves, not for valves built of materials that are biologically active. Biologically active tissues require proper nutrient and waste exchange, pH, temperature, and freedom from attacks by microbial organisms in order to survive. Pulsatile bioreactors have been developed to provide the aforementioned biological requirements to developing tissue engineered valves [1, 2], but these systems offer very limited hemodynamic control.

Therefore, in order to better understand the hemodynamic functioning of biologically active heart valves (BAHV), and to thereby create better BAHV designs, a new type of pulsatile bioreactor should be created that also incorporates more of the hemodynamic control of mock circulatory loops. This thesis details both the creation of such a device and the process of evaluating its functionality.

1.1 THE HEART

The heart is a four chambered muscular organ which actively contracts to pump blood throughout the body. The names of the four chambers in order of which they received blood are the right atrium, right ventricle, left atrium, and left ventricle. The four chambers are each separated by a valve in order to maintain flow in one direction. The names of these valves in order is the tricuspid, pulmonic, mitral, and aortic. The names of the phases of ventricular pumping and filling can simply be called systole and diastole respectively. During systole, deoxygenated blood returns from the body via the systemic venous circulation and is emptied into the right atrium. Once right ventricular pressure drops below that of the right atrium, the

tricuspid valve opens letting blood fill the right ventricle during diastole. As the ventricle contracts during systole, the pressure builds until the ventricular pressure in the ventricle exceeds that of the atrium and the tricuspid valve closes. The pressure isovolumically increases until the ventricular pressure exceeds that of the outflow vessel, the pulmonary artery, and the pulmonic valve opens and blood is ejected into the pulmonary circulation. Again, once the pressure in the ventricle falls back beneath that of the outflow vessel, the pulmonic valve will close. This cycle is the same for the left side of the heart except the left atrium receives oxygenated blood from the pulmonary veins and the left ventricle pumps blood to the systemic circulation.

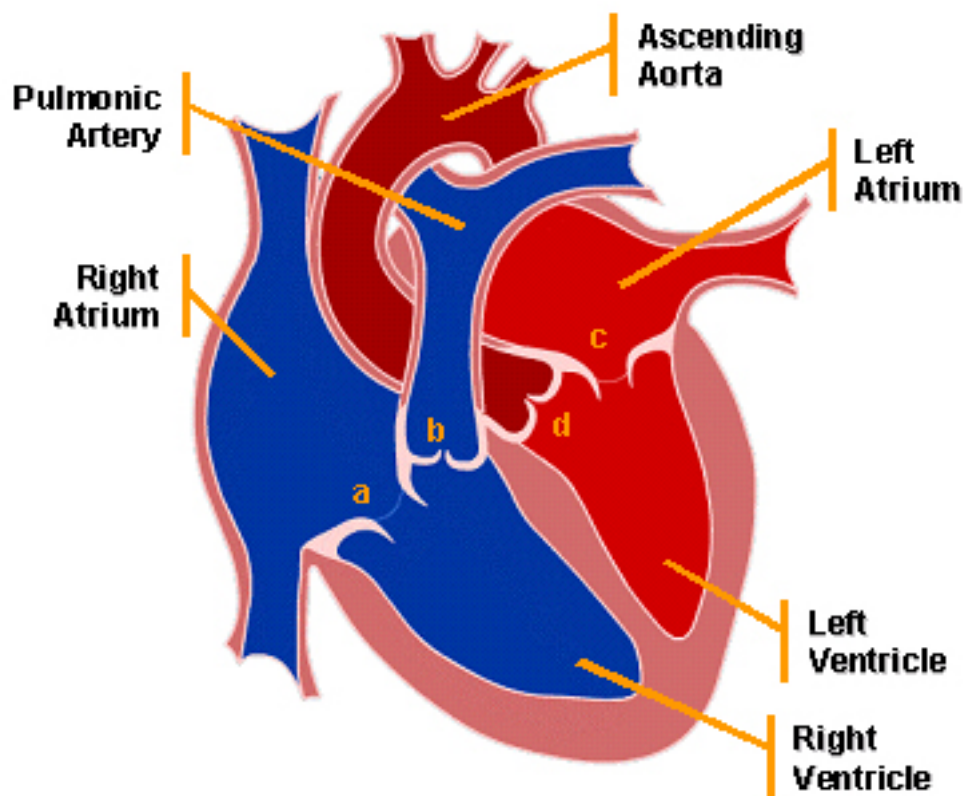


Figure 1 Diagram of the heart: tricuspid valve, a; pulmonic valve, b; mitral valve, c; aortic valve, d.

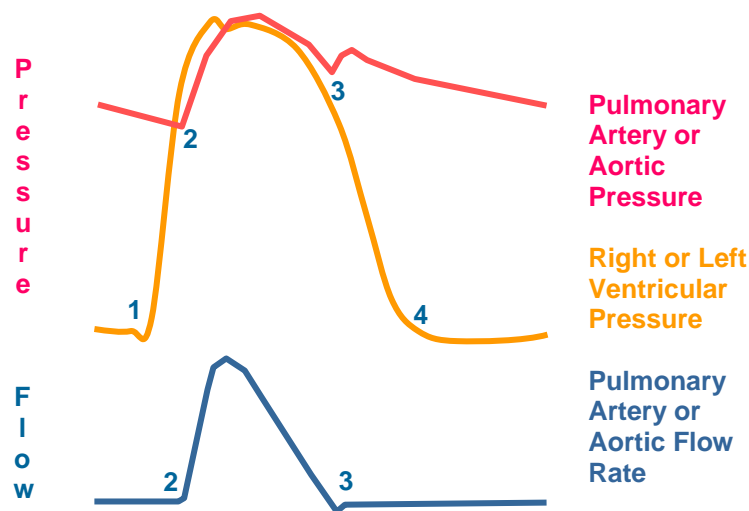


Figure 2 Pressure and flow waveforms of the aortic or pulmonary circulations: ventricular contraction starts & inflow valve closes, 1; Isovolumic contraction, 1-2; outflow valve opens, 2; ejection, 2-3; outflow valve closes, 3; isovolumic relaxation, 3-4; inflow valve opens, 4; ventricular filling, 4-1.

1.2 NATIVE HEART VALVES

1.2.1 Structure and Composition

The aortic valve is a functional assembly composed of the three cusps and corresponding sinuses which together acts to distribute stresses and assures proper and timely valve opening and closure [9]. The three leaflets of the aortic valve are attached to the wall of the aorta and are shaped to come into contact with the other leaflets in a region along the free edge called the coaptation region. The tissue at the center of the coaptation region, the nodulus, is a thickened area compared to the rest of the leaflet tissue. The aortic valve is a tri-layered structure consisting of the fibrosa, spongiosa and ventricularis. The ventricularis faces the ventricle, has a smooth surface, and consists mostly of the extracellular protein elastin. The fibrosa faces the aorta and mainly of very large bundles of collagen surrounded by a network of elastin. Between the fibrosa and ventricularis is the spongiosa, which consists of collagen, elastin, proteoglycans and

glycosaminoglycans (GAGs). GAGs bind water readily and give the spongiosa a sponge-like consistency. Its function is still unclear but it is hypothesized that it functions as a buffer zone between the fibrosa and the ventricularis during loading and unloading [10].

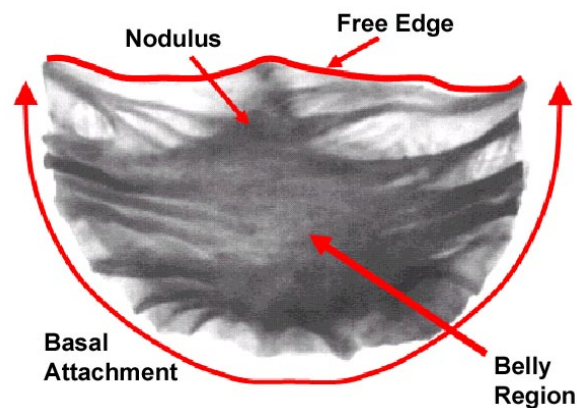


Figure 3 Picture of an aortic heart valve leaflet. Increasing gray intensity corresponds to increasing thickness. Note the very large bundles of tissue, primarily collagen, oriented circumferentially (parallel to the free edge)

1.2.2 Environment, Stresses, and Motions

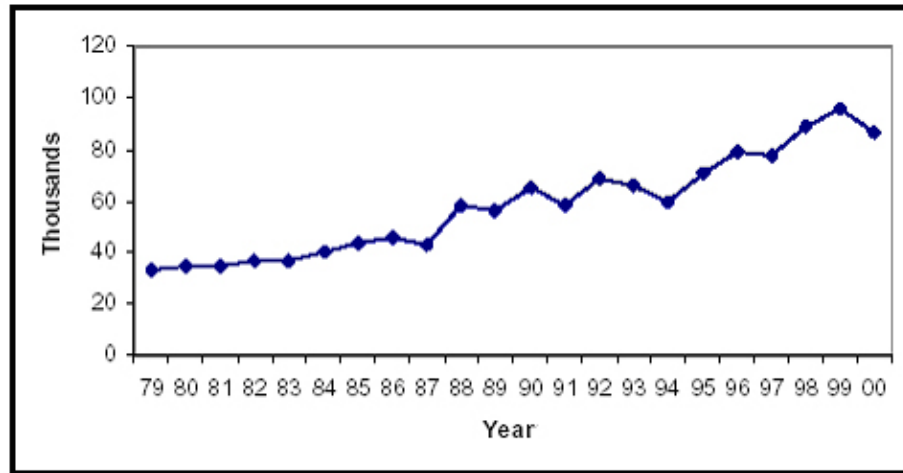
In an adult male, the aortic valve typically operates under systolic and diastolic pressures of approximately 120/80 mmHg and a peak flow rate of approximately 30 lpm and a mean flow of 5 lpm. The pulmonic valve operates under much lower pressures of roughly 30/15 mmHg with slightly lower peak flow rate of roughly 25 lpm. The mean flow rate is of course the same past both valves since the cardiovascular system is a closed circuit. The reduced peak flow rate across the pulmonic valve is compensated for by a slightly longer systolic phase in the right side of the heart than the left. The left side of the heart has a systolic/diastolic time ratio of about 33%. Other relevant physiologic information includes blood pH typically between 7.35-7.45 pH units and arterial gas tensions: oxygen, 95 mmHg, and carbon dioxide, 40 mmHg.

In vitro studies have shown that native aortic leaflet motion undergoes rapid, complex conformational changes during opening/closing. The valve opens from the belly region to the

free edge while during closing both the free edge and circumferential section close together indicating important differences between opening and closing phases [11, 12]. In vivo, aortic valve leaflets are subjected to spatially complex and time-varying cyclic bending, shearing, and tensile stresses [13]. Elastin fibers within the leaflets bear the tensile stresses at low strains and it is thought that elastin in the ventricularis acts to retract fibrosa during systole [14] while collagen bears the tensile stresses at higher strains and its super structural fiber bundles are primarily orientated circumferentially to bear the high tensile forces during valve opening, closure, and diastole.

1.3 HEART VALVE DISEASE

Eighty-seven thousand heart valve operations were performed in the United States in 2000 [15]. The chart below shows that the number of heart valve procedures has generally increased over the past two decades. There are two main conditions that can require valve surgery: valve stenosis and regurgitation [3]. Valve stenosis is a narrowing of the valve opening due to a congenital valve defect, scar tissue buildup from rheumatic fever, or from progressive valvular calcium deposition. This last cause is currently the most common cause of aortic valve stenosis [3]. Regurgitation is reverse flow back into the ventricle caused by congenital defects, aortic dilation, infective endocarditis (a bacterial infection), or a tear in the aorta [3].



Source: Health Resources Utilization Branch, CDC/NCHS.

Figure 4 Number of heart valve procedures in the United States 1979-2000 (AHA)

Birth defects of the heart valve leaflets occur in about 2% of the population and account for 20% of total heart valve disease cases [16]. Valve-related birth defects create a valve with an incorrect number of leaflets. If the deformation results in a valve with one or two leaflets, the valve will regurgitate, or allow retrograde flow while having an extra leaflet can cause stenosis. The most common defect is the formation of a bi-leaflet aortic valve. While some birth defects are not serious enough to require surgery, the presence of an abnormality generally results in a reduced life expectancy and surgery is absolutely required in cases of heart valves with mono or quad leaflet aortic valves.

Rheumatic fever is a childhood streptococcal infection that usually results in scarring of the cardiac tissue, including the valves. The scarring decreases the durability of the valve tissue and leads to damage over time or the valve leaflets can partially fuse together, resulting in stenosis of the valve. Scarring from rheumatic fever accounts for about 45% of stenotic valve cases [16].

Aortic dilation is the enlargement of the sinuses of valsalva, where the valve leaflets are situated [17] and is secondary to other heart conditions such as arteriosclerosis and hypertension.

The dilation causes the leaflets to not close properly resulting in regurgitation. Since the valve sinuses are often part of the prosthetic valve in porcine valves, depending upon the specific model, replacement of the entire conduit is usually performed [16].

1.4 HEART VALVE THERAPIES

Clinical management of heart valve disease includes both pharmaceutical and surgical intervention. Pharmaceutical therapies include beta-blockers and anti-bacterial medicines. Beta-blockers are used in the treatment of hypertrophic hearts [18] while anti-bacterial medications are used to stop the infection of cardiac tissue. Pharmaceuticals are capable of stopping or slowing down the advances of valve diseases but the only way to restore lost function is to surgically replace the damaged heart valve. Commercially available replacement valves include: autografts, allografts, mechanical valves, and bioprosthetic valves.

1.4.1 Allografts and Autografts

As with all donor organs, the supply of donated cadaveric heart valves is very limited and as a result the percentage of total heart valve surgeries performed where allograft are used is small. An autograft procedure is when one of the patient's valves is moved from one valve position to another. Autografts are primarily utilized in the Ross procedure [19], where the pulmonary valve is relocated to the aortic position and the pulmonary valve is replaced by either an allograft or a prosthesis.



Figure 5 LifeNet Allograft (St. Jude Medical)

1.4.2 Mechanical Valves

Typical mechanical valves are can last 30+ years without failure [16]. Most designs are bi-leaflet and are constructed of materials that are biocompatible such as pyrolytic carbon. Two leaflets are mounted within a rigid frame attached by hinges that are designed to open freely under minimal pressure gradients. Unfortunately, clotting factors can adsorb to leaflet surfaces requiring the patient to take anti-coagulants indefinitely.



Figure 6 On-X bileaflet pyrolytic carbon mechanical aortic valve (MCRI Inc.)

1.4.3 Bioprosthetic Valves

Bioprosthetic valves are either porcine aortic valves or bovine pericardial valves. Since both of these valve designs are made from xenograft tissue and would be immediately rejected by the host, the tissues are treated with chemicals such as glutaraldehyde to help hide antigens. Glutaraldehyde treatment also acts to crosslink collagen fibers which both stabilizes and stiffens the tissue structure. Bioprosthetic valves generally have better hemodynamic characteristics than mechanical valves and do not require anti-coagulation therapy, but they do require anti-calcification drugs since the chemical cross-linking promotes the binding of calcium and salts reducing flexibility over time. These devices can last in excess of 20 years and eventually fail due to either calcification related valve insufficiency or tissue breakdown [16].



Figure 7 Porcine aortic valve (Edwards Lifesciences)

1.1.4 Tissue Engineered Heart Valves

While the previously discussed therapies have been in use for decades, and some have freedom from complication of 20+ years [16], these therapies do have drawbacks such as chronic anti-coagulation therapy to prevent thromboembolic events in mechanical valves and chronic anti-calcification drugs in order to retard the formation of valvular calcium deposits. Another approach has been to manufacture valves into living materials using tissue engineering

technology [6]. Currently, most TEHV designs fall into one of two categories depending on the source of the scaffold used in their fabrication. Raw scaffold materials can be either of biological origin (decellularized xenograft ECM, small intestinal submucosa, collagen gels, etc...), or from manufactured polymers [4, 5, 20, 21].

1.4.4.1 Xenograft Scaffolds Currently, there are commercial attempts by Cryolife (Kennesaw, GA) and Medtronic (Minneapolis, MN) to develop a decellularized heart valve as an alternative to traditional prosthetic valve therapies [22, 23]. These valves are made from a porcine xenograft segment of the aorta or pulmonary artery that includes the valve and root. This segment is then washed in a series of detergents in an attempt to remove the cellular material while leaving the extracellular matrix proteins (ECM) in place thereby creating a decellularized scaffold. The thought behind this is that the decellularized scaffold will temporarily function as a working valve while the host's cells become incorporated within the scaffold and generate new tissue. Due to the fact that this is a foreign tissue, it is expected that there will be some form of immune response and subsequent attack by the host on the scaffold. A proper balance is needed between the degenerative effects of the immune response on the xenograft scaffold and the regenerative effects of host cell incorporation and stimulation; therein lies the current problem with this technology.

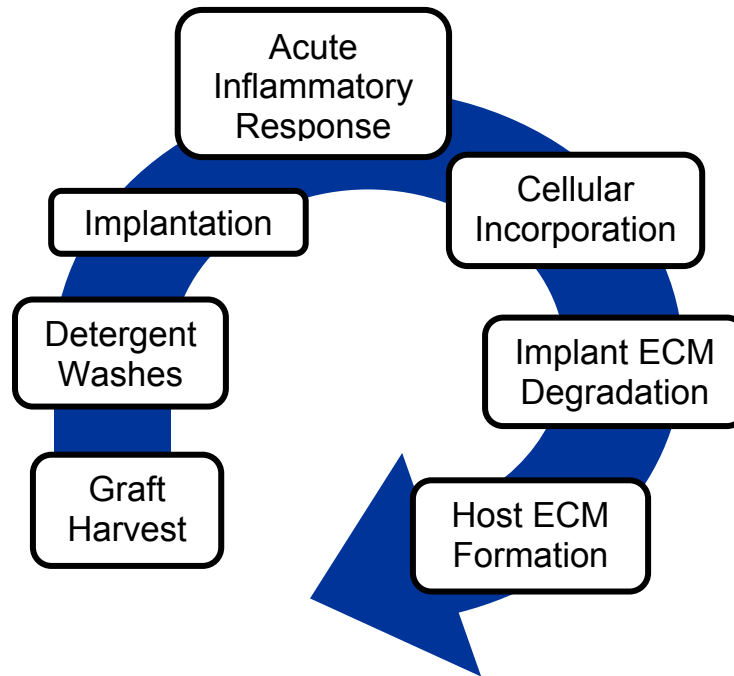


Figure 8 Theoretical lifecycle of a decellularized xenograft

The first decellularized porcine heart valve, Synergraft by Cryolife resulted in rapid failures shortly after it was introduced in Europe in 2001 as an alternative to conventional biological valves. Four Synergraft valves were implanted in four male children in the right ventricular outflow tract as needed for the Ross operation in two of the patients and the other two received homograft aortic roots. At the time of implantation, the grafts appeared macroscopically unremarkable and good valve function was demonstrated postoperatively, yet three of the children died due to device failure [22]. Two died suddenly due to severe degeneration of the valves at 6 weeks and 1 year after implantation, while the third died due to valve rupture on the seventh day. The last child had his valve removed two days after implantation as a precaution. All four of the grafts showed severe inflammation which lead to structural failure in one case and severe degeneration of the leaflets and wall in the other two deaths. It was shown that the hosts demonstrated a foreign body type reaction and significant calcific deposits were demonstrated at

all stages which are detrimental to proper long term functioning and can lead to structural valve failure. It was shown pre-implantation that the detergents used by Cryolife did not remove all of the cells and calcific deposits remained within the scaffold, and postoperatively, there was no evidence of host cellular repopulation [22].

1.4.4.2 Polymeric Scaffolds Unlike the xenograft scaffolds, this design utilizes polymeric scaffolds that are ‘seeded’ or incubated with autologous cells that are grown, at least partially, in-vitro in order to form a tissue-based replacement valve. This valve could theoretically function analogously to a healthy host valve since it would be composed of a scaffold material that would be eroded away while the host cells would continue to form tissue. The valve could subsequently offer the potential for growth and remodeling similar to a native valve without requiring pharmaceutical interventions.

The general process of creating a polymeric scaffold TEHV is illustrated in the diagram below. The process starts with harvesting cells from the host (for autologous tissues) and then isolation of the cells from the ECM. The cells are initially a relatively small population so they are expanded by passaging the cells one or more times to increase their numbers several fold. A polymeric scaffold is then seeded with these cells by placing the scaffold in a cell suspension for one or more days to allow for most the cells to attach to the scaffold [6]. The scaffold is then removed from the suspension and is allowed to incubate in static and/or dynamic conditions. During this period of incubation, the cells may change phenotype and start to produce ECM components, or in simpler terms, form tissue . The process may last for several days to weeks and at the conclusion the now biologically active scaffold can be implanted within the host.

There is as yet no consensus on many issues regarding the design of these valves such as what scaffold material will best balance mechanical properties and degradation rate, what cell

source(s) will produce the best tissue, how should the seeded valve be incubated pre-implantation, and how will in vivo hemodynamic conditions affect the tissue and valve function.

What follows is a summary of current thoughts on each of these topics.

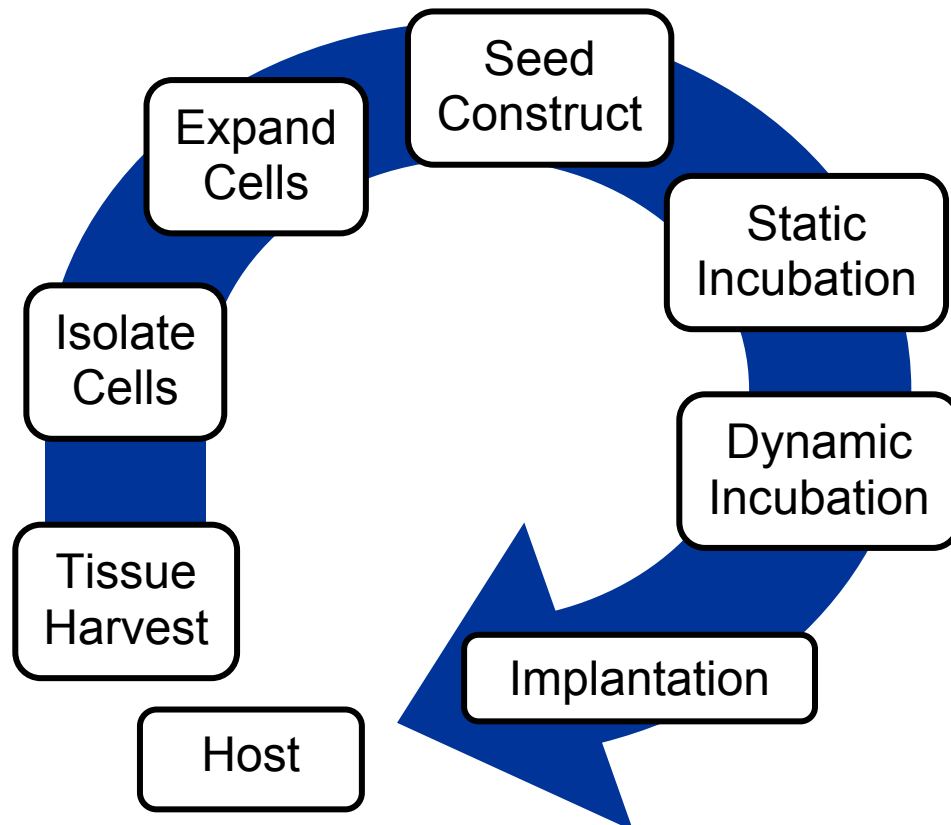


Figure 9 Process diagram of the steps used in constructing a TEHV. Note the dynamic incubation is a step that is not used by all investigators.

1.4.4.3 Cell Sources & Types There is general agreement is that the cell source should be autologous to reduce the severity of the immune response [24], but there remains no consensus as to what cell type(s) should be used to seed the scaffold. Depending on the cell type under investigation, there may be several ways of harvesting the cells from the host. This is not a trivial matter since any standardized or commercially applicable method will need a reliable host cell source and ideally the method of harvesting should be as non-invasive as possible. Currently,

most researchers are investigating cells harvested from vascular segments. It has been reported that there is a non-significant trend towards a lower cell count and reduced collagen content in venous cells [25], but generally it is easier to harvest venous segments than arterial.

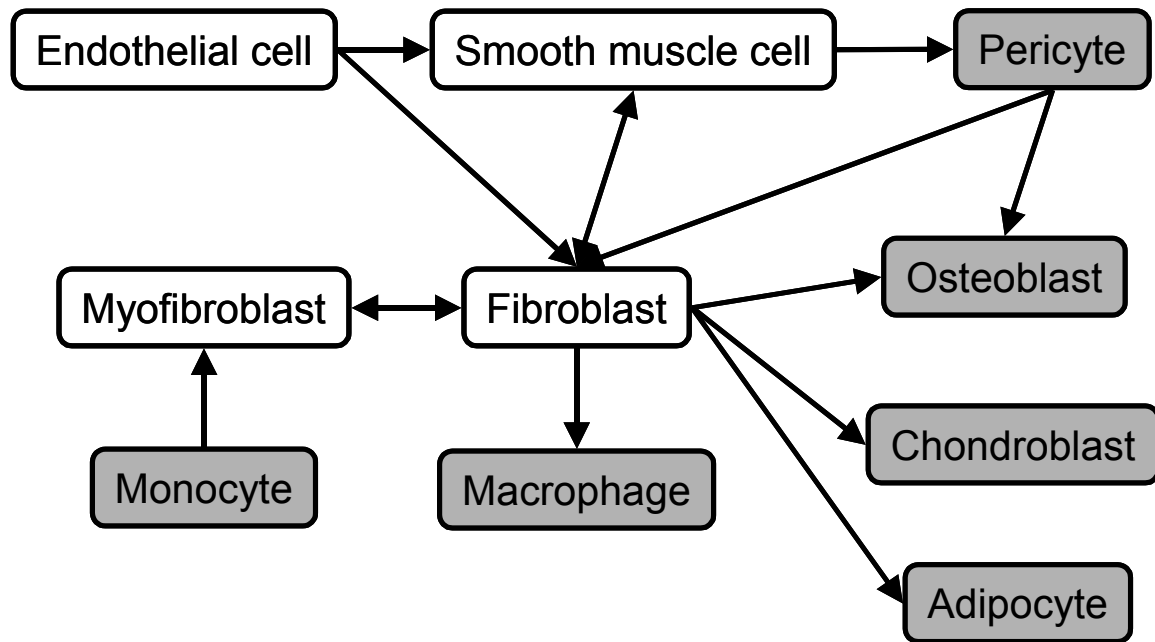


Figure 10 Transdifferentiation of cell types associated in TEHV (adapted from Fig. 37.1 in [26]). Cell types that have been used in seeding scaffolds are those in white.

The main cell types used are of mesodermal origin such as fibroblasts, myofibroblasts, and vascular smooth muscle cells. Fibroblasts are multi-potent cells of mesodermal origin that can give rise to other cells such as fat cells, bone cells, cartilage cells and smooth muscle cells. Fibroblasts make collagens, elastic fibers, glycosaminoglycans and glycoproteins found in the ECM. Fibroblasts are the least specialized of this family of connective tissue cells. The presence or absence of nearby extracellular matrix dramatically affects fibroblast differentiation, as does attachment to substrata or suspension in matrix, and the growth factor environment. Fibroblast

growth factor (b-FGF) is involved in the stimulation of fibroblasts during angiogenesis and transforming growth factor beta (TGF-b) stimulates fibroblasts to produce matrix proteins .

Myofibroblasts are cells having characteristics of fibroblasts and smooth muscle cells and are derived from pericytes associated with blood vessels. Myofibroblasts are active during tissue development, remodeling and repair. They are involved in some forms of arterial thickening and are intimately involved in wound healing. They secrete collagen and their involvement late in wound healing can cause excessive scarring. Vascular smooth muscle cells (VSMC) actively control vascular tone and vessel resistance. VSMC are multiunit smooth muscle and each cell exists as a discreet independent unit that is controlled by a single nerve ending.

1.4.4.4 Scaffold Materials Polymeric Scaffolds are shaped to resemble heart valve leaflets and optionally includes the conduit and/or sinuses. Most of these polymeric materials are hydrophobic and can be coated with ECM proteins such as laminin, fibronectin, collagen, or RGD peptides to promote cell attachment [24]. The two main synthetically derived polymers used in scaffolds are PGA, polyglycolic acid, and PLA, polylactic acid. Both are manufactured as non-woven felts where individual fibers are not directly connected to other fibers and both materials are degraded by hydrolysis in vivo [27]. Both are in-elastic, brittle materials and PGA degrades rapidly in a period of 2-4 weeks while PLA is less susceptible to hydrolysis and degrades over a period of 8-12 weeks [24]. PGA and PLA can be combined to form copolymers that will degrade over a period that is proportional to the ratio of the polymers.

Normally, polymeric TEHV valve scaffolds are assembled by hand by suturing or weaving sheets of material together which makes it difficult to mimic the complex geometry of a native valve [27]. Some studies have added P4HB, poly-4-hydroxybutyrate, a biosynthesized polymer that can be coated onto PGA or PLA scaffolds [27, 28]. This P4HB coated scaffold can then be

processed by compression molding and/or solution casting techniques which allows for greater scaffold design possibilities [27].

1.4.4.5 Seeding, Pre-implantation Culture, and Mechanical Stimulation Cell seeding involves the scaffold being placed in a cell suspension for a given period of time. The cells attach to the scaffold through adsorbed proteins or other mechanisms and begin to produce ECM components such as collagen and GAGs depending on the specific cell type(s) [6]. After this period of cell seeding, the cell suspension is removed and the valve is optionally exposed to a period of static or dynamic flow [5, 6, 29].

It has been hypothesized that culturing a valve under dynamic or pulsatile flow conditions could produce a valve with better tissue formation and mechanical properties when compared to static (non-pulsatile or steady flow) conditions [5, 6]. This exposes the valve to a combination of shearing and flexural stresses and strains which can mechanically stimulate the developing tissue. Shear stress has been shown to partially regulate proliferation, orientation, and the organization and composition of the ECM when endothelial cells have been used by themselves or in conjunction with other cell types [5, 6, 30]. It has been thought that proper modulation of the shear stress could potentially induce desired tissue structure and composition [31], but it is unclear as to what the magnitudes and directions of these stresses should be. Large cyclic strains (>9%) have been shown to produce TEHV materials with more and better oriented ECM [32]. Efforts are underway to further quantify the relationship between cyclic strain and tissue formation [33-35]. Another major mode of deformation in the native valve is dynamic flexure [36], and a recent study has shown that TEHV tissues exposed to dynamic flexure at a rate of 1 Hz for 21 days showed a 63% increase in collagen, a more uniform transmural cell distribution,

and increased vimentin (an intermediate ECM fiber) expression compared to those cultured statically [37].

1.4.4.6 Recent Studies Currently, there is only one group who is actively investigating dynamic incubation of TEHVs, the Mayer group [1, 5, 6, 24, 27, 32, 38-40]. This group's work was started primarily by Dr. John Mayer, Jr. who is trying to develop a suitable pulmonary replacement valve for pediatric patients. As previously discussed, the Ross procedure usually involves placing an allograft in the pulmonary position which are difficult to obtain and can produce a specific immune response [6]. It is thought that a TEHV would make the ideal replacement since it could potentially grow and remodel in the pulmonary position. Additionally, the pressures in the pulmonary position are much less than the aortic which is better suited for TEHV designs which are currently too weak to endure aortic pressures.

Two studies [5, 6] have been published by the Mayer group that utilize dynamic incubation of TEHVs. The system used to dynamically incubate the valves is discussed in a later section. The methods used in these studies are summarized in Table 1. It is important to note that every condition listed in Table 1 is different between the two studies. This 'shotgun' approach to valve design, rather than a more systematic investigation, makes it extremely difficult to draw conclusions and infer exactly what factors are important in modulating tissue structure and composition. Results showed that valves dynamically cultured had both more cells and more collagen, through measured DNA content and hydroxyproline assays, respectively, than those statically cultured for the same amount of time [5].

Table 1 Table summarizing previous pulsatile bioreactor studies. Note the cells, scaffold materials, and the coupled mean pressure and flow rate changes. Other relevant study parameters such as pressure and flow waveforms and heart rate were not reported.

Study	Scaffold	Cells	Cell # /Density	Incubation Time	Mean P & Q
Mayer et al [40]	PHA	Vascular (mixed population)	8 million	Static: 5 days Dynamic: 1-8 days	140 ml/min at 10 mmHg 350 ml/min at 13 mmHg
Mayer et al [5]	PGA/ P4HB	1 st Myofibroblasts 2 nd Endothelial	4.5-5.5 million/cm ² 1.5-2.0 million/cm ²	Static: 4 days Dynamic: 4- 28 days	125 ml/min at 30 mmHg 750 ml/min at 55 mmHg

1.5 MOCK CIRCULATORY LOOP DESIGN

In order to help address questions concerning the function of biologically active heart valves in a dynamic culture environment, a new type of device must be created that incorporates both bioreactor technology (explained in the next section) to provide an environment where tissues can live & grow and mock flow loop technology to provide controlled, pulsatile hemodynamics. Traditional in vitro heart valve mock circulatory flow loops are designed to subject the valves to physiologic and/or pathologic hemodynamic pressure and flow conditions. These devices offer a heart valve designer a useful tool with which to evaluate the mechanical functioning of their device in a variety of well-controlled hemodynamic situations.

Mock circulatory loops are simplified hydraulic analogs of the cardiovascular system that have been utilized in the testing ventricular assist and artificial heart devices, heart valves, and for studying arterial hemodynamics [41-43]. These systems are usually designed using multiple-element Windkessel models [44] and have a wide range of designs depending on the particular application. They are capable of producing highly accurate hydrodynamic resemblance to the desired pressure and flow waveforms, and in the more sophisticated systems, feedback control is

typically employed in order to provide stable and repeatable waveforms. Unfortunately, these systems tend to be large and were not built with sterility as a design criterion.

1.5.1 Modeling the Cardiovascular System: Windkessel Theory

Mock circulatory loops have been designed by noting that many of the laws which govern electrical circuits can be used to also describe fluid-based circuits where pressure and volumetric flow rate are analogous to voltage and current, respectively. Of particular importance is the time-varying nature of the cardiovascular system which is due to the fact that the heart pumps to produce pulsatile flow rather than steady flow. In electrical engineering terms, this relates to alternating current theory which has been well developed. Laws such as Ohm's law, Kirchoff's loop and node laws, as well as the concepts of impedance and capacitance among others, can be used to model aspects of cardiovascular system with close agreement between simulation and in vivo measurements.

These models are represented schematically as electrical circuits and numerous designs have been proposed [44]. Typically, all of these designs stem from what is called the Windkessel model proposed by Hales [45] which consists of capacitance in parallel with a resistance. Modifications to this basic design produce more physiologically accurate results at the expense of processing time. While this is in computational terms, experimentally and/or for model validation, fluid circuits can be made with the fluid analogs to these electrical concepts in order for accurate in vitro testing of the cardiovascular system. All mock circulatory loops must at least have resistive and compliance producing elements in order to simulate the cardiovascular system.

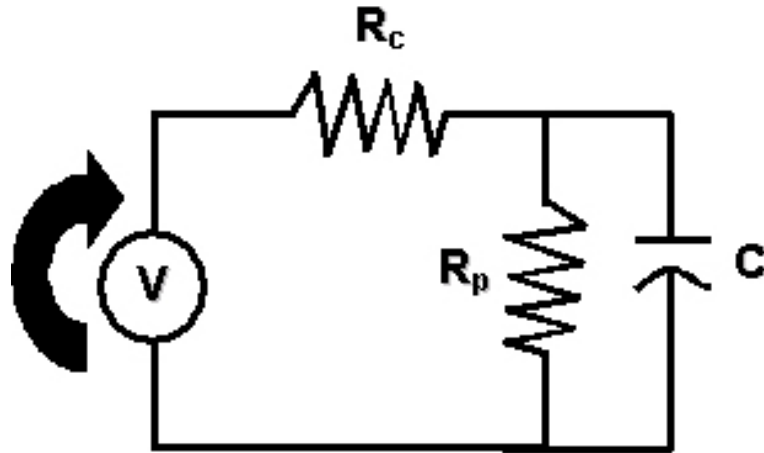


Figure 11 Equivalent electrical circuit of a 3 element Windkessel system: characteristic resistance, R_c ; peripheral resistance, R_p ; and compliance, C .

1.5.1.1 Resistance & Impedance In the body, peripheral resistance is defined as the ratio of mean pressure to mean flow and it is analogous to electrical resistance. Ohm's law states that linear electrical resistance is defined as the ratio of mean (DC) voltage to current. Therefore, the resistance in the system dictates for a given mean pressure what the resulting mean flow will be. Since blood flow is pulsatile by nature, there have to exist higher frequency components to flow and pressure other than mean values (DC values or 0th harmonic terms). Therefore, it follows that there must to be a spectrum of impedances which describe the system. The impedance spectrum can be calculated from Fourier analysis of a single beat, 'steady-state' pressure and flow waveform as discussed by McDonald [46].

It is common to define two of these spectral values when describing the cardiovascular system, the peripheral resistance/impedance, and the characteristic resistance/impedance. Peripheral resistance is the 0th harmonic term in the impedance spectrum and has the largest value by an order of magnitude compared to the other harmonics and accordingly dominates the system response. Characteristic impedance represents input impedance in the absence of wave

reflections, though physiologically there are some wave reflection presents, making most measured values estimates [46]. The characteristic resistance describes the higher frequency content of the system and is defined usually as the average value of the 8th to 12th harmonics. Above this frequency, the contribution to the waveform becomes negligible. The high frequency content of the system primarily relates to the stiffness of the vessels at the point pressure measurement. The stiffer the vessel, the higher in magnitude of the upper harmonics and subsequently the characteristic impedance.

In the cardiovascular system, the peripheral resistance is changed in the body by dilating or contracting ‘peripheral’ blood vessels (arterioles and capillaries) through control of vascular smooth muscle. This in part, along with increased ventricular contractility, ensures that various parts of the body are well supplied with oxygen-rich blood during periods of increased activity. The peripheral resistance that the pulmonary circulation experiences is similarly due to the vasculature surrounding the alveoli in the lungs. To make a distinction in peripheral resistances, I will refer to pulmonary resistance and systemic resistance separately as needed. In atherosclerotic disease, vessels can narrow due to fatty deposits which thereby increases resistance and in turn means the ventricle must pump harder, generate higher pressures, to maintain needed flow.

Typical physiologic levels of peripheral resistance can be readily calculated from simply measuring mean blood pressure and mean blood flow past the area of interest. The areas of interest in this case are the pulmonary and aortic valves where mean flow and pressure are roughly 5 lpm at 20 mmHg and 5 lpm at 80 mmHg, respectively. Again using Ohm’s law, this yields peripheral resistances of 0.24 to 0.96 mmHg s mL⁻¹. Typical values of characteristic

impedance for the pulmonary and systemic circulations are approximately 0.02 and 0.08 mmHg s mL⁻¹, respectively [44].

1.5.1.2 Compliance In the cardiovascular system, compliance is defined as the ratio of the change in fluid volume to the pressure difference that produced the volume change and it is analogous to electrical capacitance. Compliance/capacitance acts to oppose a change in pressure/voltage by storing and releasing energy. Physiologically, the need for this property in the cardiovascular system is to increase pumping efficiency. Since the cardiovascular system is pulsatile, having compliant vessels increases pumping efficiency by allowing energy stored in the vessel walls during systole to be returned during diastole to continue pushing the fluid forward. Diseased arteries can harden becoming less compliant resulting in the ventricles having to work harder to maintain needed flow. Loss of aortic wall compliance at the level of the sinuses has been shown to lead to significantly higher stresses on the aortic leaflets which can lead to changes in their microstructure, sclerosis, and gross distortion or calcification of the cusps [9]. Compliance can be measured a variety of ways and there is as yet a consensus as to the preferred method. An excellent discussion on the various methods is provided by Liu et al [47]. Physiologic values for compliance are roughly 1 and 3 mL mmHg⁻¹ for systemic and pulmonary circulations, respectively.

1.5.1.3 Features in Pressure and Flow Waveforms It is important to note some typical features in pressure and flow waveforms that are common references in discussions on hemodynamics around the cardiac circulation. The dichrotic notch is probably the best known waveform feature since it is easily observable. The dichrotic notch is a secondary pressure spike in the aortic signal due to the inertia of the blood pushing back against the aortic valve after valve closure. Regurgitant flow is any flow that is negative or backward. The most prominent instance of regurgitant flow takes place when the valve is closing frequently called the closing volume and the subsequent regurgitant flow is then the leakage volume.

It is important to realize that there are two components to the overall shape of cardiovascular pressure and flow waveforms; a component that travels forward due to the incident (driving) pressure and a backward traveling component that due to wave reflections. These components can be calculated as follows from [48]:

$$\begin{aligned} P_f &= Z_0 F_f = (P_m + Z_0 F_m)/2 \\ P_b &= -Z_0 F_b = (P_m - Z_0 F_m)/2 \end{aligned} \quad (1)$$

where: the measured pressure and flow, P_m and F_m ; the forward pressure wave, P_f ; the backward pressure wave, P_b ; the forward and backward flow components, F_f and F_b ; the characteristic impedance, Z_0 .

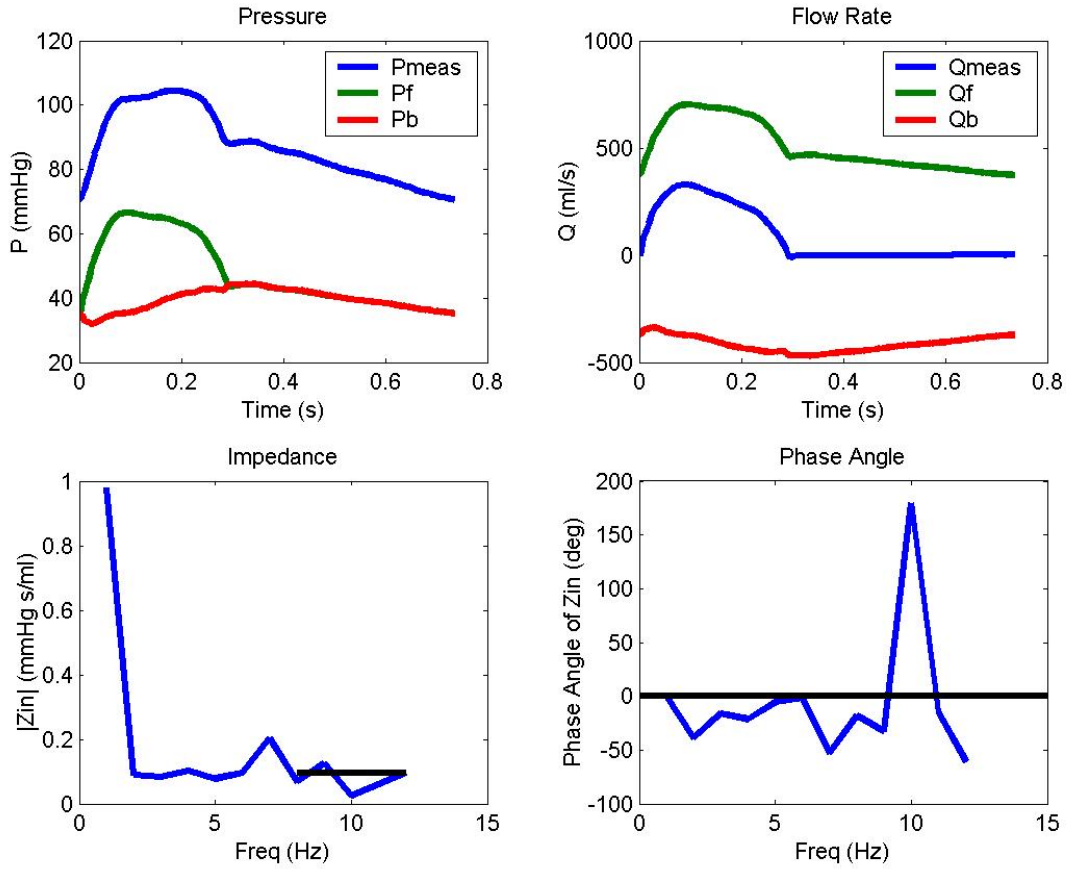


Figure 12 Plots of human aortic pressure and flow data with forward and backward components as well as aortic input impedance spectrum (magnitude and phase). Note dichrotic notch shown as a slight secondary pressure pulsation after the main pressure pulse. Raw pressure and flow data was provided by Dr. Sanjeev Shroff of the University of Pittsburgh and was analyzed with the Matlab script in Appendix C.

1.5.2 Hemodynamic Control Systems

Methods of controlling the hemodynamics of mock circulatory loops incorporate feedback systems of varying complexity to automatically control the driving pressure waveform [49-51] as well as adjustable resistance(s) and compliance(s). However, these systems have primarily necessitated substantial manual intervention to adjust resistance and compliance in order to control pressure and flow waveforms. This is not ideal for a sterile incubation situation where continual user intervention could provide a source for contamination. Another concern is that

most mock loops are designed to mimic the left side of the heart where the pressure and flow are too high to provide a suitable environment for initially mechanically weak TEHV or pulmonary valves. A more desirable system would be one that could run at a wide range of pressures and flows in order to simulate both right and left heart physiologic levels as well as non-physiologic levels. Additionally, the size and complexity of many of these loops would not lend themselves to being placed within an incubator.

The most common design [50, 52-54] for a producing compliance in a mock circulatory loop is to simply have a cylindrical chamber that is partially filled by the circulating fluid and the rest filled with trapped air. During systole pressure increases and the incompressible fluid performs work on the compressible air within the chamber thereby storing energy within it. As systole ends and the pressure starts to decrease, the compressed air resists this change by releasing its stored energy driving the fluid forward in the circuit. The method for adjusting the compliance would be to then control the amount of air or fluid in the chamber by either releasing or pumping in air.

Conventional mock circulatory loops have used several different designs for providing variable circuit resistance. Most have used some type of clamp [55] or valve [53] which is manually adjusted until a desired resistance is achieved. The system must be manually tuned until the proper setting is achieved during which time the resistance could be changing drastically subjecting the valve to undesirable pressure and/or flows. Additionally, many of these valves have small internal features and components that could be difficult to clean or sterilize for use in a pulsatile bioreactor. Another method that provides more predictable control employs a number of small tubes in parallel with a motor positioned slide that can block off flow to some of the tubes [56] and in this way provide computer-based control for resistance.

1.5.3 Actuation Methods

Several different methods of pumping the circulating fluid have been utilized in the construction of mock circulatory loop. The three main actuation systems have been rotational motors employing cams and a driving piston [57-59], an electromagnetic voice coil and piston [50, 53], and a pneumatic system driving a sac or bladder [43, 55, 60]. Both the cam and voice coil designs employ a piston attached to either the cam arm or voice coil respectively which when actuated compresses the hydraulic fluid surrounding a sac that functions as the ventricle. The pneumatic type relies on driving the ventricular sac with a compressed gas, usually air, instead of an incompressible liquid.

The exact hydrodynamic performance of these systems varies largely on the details of the designs and their target application, but generally cam-piston designs have been used in systems that are meant to drive circuits at hyper-physiologic frequencies usually in order to perform accelerated flow/wear studies. Once the proper cam shape is designed, a highly repeatable ventricular pressure-volume relationship can be achieved. A drawback to using this system is the lack of flexibility and control in producing different ventricular waveforms since the shape of the ventricular pressure waveform is specific to the shape of the cam.

Voice coil systems can generate highly controllable pressure-volume curves and can utilize robust feedback control algorithms. These systems have largely been used in studies where exacting ventricular volume control is of utmost concern. Some potential drawbacks to these systems are that the coils heat up dramatically after prolonged actuation and usually have exposed electromagnetic coils which could pose problems in humid environmental conditions such as those found in incubation systems. The voice-coil would then need to be external to the

incubator and the hydraulic driveline would then be passed into the incubator. Maintaining sterility of the hydraulic fluid could pose an additional complication.

Pneumatic systems have been used for many years as the actuation method of choice for a host of medical devices such as sac-type ventricular assist devices which have been in use for over 20 years. In mock circulatory loops, however; usually this mode of actuation is still not as favorable as the voice coil for short-term in vitro testing due to the fact that pneumatic systems don't directly control ventricular volume due in large part to the compressibility of the air. However, feedback systems can still be employed to control the driving pressure waveform, pneumatic drivers can offer trouble-free function for months at a time, and the drive line can be passed easily into the incubator.

1.6 HEART VALVE BIOREACTOR DESIGN

A pulsatile bioreactor is a device meant to subject living or developing cardiovascular tissues to pulsatile flow while providing an environment that maintains biological activity. This pulsatile flow is meant to simulate the flow in the cardiovascular system which may possibly better direct proper tissue growth and formation, as already discussed.

Design requirements for pulsatile bioreactors include providing a biologically suitable & stable environment (proper nutrient & gas exchange, pH, temperature, sterility), stable hemodynamic control, a relatively easy method for attaching the outflow valve (BAHV), and proper sizing to fit into a commercial incubator [1, 61-63]. Pulsatile bioreactors have been designed for dynamic incubation of tissue engineered cardiovascular structures, and unlike the more technologically sophisticated mock circulatory loops, most use manual feedback control

systems in order to alter the pulsatile pressure and flow waveforms. They utilize fluid circuit resistances that are either manually operated [2] or have a fixed value [1, 61-63] resulting in a system that requires substantial manual intervention to achieve different mean pressure and flow levels. The pressure and flow waveforms these systems produce are largely non-physiologic, with exception of Dumont et al. [2] whose design has been shown to produce aortic hemodynamics. Additionally, most of these systems have to at least partially rely on changing the beat frequency (heart rate) rather than the stroke volume in order control the volumetric flow rate. This removes beat frequency (heart rate) as a possible experimental variable which is a potentially important factor in developing tissues [31].

There have so far been only two published designs of pulsatile bioreactors for the dynamic incubation of tissue engineered heart valves [1, 2]. The only group to report a design tested with an actual tissue engineered heart valve is by Mayer et al whose only hemodynamic control is the magnitude of driving pressure waveform. The device is pneumatically driven by a respirator and produces a waveform which is sinusoidal in shape. This design features very low flow rates for a given pressure (mean 125 mL/min at mean 35 mmHg) probably due to several factors such as the small caliber of the tubing used, the static tension in the deforming ventricular bladder, and the lack of a compliance source. These perceived limitations however are in keeping with the authors' design intent which was to provide pulsatile pressure and flow to a maturing tissue engineered heart valve under sterile conditions, with an emphasis on the sterility.

1.7 STUDY AIMS

Finding adequate in vitro models for investigating human biological phenomena has been an ongoing problem within the scientific community and especially within the medical device community. The costs of using animal models can be prohibitive and are often difficult to adequately control, but it is currently the only way to model complex physiological processes. Making in vitro experiments more physiologically accurate is a more tractable approach to answering more fundamental questions that can be helpful in the initial design phases of a medical device. In vitro experiments generally provide enhanced control while offering an approximation of a biologically active event.

Altered hemodynamics is a physiological event that can exist in many pathologic or post-implant states that can potentially have a dramatic effect on biologically active heart valve function as previously discussed. While it is unclear what pressure and flow waveforms (overall shapes and/or magnitudes) are required for alteration in BAHV function, it is clear that in order to investigate the effects of altered hemodynamics on BAHV in vitro, a new type of pulsatile bioreactor that incorporates greater hemodynamic control must be developed.

To this end, the study aim is to develop an in vitro system capable of subjecting a biologically active heart valve to well controlled pulsatile pressure and flow waveforms under biologically relevant conditions. The steps used in completion of the study aim are the following:

1. Analysis of the design problem to form design requirements
2. Create and fabricate design hardware based on design requirements
3. Develop a suitable control system
4. Test the design for both mechanical and biological functionality

2.0 METHODS

It was realized that in order to accomplish the study aim the project would have to be executed in two distinct phases: the design phase which consists of establishing needed device requirements, create possible design solutions, quantitatively select the best solution, create fabrication solid models/schematics, and reevaluation of device requirements. The second phase is evaluation which entails machining components, assemble prototype device, writing control code, and testing comprising hydrodynamic characterization of the system with a prosthetic valve, a sterility challenge and full test with biologically active heart valve.

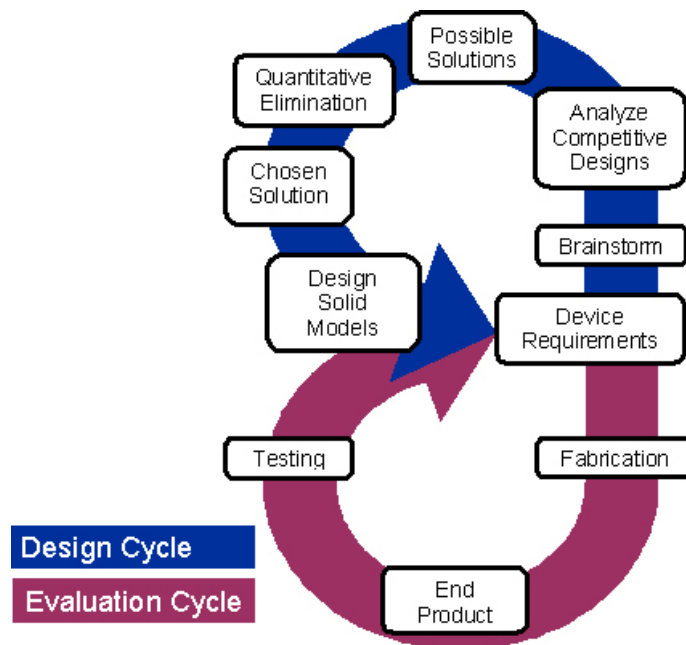


Figure 13 Diagram of design and evaluation processes

2.1 DEVICE DESIGN PROCESS

The first step and the most important part of the design process is establishing the device requirements. This is done by determining the true needs/problems of the end-user (customer) which will result in a problem set that is almost certainly at least somewhat different than the problems initially expressed by the end-user. An example of this would be if an end-user said they required an improved wheelchair so they can travel from point A to point B more easily. The expressed need is an improved wheelchair whereas the true problem is a way of getting from point A to point B more easily. A solution to the true problem may not be best addressed by an improved wheelchair since the designer could possibly come up with a more effective solution.

Once the device requirements are firmly established, the designer can start to think of ways of addressing the problem. Brainstorming ideas, no matter how unrealistic they might seem to at first be, can be incredibly helpful. Momentarily and purposefully forgetting preconceived solutions can result in truly inspired designs. The next step involves analyzing competitive designs which is necessary to ensure that the designer is not wasting his/her efforts on a product that has already been devised. This step serves to help establish expected performance specifications, provide more ideas, and save time. This step also involves looking at the possibility of incorporating existing, off-the-shelf (OTS) components, which can cut down on costs as well as save time.

After these steps have been completed the designer should have several possible solutions to the problem. The way of eliminating or refining the solutions is to analyze them as quantitatively as possible through either performing calculations, running simulations, administering surveys, hazard/risk assessment, conducting feasibility studies, etc.... After

weighting the results of the different design solutions the winning design should become apparent. If this is not the case, it is quite likely that not enough analyses have been performed.

Once the solution is chosen, it is time to design any parts that must be fabricated as well as ensure the functionality of the assembled device. For mechanical or structural components, this is usually accomplished through the use of computer aided design (CAD) programs that can generate 2D or 3D models of the parts and assemblies. The resulting files used for fabrication purposes are either 2D schematics showing the parts with dimensions and notes on various faces or are 3D triangulated mesh files (*.STL). STL files can be used directly by some manufacturing operations such as the rapid prototyping techniques of fused deposition modeling (FDM) and stereolithography (SLA).

Once the solid model part or assembly is complete it is important to now revisit the device requirements in order to attempt to ensure that all of the design intent is still being met. By running virtual simulations (stress analysis, computational fluid dynamics, heat transport, etc...) on the solid models within the computer, actual real-world device performance can often be predicted with great accuracy. Fabrication is expensive, both in terms of money and time and this is the last step that the designer has direct and total control over the actual design. If the device requirements are still met at this stage it is safe to go onto fabrication. If any requirement is in jeopardy of failure, it is very important to go back through all of or as many of the steps already covered that are required to ensure success before fabrication.

The degree of control the designer has over the fabrication/manufacturing process may vary, but regardless it is critical that the designer accurately convey the design intent to the manufacturer so that the most appropriate fabrication techniques are used. The result of the fabrication step will be the end product which should be tested to evaluate its performance with

respect to the device requirements. Testing can reveal faults in either the design itself or with the fabrication steps used to create the device. Depending on which of these cases is true, either process can be repeated as many times as needed.

2.2.1 Device Requirements

The device requirements are determined from analyzing the study aims and their implications: for the device to subject a heart valve to well controlled pulsatile pressure and flow waveforms that can span physiologic and non-physiologic ranges and can also be modulated over an extended period of time, it is clear that a robust hemodynamic control system be in place. Deconstructing the previous statement into design parameters, it is noted that there are three levels or aspects of the control system that need to be in place: pulsatile hemodynamics, predictable response to adjustments, and time-varying control.

To detect meaningful cellular changes in of biologically active heart valves due to altered hemodynamics, they must be cultured for a period of days to weeks. This has a broad impact on the design since nearly all aspects of the system will be affected by having to function properly for extended durations. Two of the most important impacts are the type of actuator, as discussed in the introduction, and the control system. This affects the control system in that user intervention will be of a limited nature since the timeframe of testing is over days, and accordingly, the system should have as high a capacity for auto regulation as possible.

Sterility is needed in any biological setting where the system is incapable of providing a sufficient immune response to remove or prevent infection or where the presence of such an immune response would interfere with the study aims. System sterility implies two design

parameters: that the system is capable of being sterilized and that the system can maintain sterility over the duration of the test.

The outflow valve, the biologically active heart valve, must be easily mounted to the system. This is due to the fact that increased handling time both negatively impacts sterility and excessive handling also could mechanically damage the possibly fragile valve.

Since the device must be kept at physiologic temperature, pH, and gas concentrations, it would be ideal to have the device reside in an incubator which is capable of maintaining these environmental conditions. This creates an added design requirement in that commercial incubators have given interior dimensions to which the device must fit.

Table 2 Table of the design requirements for the pulsatile BAHV bioreactor

Requirement	Motivation	Solution(s)	Qualitative or Quantitative Values
Pulsatile hemodynamics	Simulate cardiovascular system	2 Element, RC, Windkessel system	R: 0.3-1+ mmHg s mL ⁻¹ C: 1-3 mL mmHg ⁻¹ HR: 70+ bpm
‘Un-couple’ mean pressure & flow rate	Automatic control of mean pressure and flow rate	Variable resistor Pneumatic controller	P: 120+ mmHg Q: 5 lpm
Sterility	Prevent biological attacks on valve	All components can be disassembled Materials can be EtO sterilized	No bacterial or fungal colony formation
Easy valve attachment	Prevent handling damage Sterility	Screw-in stent	
Biological environment	Cellular metabolism	Tri-gas incubator	pH 7.4, 37°C pO ₂ 95 mmHg
Size	Fit into incubator		450x450x750 mm

2.1.2 Hardware Design & System Overview

All device hardware, with exception of the pneumatic system, was designed with the CAD platform SolidWorks (version 2003, SolidWorks Corporation, Concord, MA). All of the individual part solid models were generated within separate component assemblies (ventricle, atrium, resistor, etc...) to maintain proper parametric functionality. These component assemblies were then incorporated into a single master assembly in order to ensure proper component interconnectivity.

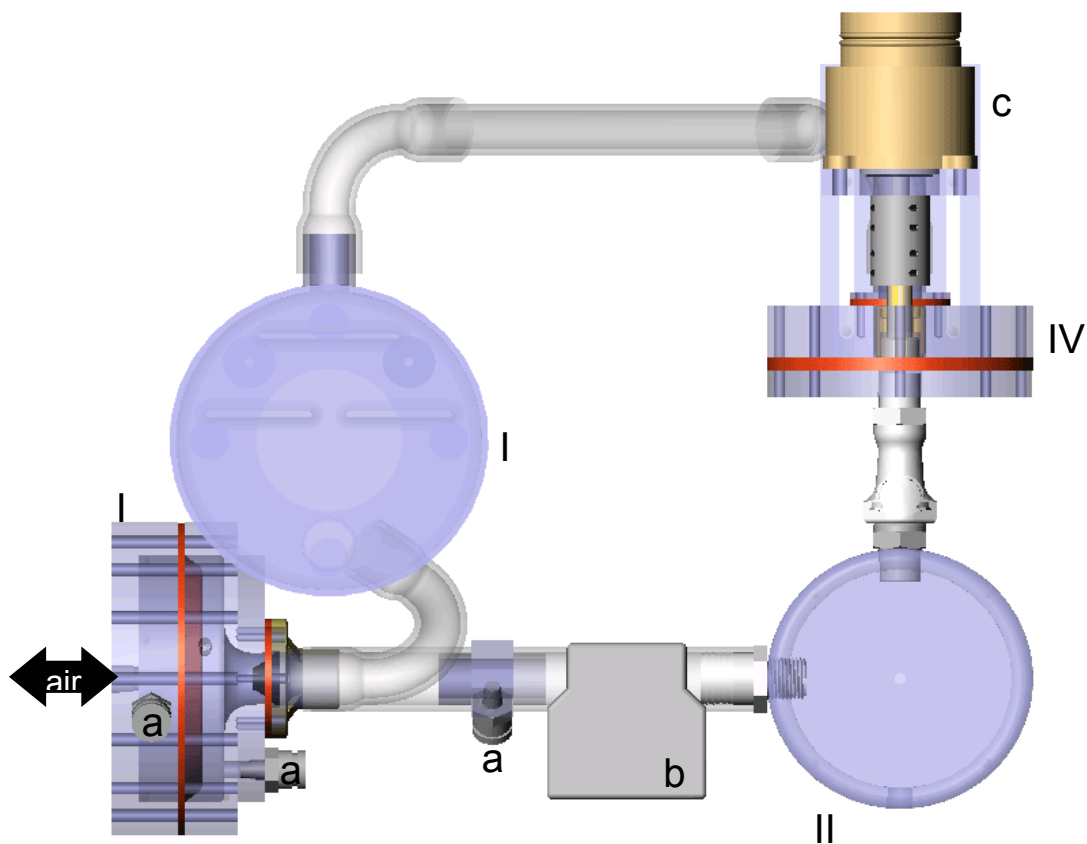


Figure 14 CAD assembly of an overhead view of the pulsatile bioreactor: atrium, I; ventricle, II, compliance chamber, III, variable resistor, IV; pressure sensors, a; flow sensor, b; stepper motor, c.

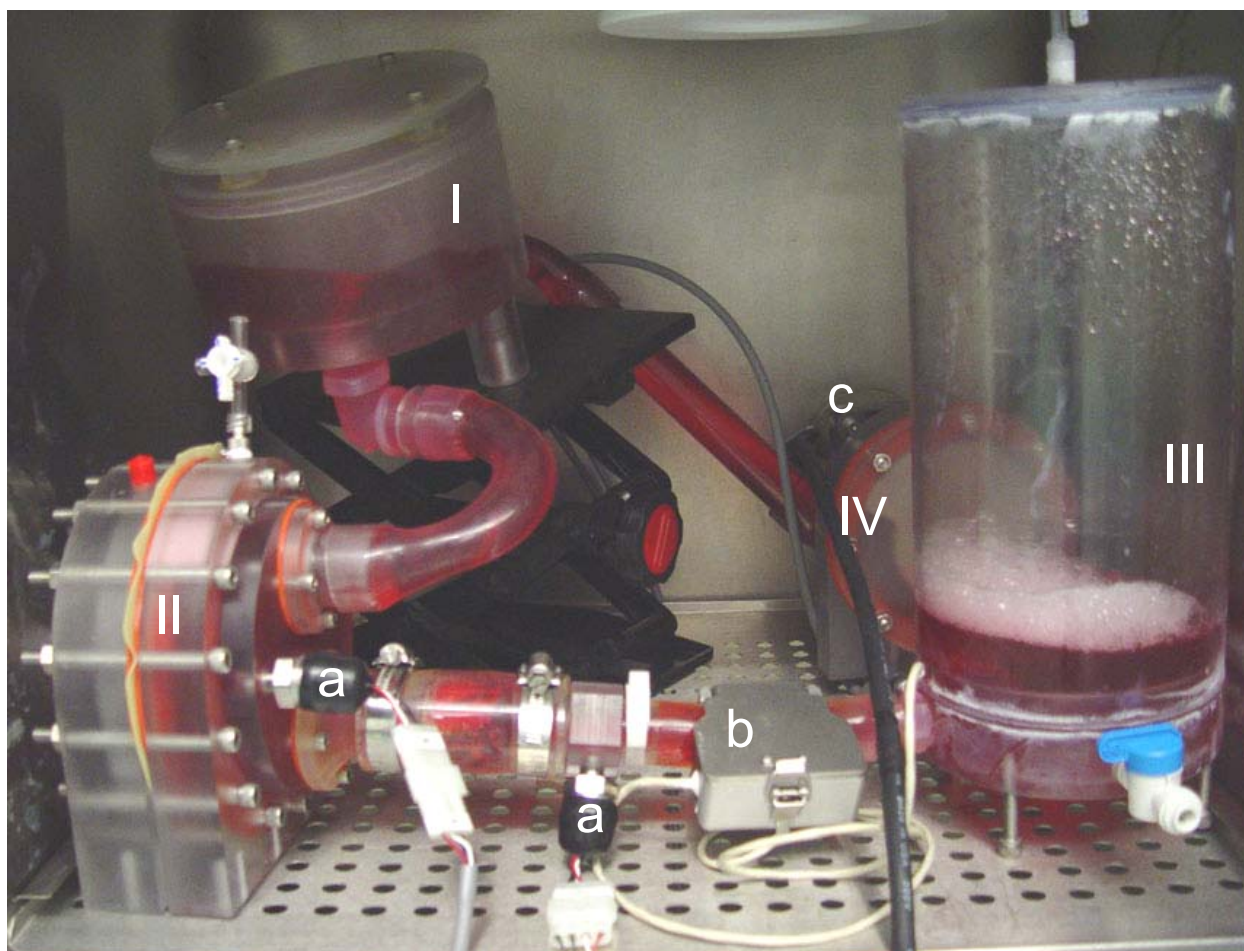


Figure 15 Picture of the pulsatile bioreactor in operation within the incubator: atrium, I; ventricle, II, compliance chamber, III, variable resistor, IV; pressure sensors, a; flow sensor, b; stepper motor, c.

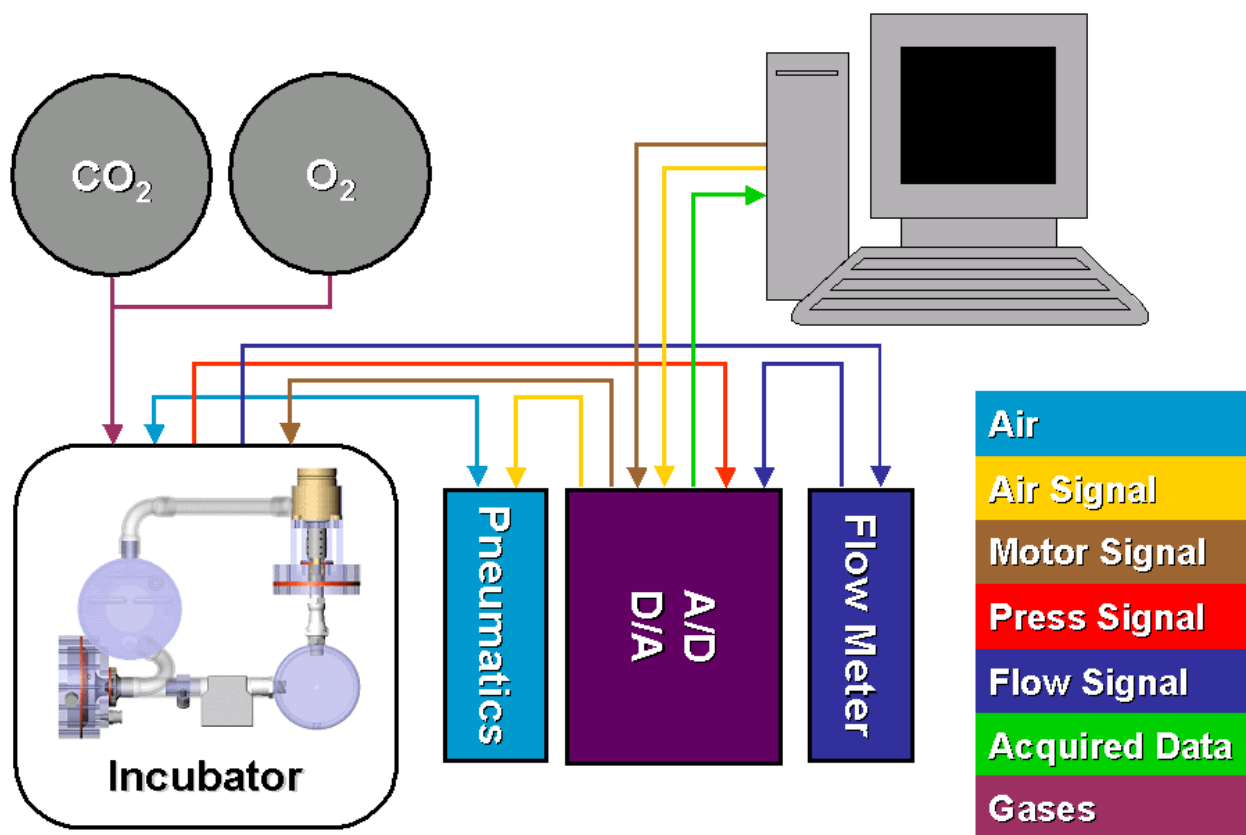


Figure 16 Schematic of the entire system

The schematic of the entire system is illustrated in Figure 16 which shows the pulsatile bioreactor located within the incubator. The pulsatile bioreactor is driven pneumatically and the compressed air is generated by an external pneumatic system. A computer through a digital to analog converter (D/A) generates the signals to control the pulsatile bioreactor through both the pneumatic pressure waveform (air signal) and the resistor's stepper motor (motor signal). Pressure and volumetric flow rate measurements are acquired by the computer with an analog to digital converter (A/D). Carbon dioxide and oxygen gases are supplied to the incubator to maintain proper media pH and oxygen tension respectively.

2.1.2.1 Pneumatic System Most pneumatic controllers in mock loops utilize simple on/off solenoid type valves for dispensing air into the ventricle which produces a mostly square driving

pressure waveform and accordingly, for many applications this does not provide enough control over waveform shape. However, it was realized that if a different type of valve controller, called proportional pressure regulators, could be employed in dispensing the air to the ventricle in a more controllable manner that this would be the ideal actuation scheme for our system. Proportional pressure regulators can generate highly detailed pressure waveforms through piezoelectric valve technology. Such a pneumatic system would provide: dependable and adjustable pressure waveforms over millions of cycles, the pneumatic line can be easily passed into the incubator, and can incorporate feedback control. Thus, we adopted a pneumatic system for the current design.

The pneumatic system starts with a bench-top compressed air supply that is connected to a pressure regulator & air filter (R18, Wilkerson) which steps down the inlet pressure to 10 psi and is passed into a buffer chamber to dampen transient pressure spikes. The air line then runs into a voltage-controlled piezoelectric proportional pressure regulator (Airfit Tecno, Hoerbiger-Origa, Glendale Heights, IL) that features a 43Hz update rate to produce a smooth and highly detailed pressure waveform controlled by the computer generated voltage waveform. Next, the air flows to a 3-way solenoid valve (225B-601BA, Mac Valve, Wixom, MI) and is either sent to the ventricular chamber for driving the system (systole) or is allowed to exit from the ventricle through an exhaust port (diastole). The air is passed through the incubator and into the ventricle via reinforced Tygon tubing.

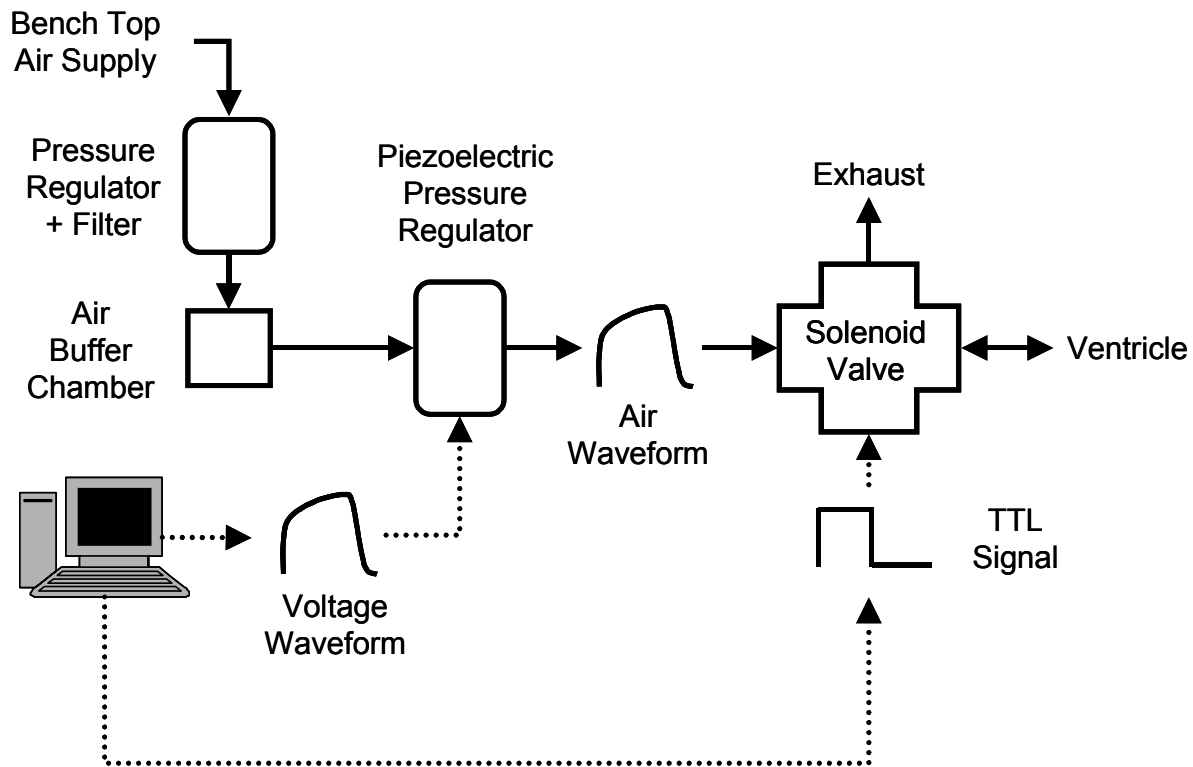


Figure 17 Schematic of the pneumatic system

2.1.2.2 Atrium The atrium provides a location for the circulating media to collect before passively filling the ventricle. For bioreactors there is added need to provide a means for gas exchange between the media and the incubator interior. The atrium is an ideal location for this function since it can be designed to have a large surface area and is open to the interior of the incubator. Our atrium design incorporates panels to encourage mixing to enhance gas exchange and it is made out of a solid piece of polycarbonate to avoid gaps or spaces that could be difficult to clean. The lid, also made of polycarbonate, is easily removable and features a cover which allows gas exchange but hinders particles from falling directly into the media. The atrium is mounted onto a plastic lab jack (Cole-Parmer) which allows for height changes for varying ventricular filling pressure.

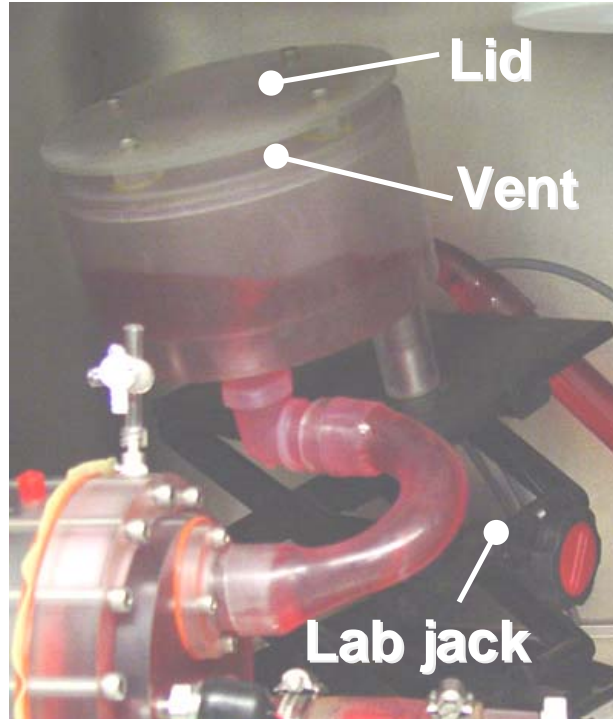


Figure 18 Picture of the atrium

2.1.2.3 Ventricle The ventricle consists of two polycarbonate chambers separated by a thin latex (~0.5 mm) bladder. One chamber is filled by the circulating fluid, the media side, that has a working volume of ~200 ml while the other is filled by air from the pneumatic system. Filling the air chamber causes the bladder to deform and drive the fluid forward. The direction of flow in the ventricle is maintained by a mechanical inflow valve (On-X, MCRI, Austin, TX) and an outflow valve which can be a BAHV or a prosthetic valve. A stopcock is on the top of the media side to allow for removal of trapped air during initial filling. The media side is also ported for a pressure sensor.

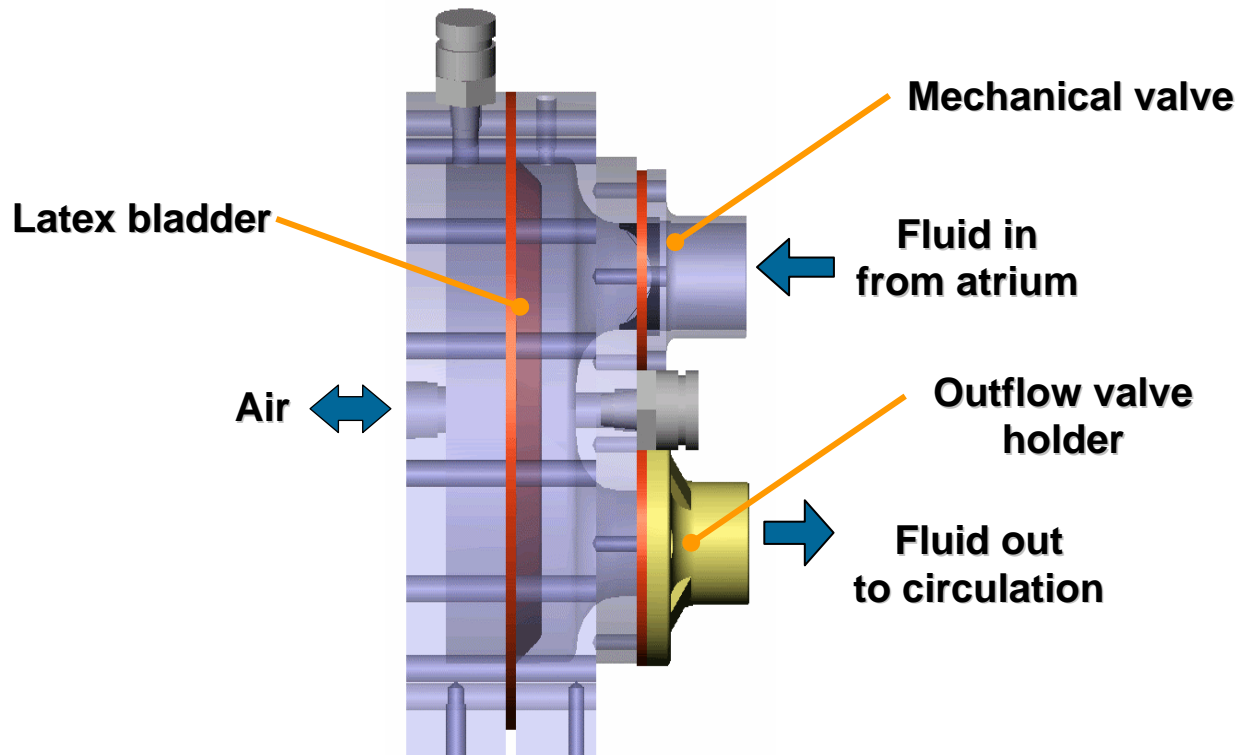


Figure 19 Diagram of the ventricle

2.1.2.4 Outflow Valve Holders For hydrodynamic characterization purposes, a bioprosthetic valve (Perimount, Edwards Lifesciences Corp.) was used in the outflow position since it is more robust than a tissue engineered construct. The bioprosthetic valve is mounted in a conduit held in place between the lip of the outflow conduit and an o-ring mounted on the inflow side.

Other outflow valve holders have been designed for attaching biologically active valves such as TEHV and native heart valves to the ventricle. The sterility challenge utilized a TEHV holder which consists of two parts, a mount with a female threaded hole and a stent with curved suture holes and male threads at its base. The valve is sewn to the stent using ~3 continuous sutures (684H, Ethicon, Johnson & Johnson) which is greatly facilitated by having the suture

holes curved the same radius as the suture needle. All of the valve holders were made from stereolithography resin (Accura Si40, 3D Systems, Valencia, CA)

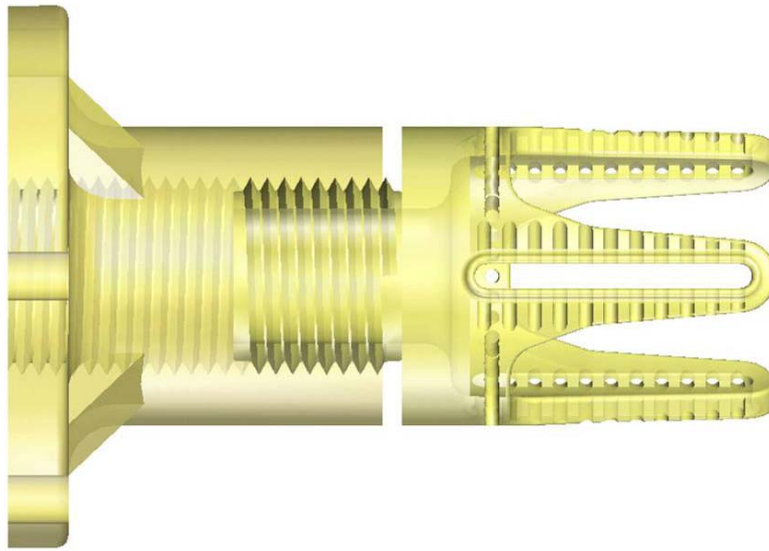


Figure 20 Tissue engineered heart valve holder assembly showing the stent and base

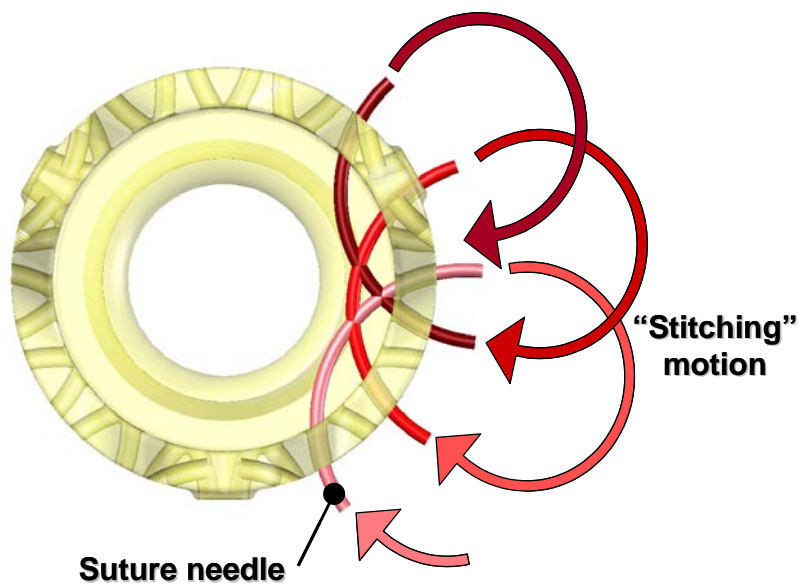


Figure 21 Diagram showing the method for suturing the TEHV scaffold into the stent. Note the holes within the stent are curved the same as the needle allowing for easy suturing since the needle never has to be manipulated within the inflow aspect of the scaffold

2.1.2.5 Compliance Chamber As previously stated, most mock circulatory loops utilize a compliance element that is a cylindrical chamber located downstream of the heart valve. In order to calculate the needed volume of the compliance chamber one must look at the limiting case which is the pulmonary compliance which is approximately 3.5 mL mmHg⁻¹, C_{max}. The needed empty volume of the compliance chamber was determined using formulations given by Knierbein et al [52] and assuming pulmonary systolic/diastolic pressures of 40/20 mmHg:

$$\begin{aligned}
 P_{sys} &= 40 \\
 P_{dia} &= 20 \\
 P_{atm} &= 760 \\
 P_1 &= P_{sys} + P_{atm} \\
 P_2 &= P_{dia} + P_{atm}
 \end{aligned} \tag{2}$$

Noting that compliance is defined as $C = \Delta V / \Delta P$ and assuming isothermal expansion and contraction, PV=constant:

$$\begin{aligned}
 P_{atm} V_{atm} &= P_1 V_1 = P_2 V_2 \\
 C_{max} &= V_2 / P_1 \\
 P_{atm} V_{atm} &= P_1 V_1 = P_1 P_2 V_2 / P_1 = P_1 P_2 C_{max} \\
 V_{atm} &= P_1 P_2 C_{max} / P_{atm}
 \end{aligned} \tag{3}$$

the needed chamber volume, V_{atm}, is approximately 2.8 L. The height and diameter are then constrained parameters that must satisfy the relationship:

$$V_0 = 2.8 \text{ L} = \pi D^2 H / 4 \tag{4}$$

The chosen dimensions are roughly 120 mm inner diameter by 250 mm in height.

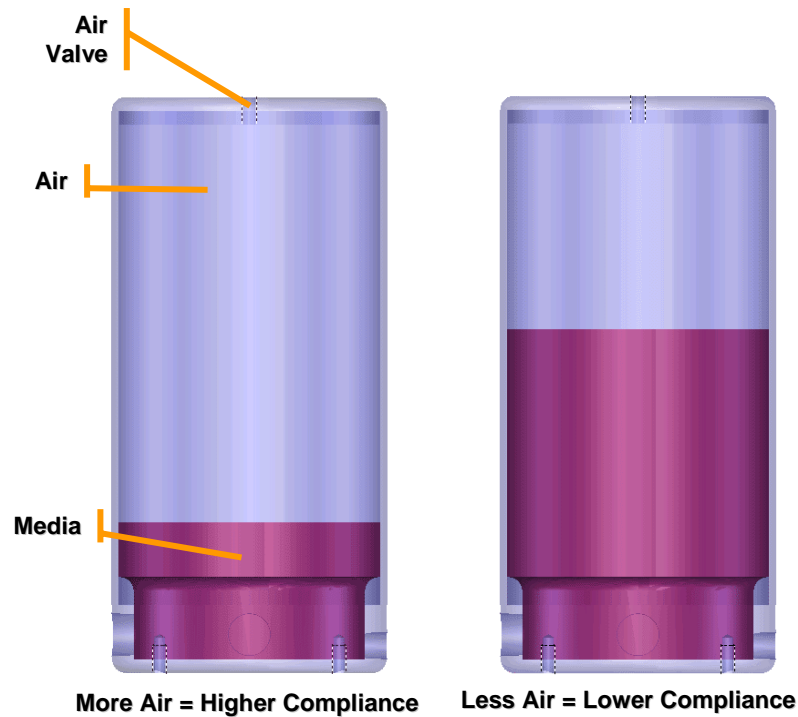


Figure 22 Diagram of the compliance chamber: the compliance is proportional to the amount of air trapped within the chamber

2.1.2.6 Variable Resistor The resistor provides a variable resistance to flow within a predetermined range. The needed working range is dictated by physiology where the typical resistance range is roughly 0.25 and 1.2 mmHg s ml⁻¹ for pulmonary and systemic circulations respectively. In order to fill the design requirements, the system would have to be able to automatically adjust to and maintain the desired resistance indefinitely as well as provide high resolution in order to provide the level of control needed for mean pressure and mean flow.

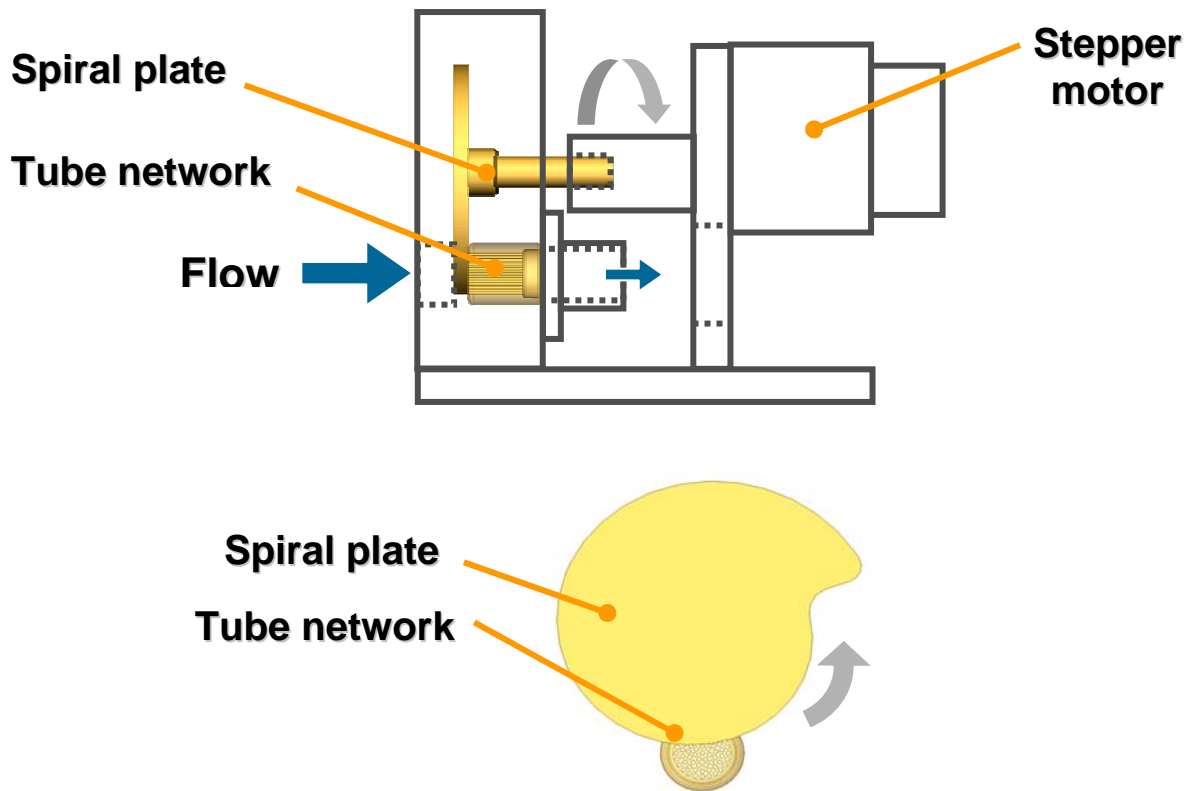


Figure 23 Diagram of the variable resistor. Flow is restricted depending on the position of the spiral plate in relation to the tube network. Adapted from a design used in [41].

The design that was chosen for our system utilizes a rotating spiral shaped plate in contact with a tube network of approximately 60 1.3 mm diameter tubes manufactured from a stiff stereolithography resin formulation (Accura Si40, 3D Systems). The rotation of the plate is provided by a high angular resolution (0.0375 degrees/step) stepper motor (C57L, Thompson Airpax, Danaher Motion, Port Washington, NY) and provides high torque (10 ft-lbs). The reason for needing a high torque motor is due to the friction that is present in both maintaining the water-tight seal around the shaft of the plate and in the contact of the plate against the tube network. In order to maintain this contact, an o-ring is placed between the inflow side of the plate and the resistor housing as well as the outflow end of the tube network and the outflow gasket. Tightening of the outflow flange then presses the tube network into the plate.

The number and diameter of the tubes were determined from using the Hagen-Poiseuille equation for fully-developed, laminar flow of a Newtonian fluid in a tube as an approximation for calculating resistance:

$$R_{tube} = \frac{8\mu L}{\pi R^4} \quad (5)$$

where: fluid viscosity, μ (0.7×10^{-6} N s m⁻² for water at 37°C); tube length, L (25 mm); tube radius, R (0.65 mm). For resistors in parallel, $R_{tot} = R_{tube} / N$, where number of tubes, N. A pilot study was performed to check the error of using equation (5) as an estimate using a resistor with 30 tubes. The measured resistance was found to be approximately 4.6 times the calculated resistance which was calculated based on the Hagen-Poiseuille equation. Noting that pulmonary resistance is typically 0.25 mmHg s ml⁻¹, the maximum number of tubes needed is then shown as below:

$$\frac{R_{tube}}{R_{total}} HP_{error} = \frac{R_{tube}}{R_{pulmonary}} HP_{error} = \frac{\left[\frac{8\mu L}{\pi R^4} \right]}{0.25} 4.6 = N = 57 \quad (6)$$

A constraint on the number of tubes is the overall diameter of the tube network which was desired to be less than 25 mm, the diameter of the inlet and outlet tubing, and to limit the overall size of the entire resistor as the resistor plate diameter also depends on the tube network diameter. A constraint on the diameter of the tubes is due to fabrication and also ease of cleaning. Too small of a diameter would be difficult to accurately machine for every hole and could cause some holes to be larger than others which can cause large differences in resistance since radius is raised to the 4th power in the equations.

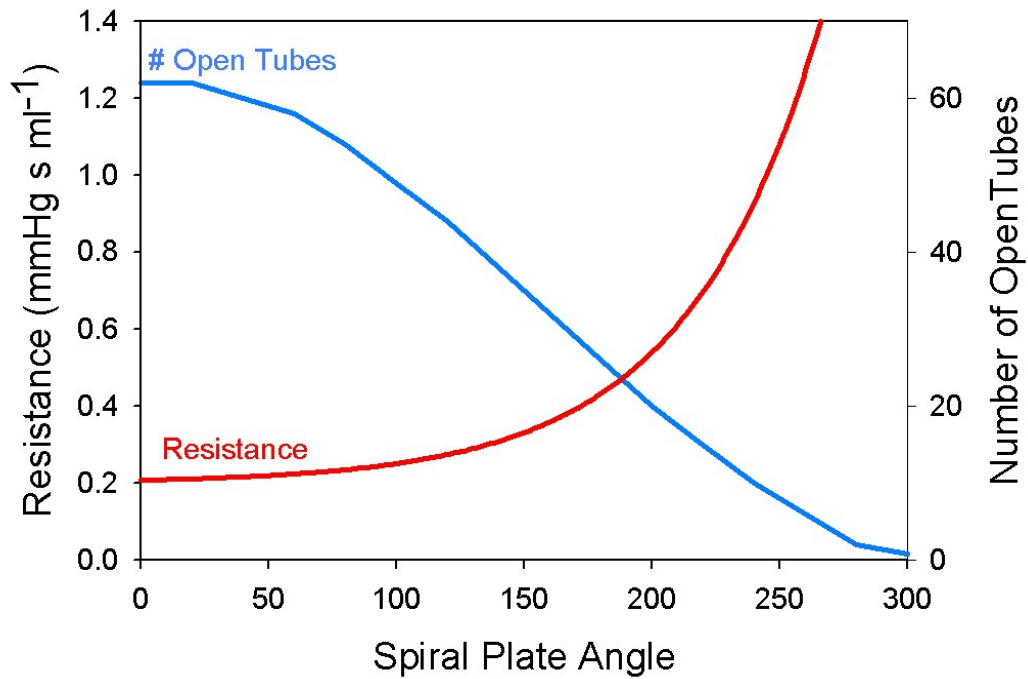


Figure 24 Number of open tubes vs. angle of spiral plate in the resistor

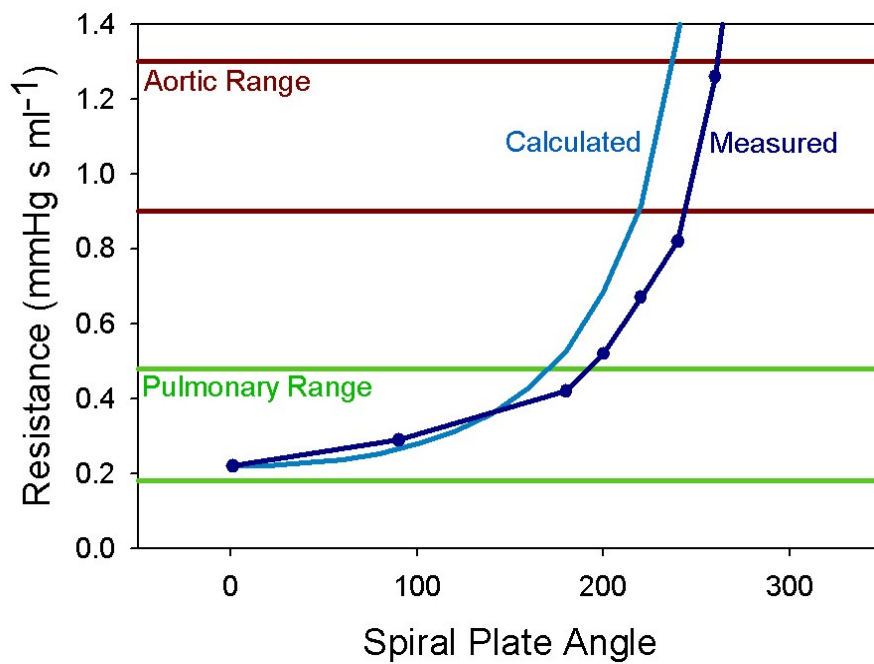


Figure 25 Resistance vs. angle of the spiral plate in the resistor. Resistance was calculated by measuring mean pressure and flow across the resistor.

2.1.2.7 Sensors The pressure is monitored with pressure transducers (19C series, Sensym ICT) in direct contact with the circulating fluid in both the ventricle and in the outflow stream. The pressure sensors were chosen for being constructed of 316 grade stainless steel which is extremely resistant to corrosion. The sensors are also temperature compensated and have the desired pressure range. Volumetric flow is measured using an ultrasonic flow probe (C series, Transonic Systems, Ithaca, NY) placed after the valve and before the compliance chamber.

2.1.2.8 Incubator The incubator is a tri-gas model (Isotemp, Fisher Scientific, Hampton, NH) which allows for controlling both the concentration of oxygen as well as carbon dioxide the within the incubator environment by adding oxygen or nitrogen to increase or decrease the oxygen concentration respectively. In this way, the concentrations of oxygen and carbon dioxide in the media can be controlled. The media pH is consequently controlled since it is buffered by the reaction between carbon dioxide and the bicarbonate ion within the media.

2.1.2.9 Computer Interfacing Electronic control of the device is performed by a PC with a multifunction data acquisition card (PCI 6035E, National Instruments, Austin, TX) running custom written control software (Labview, National Instruments). Two metallic enclosures that are external to the inter-incubator components of the loop house the pneumatic system, the pneumatic enclosure, and the data acquisition & stepper motor controller, the DAQ enclosure. The breakout terminal for the DAQ card is located in the DAQ enclosure along with the power supplies for the stepper motor, an inexpensive multi-output DC supply (Techtronix), and for the pressure sensors, a regulated 12 V DC supply (Sola). The stepper motor controller (TM98CTL3145, Herbach and Rademan) is controlled bit-wise by using the digital I/O

functionality of the DAQ card. The two analog output channels of the DAQ card are used for generation of the voltage waveform that controls the piezoelectric proportional pressure regulator and for producing the square wave (TTL signal) which controls the solenoid valve. An analog output channels are used for both signals since they can be easily synchronized with each other in the Labview software.

2.1.3 Software Design

The requirements of the software are to produce a tunable pulsatile driving waveform, automatically control mean pressure and flow over time, and acquire and store data. All code was created in the LabView software environment.

2.1.3.1 Driving Waveform A numerical function is used for producing the driving voltage waveform for the piezoelectric pressure regulator since the pressure waveform that the valve is exposed to should be the same for successive tests. Additionally, a numerical waveform that has parameters to finely control its shape gives the user an easy way to predictably alter the waveform shape over time if so desired.

The driving voltage waveform for the piezoelectric pressure regulator is generated using the function shown below:

$$f_{act} = \left[\frac{\left(\frac{t_n}{\alpha 1} \right)^{n1}}{1 + \left(\frac{t_n}{\alpha 1} \right)^{n1}} \right] \left[\frac{1}{1 + \left(\frac{t_n}{\alpha 2} \right)^{n2}} \right] \quad (7)$$

where $t_n = t_{abs} / t_{p \max}$ and f_{act} , normalized air valve function; n1, n2, $\alpha 1$, adjustable parameters; t_{abs} , absolute time; $t_{p \max}$, time to peak pressure; T, period. A typical f_{act} waveform is shown in Figure 26 as the standard case. The amplitude of the output waveform is controlled by multiplying f_{act} by the computed magnitude of the control voltage, V, as discussed below. The shape of the waveform can be modified by adjusting n1, n2, and $\alpha 1$ as well as the systolic/diastolic time ratio by controlling $t_{p \max}$. Physically, the parameters n1, n2, and $\alpha 1$ are analogous to the rise time, the decay time, and the width of the peak respectively.

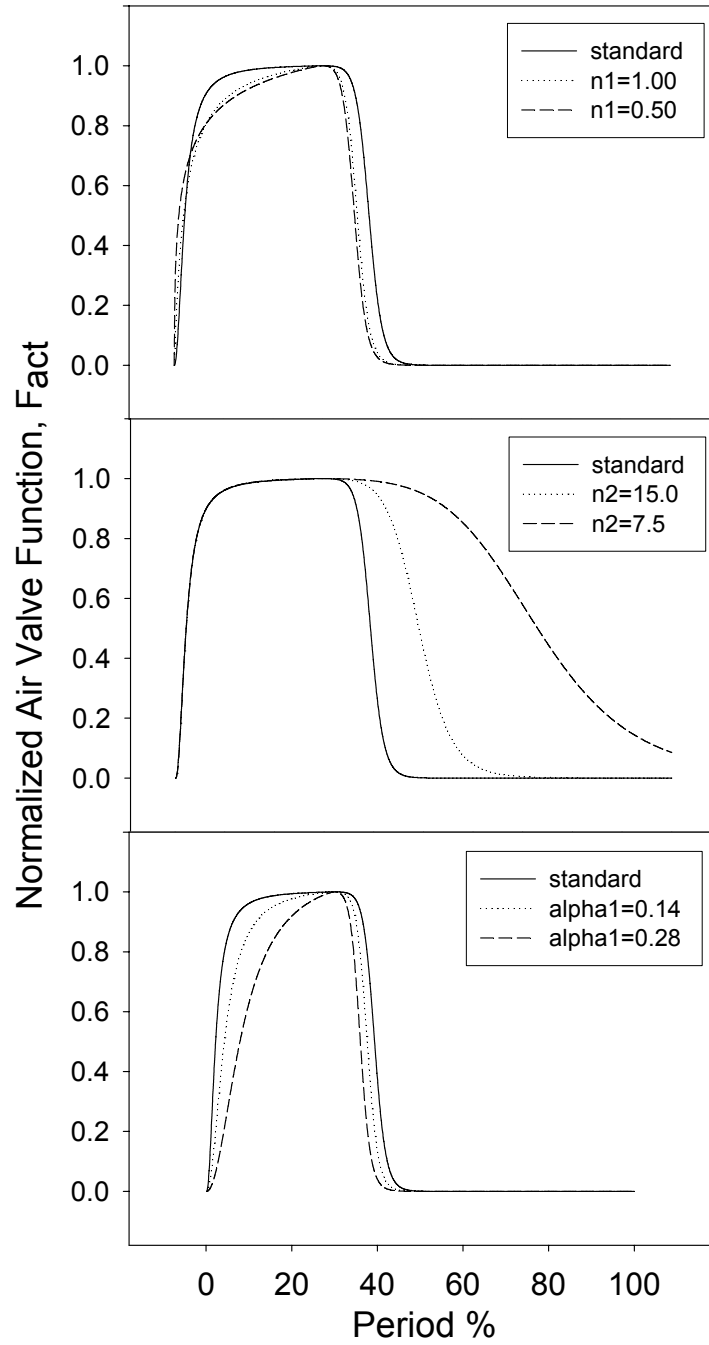


Figure 26 Plots of varying the waveform parameters $n1$ (a), $n2$ (b), and $\alpha1$ (c) in the normalized air valve function, fact, which controls the driving ventricular pressure waveform. Standard parameter values: $tp_{max} = 30\%$ period, $n1=2.00$, $n2=30.0$, $\alpha1=0.07$

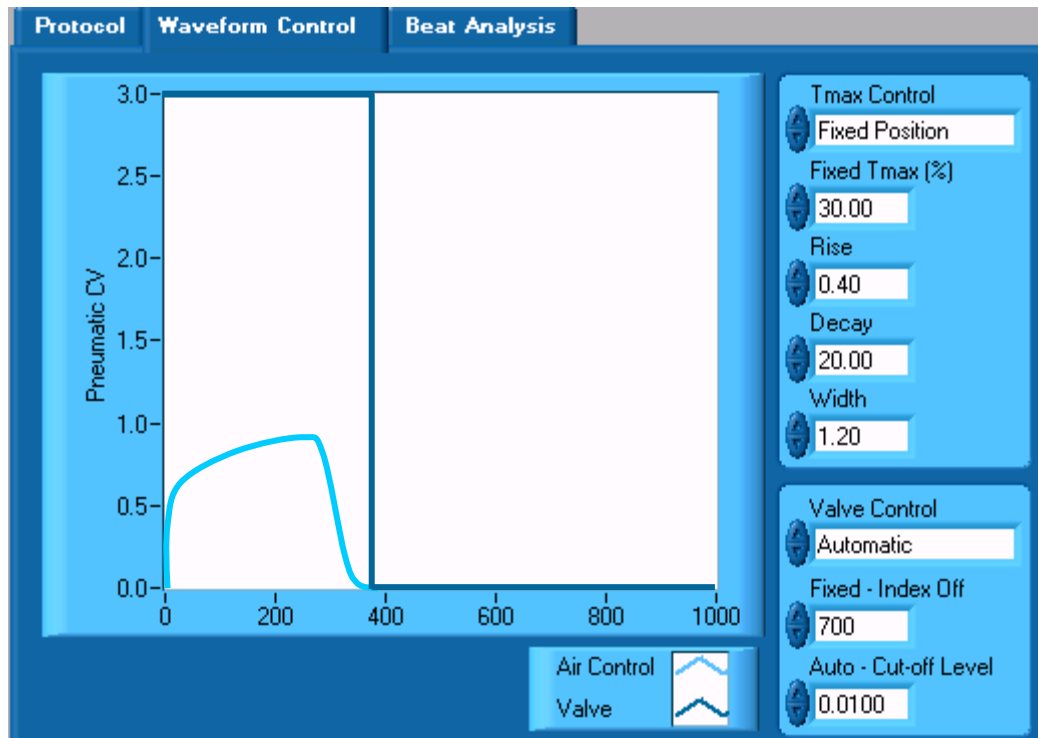


Figure 27 Screenshot of flow loop software showing the waveform control interface

2.1.3.2 Mean Pressure and Flow Control Code In order to limit user intervention and to reduce risk of contamination in our system, mean pressure, P , and mean flow, Q , are primarily controlled electronically by simultaneously modulating the magnitude of the driving pneumatic pressure waveform, V , and the circuit resistance, R , as shown in Figure 28.

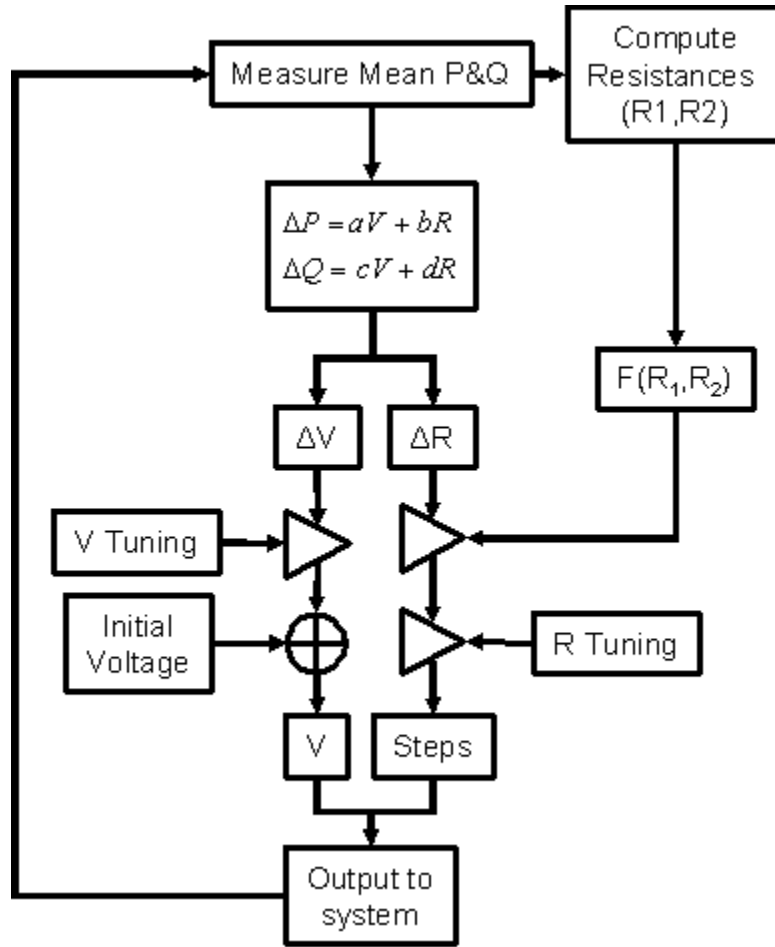


Figure 28 Diagram of the control system for mean pressure, P, and mean flow, Q. Errors from the target values, ΔP and ΔQ , are functions of the magnitude of the pneumatic waveform, V, and resistance, R.

Measured pressure and flow errors from the command, ΔP and ΔQ , are used in solving for the needed change in circuit resistance and control voltage, ΔR and ΔV , using the equation:

$$\begin{aligned}\Delta P &= aV + bR \\ \Delta Q &= cV + dR\end{aligned}\tag{8}$$

where: ΔP , pressure difference; ΔQ , volumetric flow difference; V, control voltage to piezoelectric pressure regulator; R, resistor control explained below; a-d are constants determined from linear regressions of tuning the system response as shown:

$$\begin{aligned}
P &= aV \\
P &= bR \\
Q &= cV \\
Q &= dR
\end{aligned} \tag{9}$$

Constants a (mmHg V^{-1}) and c (lpm V^{-1}) were computed from the regressions of system pressure and flow while changing voltage only and constants b (lpm) and d (mmHg $^{-1}$) while changing circuit resistance only. Constants a, b, c are positive values while d is negative.

The resistor history function, below, relates the number of steps needed to be output to the stepper motor to provide the needed change in resistance:

$$\begin{aligned}
A &= |1 - R_1/R_t| \\
B &= |1 - R_2/R_t| \\
F &= |A - B| \\
motor\ steps &= \Delta R \cdot S \cdot [1 - F]
\end{aligned} \tag{10}$$

where: R_t , target (command) resistance; R_1 , the current measured resistance; R_2 , the resistance measured in the previous running of the control loop; S , a scaling factor. F is then a weighting factor that approaches zero when the resistor is fully open and increases as the resistor becomes closed. Both the number of motor steps and control voltage output to the system are tuned by scaling factors, S , to achieve a stable and fast system response.

When the user requires the target mean pressure and flow levels to change over time, the control code generates a protocol that consists of the beat or cycle number and the desired values of mean pressure and flow at this beat. The software keeps track of the number of elapsed beats and the appropriate target mean pressure and flow level are fed into the control code. It was decided that the beat number should be used rather than time as to anticipate tests where the heart rate could be modulated over time as well.

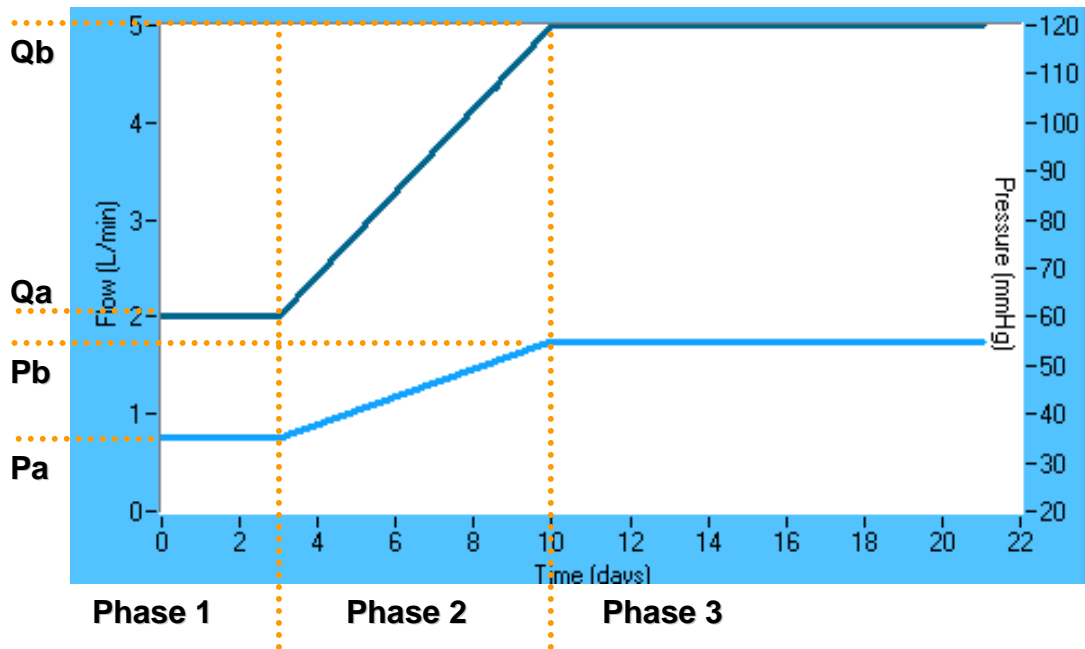


Figure 29 Partial screen capture of the flow loop software showing the mean pressure and flow vs. time protocol where: initial and final mean pressure, Pa and Pb; initial and final mean flow rate, Qa and Qb; initial phase, Phase 1; ramping phase, Phase 2; and final phase, Phase 3

In the event of a system malfunction where mean pressure and/or mean flow can no longer be accurately maintained, as would happen if there was a leak, a problem with the air line, structural valve failure, etc..., the control code will automatically stop the actuation of the system. It does this by having the user input limits on the mean pressure and flow errors from the command, ΔP and ΔQ , and if these limits are exceeded for a user defined period, the system will change the control voltage to 0 V thereby halting actuation. The data acquisition portion of the code will continue to run since the acquired data could be helpful in failure analysis.

2.1.2.4 Data Acquisition Pressure and flow data are acquired at a frequency dependant on heart rate which ensures that 4 beats are always acquired regardless of the heart rate. This is easily accomplished since the heart rate, or period, is already controlled by software. Mean pressure and flow data are the given as the average of these 4 beats. The rate at which the data is saved to

file is user defined due to the fact that tests could be quite long (weeks) and generate large file sizes. Two separate files are generated, one with extracted pressure and flow data (mean, max, min), stroke volume, heart rate, target pressure and flow, and another file that consists of the waveforms of outflow valve pressure & flow, ventricular pressure, and driving voltage.

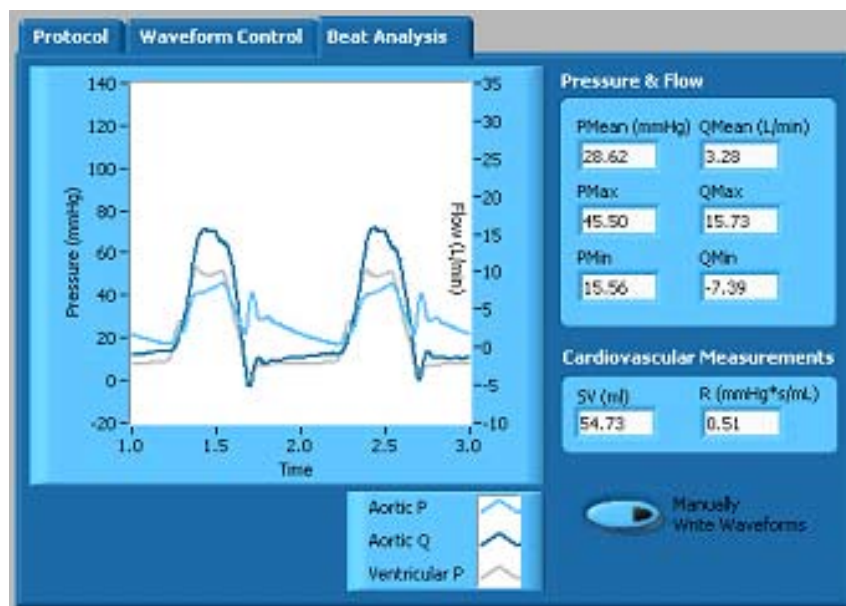


Figure 30 Screenshot of the flow loop software showing acquired waveforms and displaying various measured parameters

2.1.3 Tissue Engineered Heart Valve Design

2.1.3.1 Scaffold Design The TEHV outflow valve that was used for the sterility challenge, TEHV#1, and the valve used in the TEHV ramped flow study, TEHV#2, were constructed from a non-woven 50:50 blend PGA/PLA (Albany International Research, Mansfield, MA) scaffold approximately 2 mm thick. TEHV#1 was constructed out of 2 layers of scaffold material stitched together along the edges while TEHV#2 was constructed from 1 layer. This was due to the results of TEHV#1 showing the two layers delaminated after incubation.

The geometry of the valve was determined by first constructing a valve with rectangular leaflets (28 mm x 25 mm) that had a straight free edge out of a thin latex sheet (~0.3 mm) and suturing it in the TEHV holder which recreates the dimensions of the valve designed for the sterility challenge, TEHV#1. This valve was run in the loop at various hemodynamic conditions and its open and closing behavior, leaflet flutter and extent of opening, was qualitatively evaluated and recorded onto digital video (9000, Sony). An examination of the literature [9] provided useful native valve leaflet geometry which suggested that the length of the leaflet from base to center of free edge should be roughly 70% of the valve diameter. The latex valve was modified by cutting away excess leaflet, as shown below, and then re-evaluating it. Both the amount of flutter and degree of opening appeared to be improved. It was this valve design that was duplicated for use as the TEHV design for the TEHV ramping study explained below, TEHV#2.

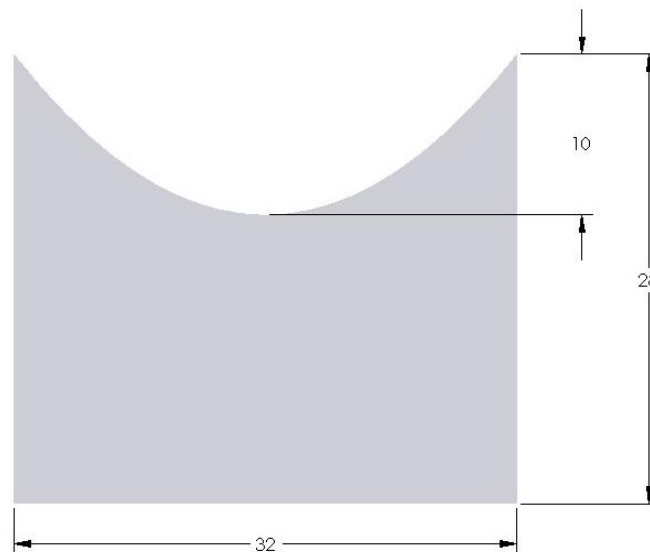


Figure 31 Diagram showing the geometry (in mm) of a single TEHV leaflet in the TEHV#2 design. TEHV #1 featured the same height and width dimensions without the parabolic cutout

2.1.3.2 Cell Expansion and Scaffold Seeding The seeding apparatus and methods used in this study were adapted from Sutherland et al [64] and Nasser et al [65]. One vial of vascular smooth muscle cells (SMC) (approximately 7.5×10^6 cells, passage 9) cryo-preserved in culture medium supplemented with 5% dimethyl sulfoxide (DMSO; Sigma, St. Louis, MO) was thawed, resuspended in culture medium, and plated into three 185 cm² flasks (Nuclon™Δ SoLo flask; Nalgene Labware). After 3 serial 1:3 passages (approximately 28 days), a total of 54 confluent 185 cm² flasks (passage 13) were ready for use. The flasks were trypsinized (0.25% trypsin, 1 mM EDTA; GIBCO™), and the SMC were resuspended to yield a seeding solution of approximately 8×10^6 cells/ml, as determined by cell counts with a hemacytometer (Hausser Scientific, Horsham, PA).

Each valve was seeded with ovine vascular smooth muscle cells ($\sim 17 \times 10^6$ cells/cm², starting passage number 9, final passage number 13). The culture media was Dulbecco's modified eagles medium containing 4.5 g/L glucose, L-glutamine (#11965, Invitrogen, Grand Island, NY) with 10% fetal bovine serum (#16000, Invitrogen) added 1% antibiotic-antimycotic (#152400, Invitrogen) containing penicillin, streptomycin, and amphotericin, and 2 ng/ml human recombinant basic fibroblast growth factor (bFGF, BD Biosciences, Bedford, MA) as well as phenol red for visual pH estimation. The cell-seeded valves were incubated for 7, TEHV#1, and 10 days, TEHV#2, prior to testing at 37°C and 5% carbon dioxide in a 140 cc hybridization tube (Pyrex, Corning, Corning, NY) with a vented filter cap on a rotisserie at 8 rpm (Labquake rotisserie rotator, Barnstead-Thermolyne, Dubuque, IA) in 90 ml of media that was changed daily.



Figure 32 Tissue engineered heart valve, TEHV#2, after rotisserie incubation

2.2 HYDRODYNAMIC TESTING

Aspects of system response time, stability, and control were tested as well as the system's ability to produce physiologic waveforms with water as the circulating media. Pressure sensors were first placed in the incubator overnight in order to heat to 37°C. They were then calibrated with a mercury manometer (Baumanometer, Baum) using measurements taken at 40, 80, and 120 mmHg. The scales were found to be very similar with slope of 6.4 to 6.5 mmHg/mV. Given the low output of the pressure sensors, the programmable gain functionality of the DAQ board was used to maximize the resolution. The ultrasonic flow meter was calibrated at the factory at 37°C. This was verified by attaching it to a tube connected to a lab faucet. The temperature of the water was adjusted roughly to 37°C and the flow was collected in a graduated cylinder while the elapsed time was recorded with a stop watch.

2.2.1 System Calibration, Response, and Stability

In order to first tune the system response time, a step pressure and flow test, 3 to 3.5 lpm at 30 to 40 mmHg, was run and control voltage & resistor tuning parameters were adjusted until a fast and stable system response was achieved. System stability was addressed by running two constant set point tests of 5 lpm mean flow (MF) at 30 mmHg mean pressure (MP) and 1 lpm at 35 mmHg for 16 hrs each.

2.2.2 Control and Flexibility

System control and flexibility was tested by performing two series of gradual ramp tests at high and low flow rates. For the high flow rate series, MP was gradually increased from 30 to 40 mmHg and back while MF was held at a constant of 4 lpm (Fig. 37a). Next MF was gradually increased from 4 to 5 lpm and back while MP was held at a constant of 30 mmHg (Fig. 37b). Finally both MP and MF were increased and decreased at the same amounts as the prior ramp tests (Fig. 37c). For the low flow rate series, MP was gradually increased from 25 to 35 mmHg and back while MF was held at a constant of 1 lpm (Fig. 38a). Next MF was gradually increased from 1 to 2 lpm and back while MP was held at a constant of 25 mmHg (Fig. 38b). Finally both MP and MF were increased and decreased at the same amounts as the prior ramp tests (Fig. 38c).

2.2.3 Waveforms

The system was tested to see if it could produce reasonably accurate physiological waveforms of both aortic and pulmonary circulations. The beat frequency was set at 60 BPM and the MF at 5 lpm for both cases while MP was 105 mmHg (systolic/diastolic pressures of 125/85 mmHg) for the aortic case and 27 mmHg (systolic/diastolic pressures of 35/20 mmHg) for the pulmonary

case. The waveforms were analyzed with a custom Matlab script (Appendix C) which calculated the input-impedance spectrum (magnitude and phase), and the forward and backward waveforms as previously discussed.

2.3 TESTS OF BIOLOGICAL RELEVANCE

2.3.1 Sterility

A 21 day test of system sterility was performed using culture media and TEHV#1 as previously described. The system was sterilized with ethylene oxide gas before loading the valve. The incubation conditions were 37°C, 5% carbon dioxide, and 21% oxygen. During rotisserie culture it was found that the rate of media consumption was approximately 90 ml per day and accordingly, 2 L of media was used to fill the system initially and at no other time was media was added or removed. The mean flow and pressure was set at 2.5 lpm at 40 mmHg. Sterility was macroscopically qualified by daily inspection of the media and also at the test conclusion by disassembling the device and inspecting each part for bacterial, mold, or fungal colonies.

2.3.2 Measuring Dissolved Gases and pH

It is known that a stagnant fluid will have will have gas mass transport rate that is diffusion limited while a well-mixed fluid will have a mass transport rate that is limited by convection. In between the stagnant and well-mixed situations, gas tension of a particular species will be a function of the degree of mixing, or in the case of the pulsatile bioreactor, the mean flow rate. Dissolved oxygen and carbon dioxide gas tensions as a function of mean flow rate were measured using a blood gas analyzer (ABL 5, Radiometer, Radiometer America, Westlake, OH)

with samples drawn from the ventricle's luer port. Two separate tests were run with water first and then culture medium as the circulating fluids in the pulsatile bioreactor at incubator settings of 5% carbon dioxide and 37°C.

The water test was conducted first to determine only the general oxygen tension and flow rate relationship running the pulsatile bioreactor at mean flow rates of 3.5, 2, 1, and 0 lpm at an incubator oxygen setting of 21% (room oxygen level). Oxygen tension was also measured in the lab's flexure bioreactor, which has been demonstrated to effectively grow engineered tissues, to serve as a comparison [36]. Carbon dioxide values are not particularly important for the water case since it is known that carbon dioxide is 24 times more soluble than oxygen in water. pH can not be accurately measured since the blood gas analyzer is calibrated to measure pH between 7 and 8 pH units. This too is not important for the water case since the pH buffering ability of the media will be of much greater effect and importance. The water test was then repeated at an incubator oxygen setting of 35% to measure the effect of enhanced gas partial pressure on the general oxygen tension and flow rate relationship. The time in between gas measurements was no less than 2 hours and the amount of fluid within the circuit was approximately 2.5 L and the atrium was kept near full to ensure maximum diffusion distance. 3 samples were taken for each test and the average is reported.

Below is a picture of phenol red which is present in the culture medium giving it its red color. Phenol red is an acid-base indicator useful near physiologic pH (7.4) and can be used to visually detect relatively large changes in pH of ± 0.5 . Clearly, pH must be measured with means such as those described here to obtain accurate and precise pH measurements. Unlike the water test, measured pH and carbon dioxide concentrations are needed since pH is buffered in the medium by sodium bicarbonate and modulated by carbon dioxide concentration. The media test

was then conducted to determine only the relationship of the dissolved gas tensions and pH at low flow rates, 1.0, 0.5, and 0 lpm, since that was found to be transition region between the diffusion and convection limited cases in the water tests. The incubator's oxygen setting was kept at 21% (room oxygen level).



Figure 33 Picture showing the acid-base indicating ability of phenol red which is present in the culture medium. Note physiological pH is approximately 7.4. pH levels have to change at least 0.5 pH units before a noticeable change in pH can be detected.

2.3.3 TEHV Ramped Flow Study

A 5 day test was conducted to demonstrate the ability of the pulsatile BAHV bioreactor to subject a TEHV, TEHV#2 as previously described, to a gradually ramped mean flow rate at a constant pressure over the course of 4 days. On day 1, the valve was subjected to mean pressure and flow levels of 1.5 lpm at 40 mmHg and starting on day 2 the flow was gradually increased to 2 lpm until the 5th day. 1.5 lpm was used as the initial flow rate since that is the minimum flow rate that produced physiologically shaped pressure and flow waveforms. At the conclusion of the test, valve tissue composition was examined for collagen content. Additionally, the device was examined for signs of contamination in the same manner as previously discussed.

2.3.4 Tissue Analysis

Collagen was assayed by techniques adapted from Brown et al [66]. 3 samples (~ 16 x 4 x 1 mm, average wet weight 0.05 g) were cut from each leaflet: near the free edge, at the belly region, and at the basal stent region as shown below. Total collagen was extracted from samples using a solution of 0.5 M acetic acid (Sigma) and pepsin (1 mg/ml Pepsin A (P-7000); Sigma). Each sample was placed in a microcentrifuge tube and incubated in 1 ml of extraction solution overnight (~ 16 hours) on a rocker table (Orbitron Rotator I™; Boekel Scientific, Feasterville, PA) operating inside a refrigerator at 2-8°C. Following the extraction steps, the collagen extracts were assayed according to the guidelines provided with the Sircol™ assay kit (Biocolor Ltd., Newtownabbey, N. Ireland) using a Genesys 20 spectrophotometer (Thermo Spectronic, Rochester, NY).

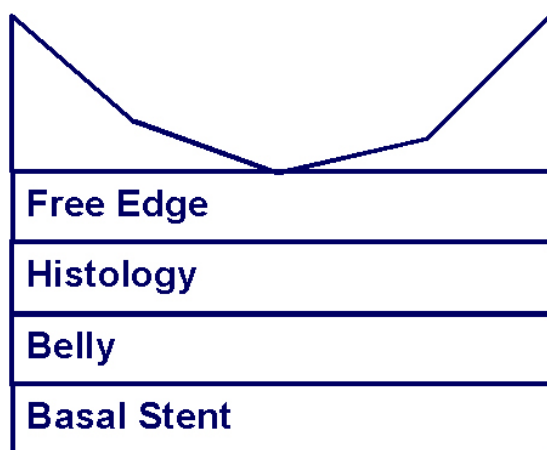


Figure 34 Sectioning diagram for performing collagen analysis. 3 sections per leaflet were used for evaluation: near the free edge, belly region, and a basal region sewn to the stent.

3.0 RESULTS

3.1 HYDRODYNAMIC STUDIES

3.1.1 System Response & Stability

The response time, or the amount of time it took the system to go from the baseline level of 3.0 lpm MF at 30 mmHg MP to a stable elevated level of 3.5 lpm at 40 mmHg, was less than sixty seconds. The results of the stability tests (average \pm standard deviation) showed a stable reading of 5.00 ± 0.06 lpm at 30.00 ± 0.04 mmHg and 1.00 ± 0.02 lpm at 35.00 ± 0.07 mmHg with maximum absolute values of the command errors of 0.15 lpm for MF and 0.21 mmHg for MP for the high flow rate test and 0.06 lpm for MF and 0.22 mmHg for MP for the low flow rate test.

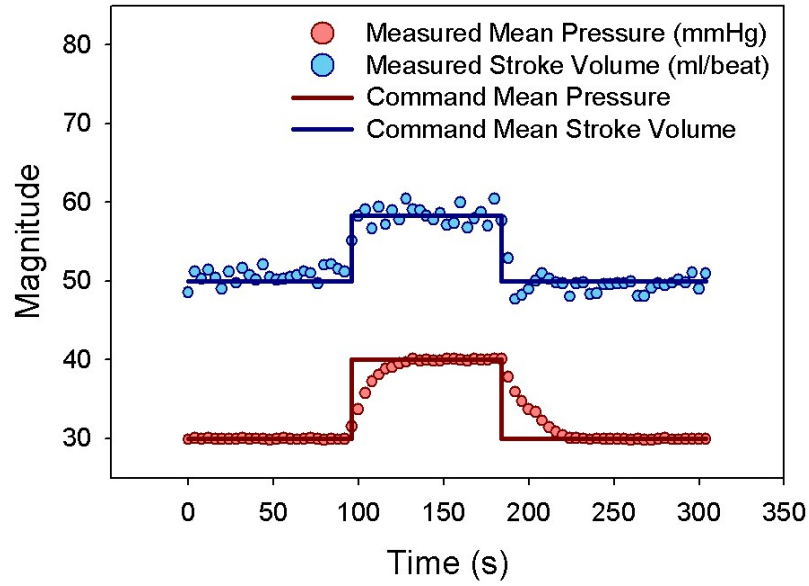


Figure 35 Results of the system response test: mean pressure and mean flow were stepped from 3.0 lpm at 30 mmHg to 3.5 lpm at 40 mmHg. Note the critically damped behavior of the mean pressure solution

3.1.2 System Control and Flexibility

Control and flexibility results for the high flow rate series showed that system followed the command signal strongly with command errors of 0.00 ± 0.27 mmHg and 0.00 ± 0.05 lpm. The maximum absolute values of command errors were 0.18 lpm and 0.83 mmHg. Results of the low flow rate series showed that system followed the command signal strongly with a mean and standard deviation for the command errors of 0.00 ± 0.12 mmHg and 0.00 ± 0.03 lpm. The maximum absolute values of command errors were 0.10 lpm and 0.32 mmHg. In both series, the command errors for both pressure and flow passed the Kolmogorov-Smirnov test [67] for following a normal distribution.

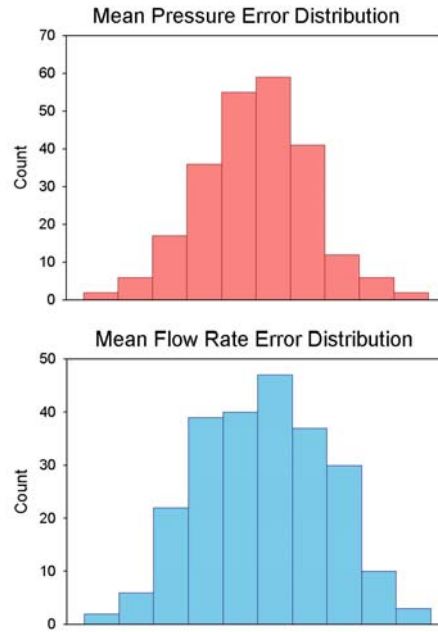


Figure 36 Histograms of the mean pressure and flow rate errors from the input (command) for the high flow ramped pressure and flow studies with a bioprosthetic valve. Both passed the Kolmogorov-Smirnov test [67] for following a normal distribution.

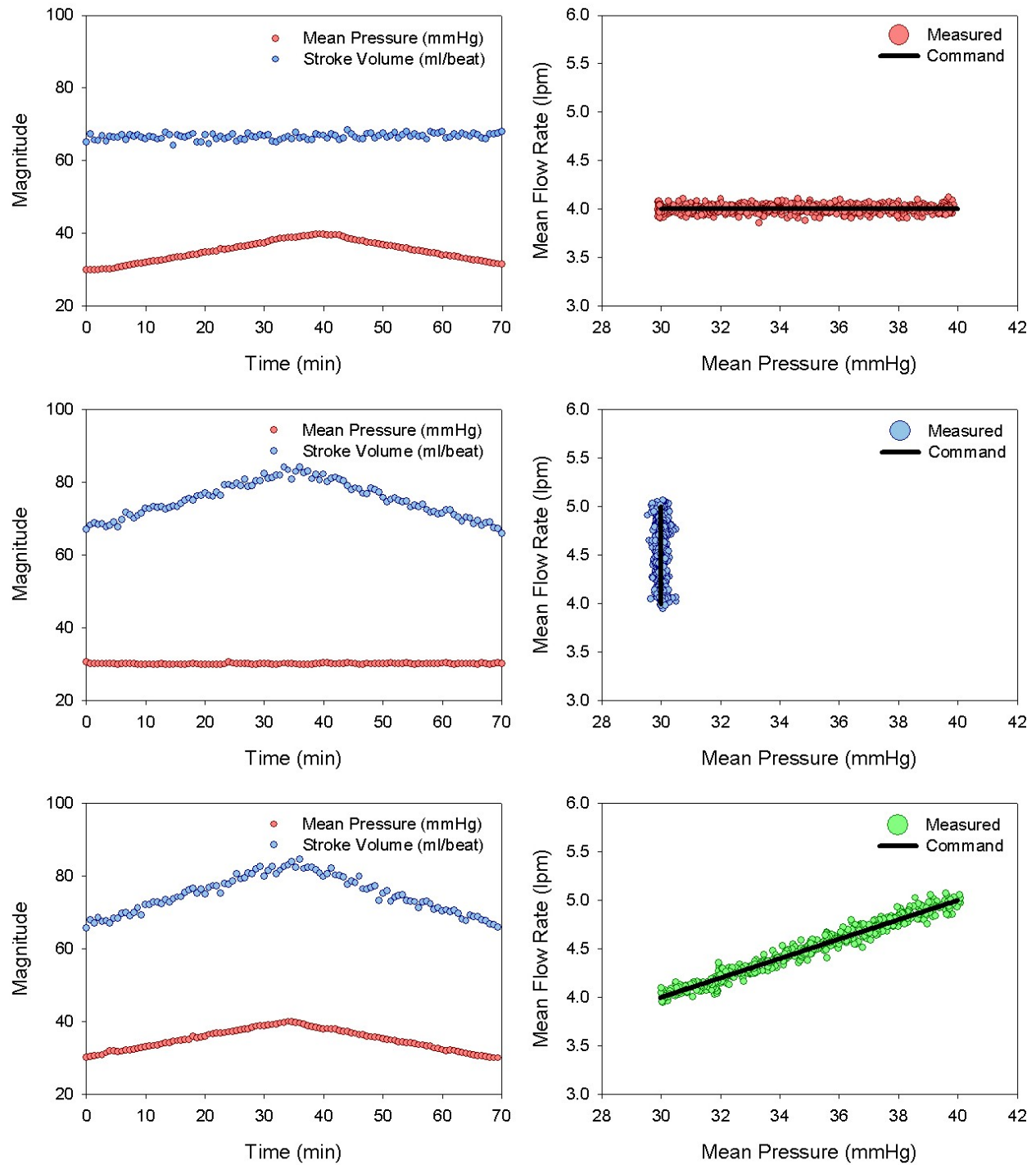


Figure 37 High flow hydrodynamic control tests: ramped mean pressure test (a), ramped mean flow test (b), ramped mean pressure and mean flow test (c). All tests are run at 60 bpm

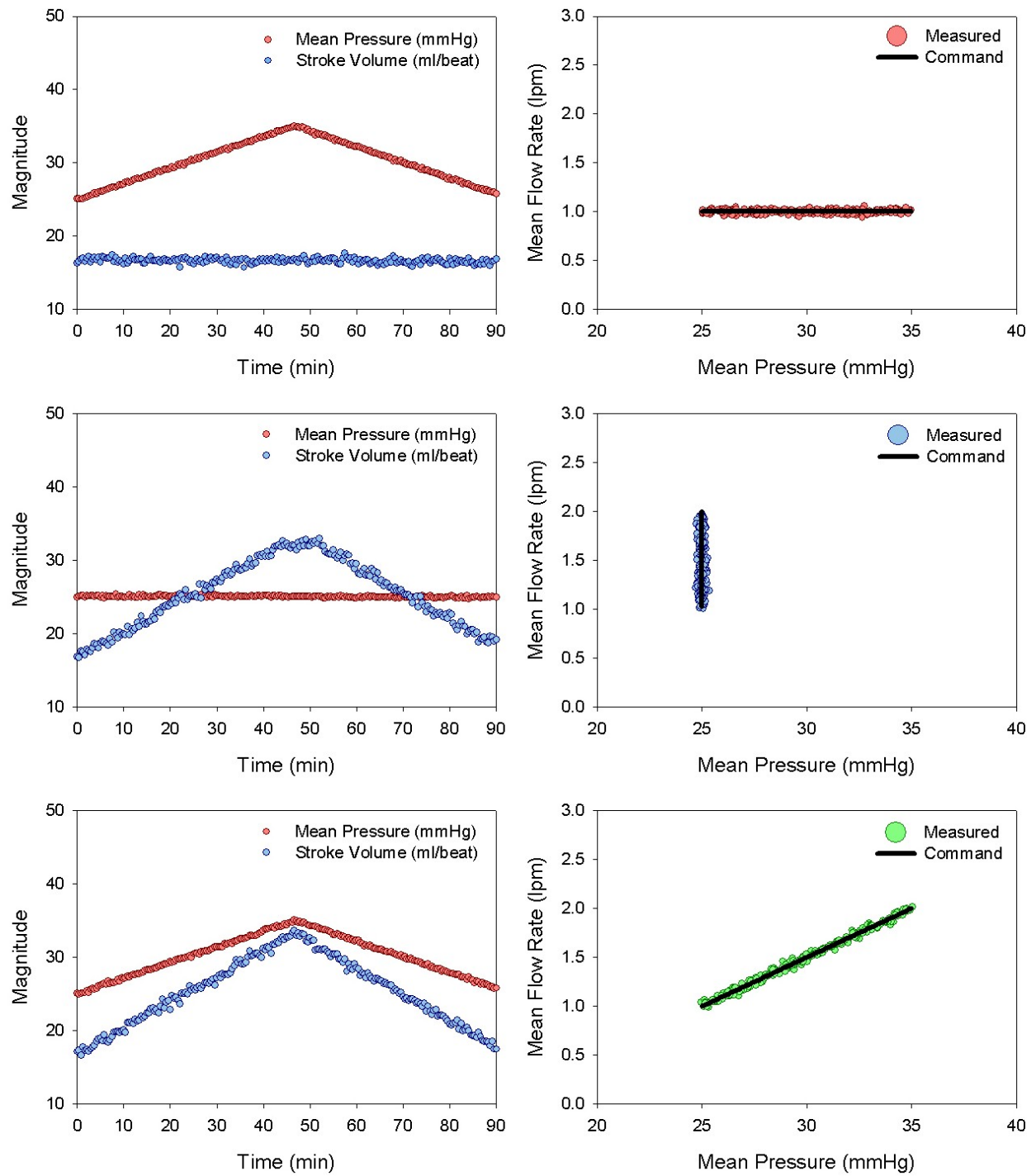


Figure 38 Low flow hydrodynamic control tests: ramped mean pressure test (a), ramped mean flow test (b), ramped mean pressure and mean flow test (c). All tests were run at 60 bpm

3.1.3 Waveforms

Resulting waveforms of the device running at pulmonary and aortic pressures and flows are shown in Figure 39, Figure 40, and Figure 41. The waveforms exhibit both similarity to physiologic waveforms as seen in the input-impedance spectrum in Figure 40 and Figure 41. The waveforms also exhibited strong beat-to-beat similarity with mean differences of 0.37 mmHg and 0.48 lpm with the largest beat-to-beat differences taking place in the first 0.5 s after valve closure (Figure 39). Mean pressure and mean flow for the aortic case was 105 mmHg and 5 lpm, and 28 mmHg and 5.14 lpm for the aortic and pulmonary circulations, respectively. The calculated peripheral resistances are then 1.26 and 0.33 mmHg s ml⁻¹ and the characteristic resistances are 0.2 and 0.15 mmHg s ml⁻¹ for the aortic and pulmonary circulations, respectively. Compliances of 1.35 and 2.98 ml/mmHg for the aortic and pulmonary circulations, respectively, were also calculated with the Matlab script in Appendix C.

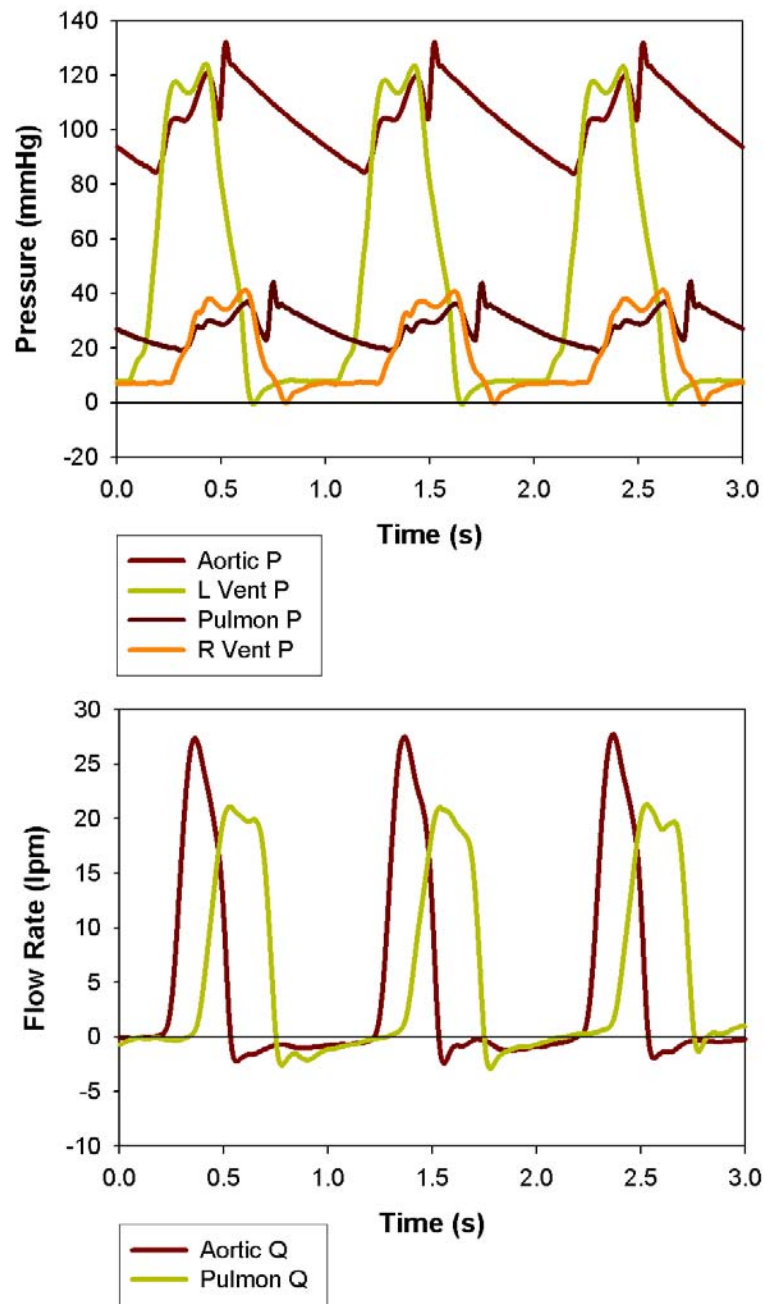


Figure 39 Acquired physiologic waveforms at 60 bpm: pressure (mmHg) and volumetric flow (lpm)

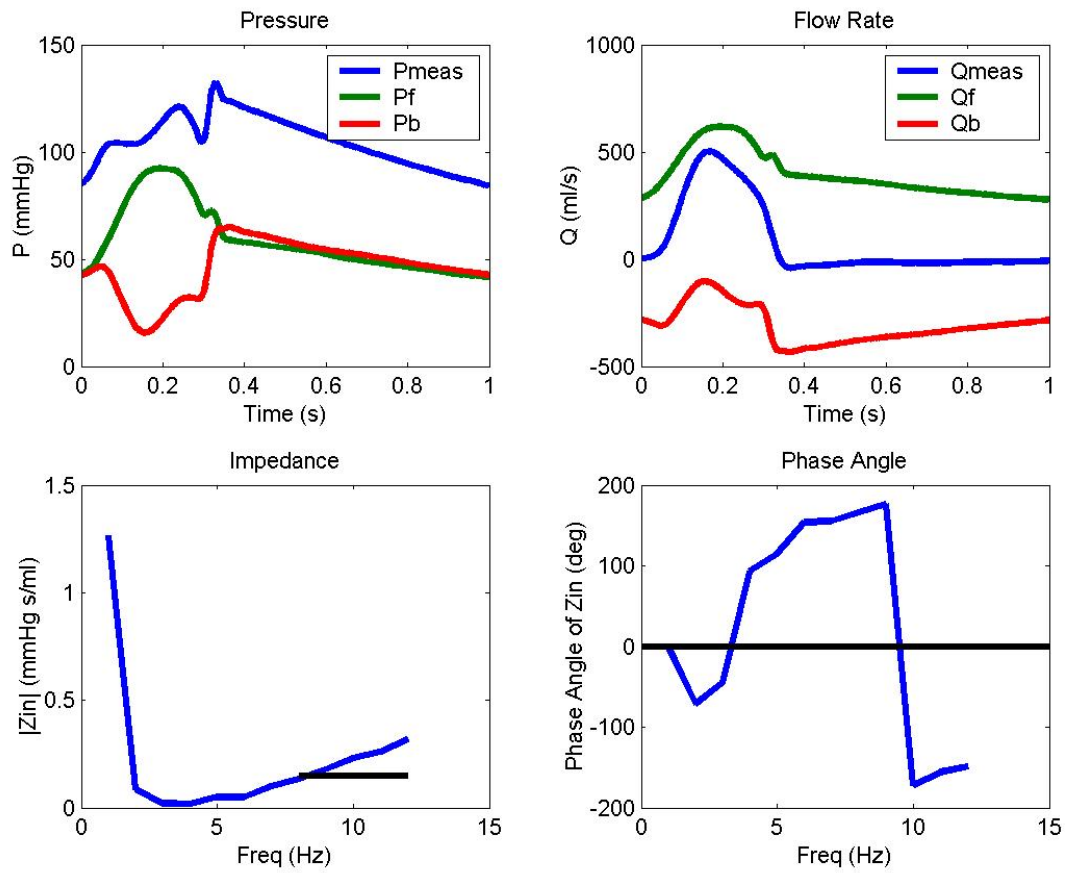


Figure 40 Analysis of the aortic waveform produced by the pulsatile bioreactor: measured, forward, and backward pressure and flow waveform components, a & b; impedance spectrum, c; phase angle, d. The black line in the impedance magnitude plot shows the average of the 8th-12th harmonics.

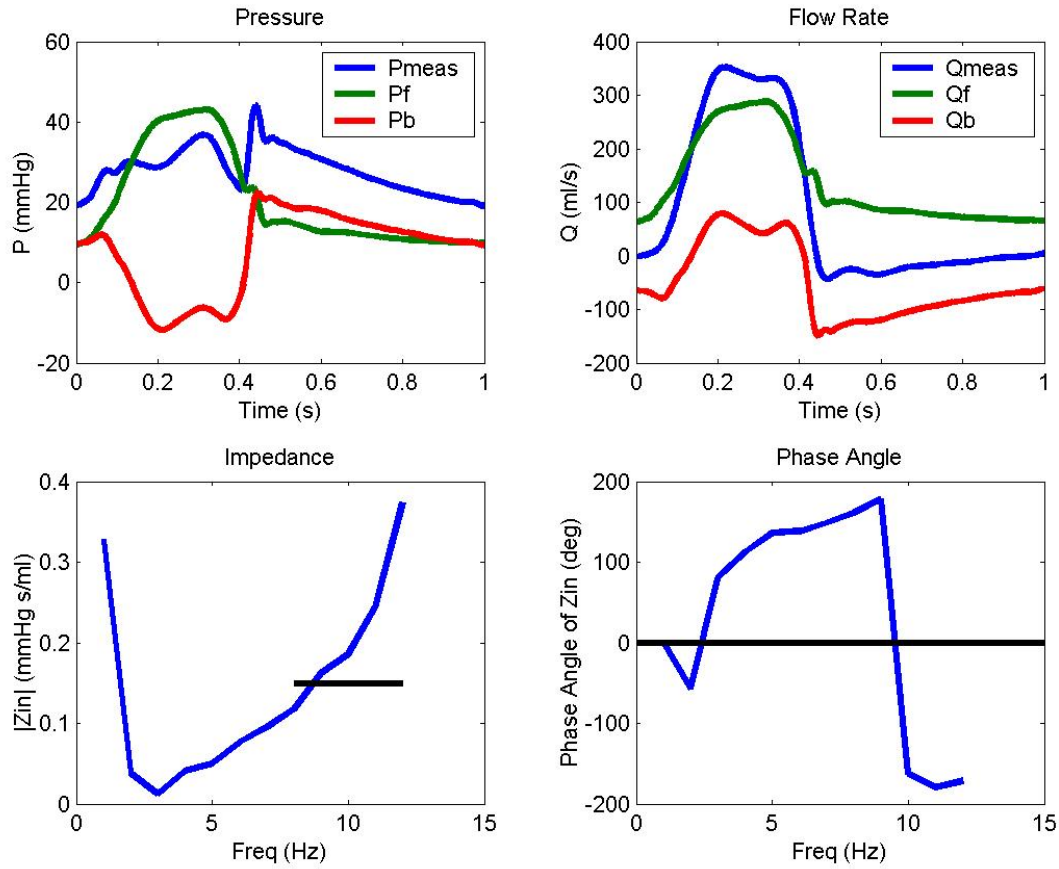


Figure 41 Analysis of the pulmonary waveform produced by the pulsatile bioreactor: measured, forward, and backward pressure and flow waveform components, a & b; impedance spectrum, c; phase angle, d. The black line in the impedance magnitude plot shows the average of the 8th-12th harmonics.

3.2 TEHV FEASIBILITY STUDIES

3.2.1 System Sterility

The valve, TEHV#1, suffered a leaflet tear at the basal attachment during the night on day 19. Due to this failure, the hemodynamic waveforms became irregular with regurgitant flow and pressure oscillations. The system attempted to maintain target pressure and flow conditions, but was unable due to the tear, which greatly lowered mean pressure and flow rates. This resulted in

the system going into standby mode as expected. Examination of the data indicates that the valve was probably exposed to zero flow conditions for approximately 12 hours. When the device was checked in the morning, the target flow rate was set to 1.3 lpm so as not to further damage the valve and to circulate fluid. The media was examined daily for turbidity, and after a total of 21 days, the device was removed from the incubator, the media was drained, and the valve and components were macroscopically examined for signs of contamination such as bacterial or fungal colonies. Every component was disassembled and inspected and no signs of contamination were found as was the case for the valve.

3.2.2 Gas Concentrations and pH

The water test at an incubator oxygen setting of 21% showed that oxygen tension was greater than 140 mmHg at flow rates of 3.5 to 1.0 lpm. The oxygen tension dropped to 80 mmHg when the loop was stagnant (0 lpm). Increasing the incubator oxygen setting 14% to 35% uniformly raised the tension 14 mmHg yielding values of 154 and 94 mmHg for the 3.5 -1.0 lpm and stagnant conditions respectively.

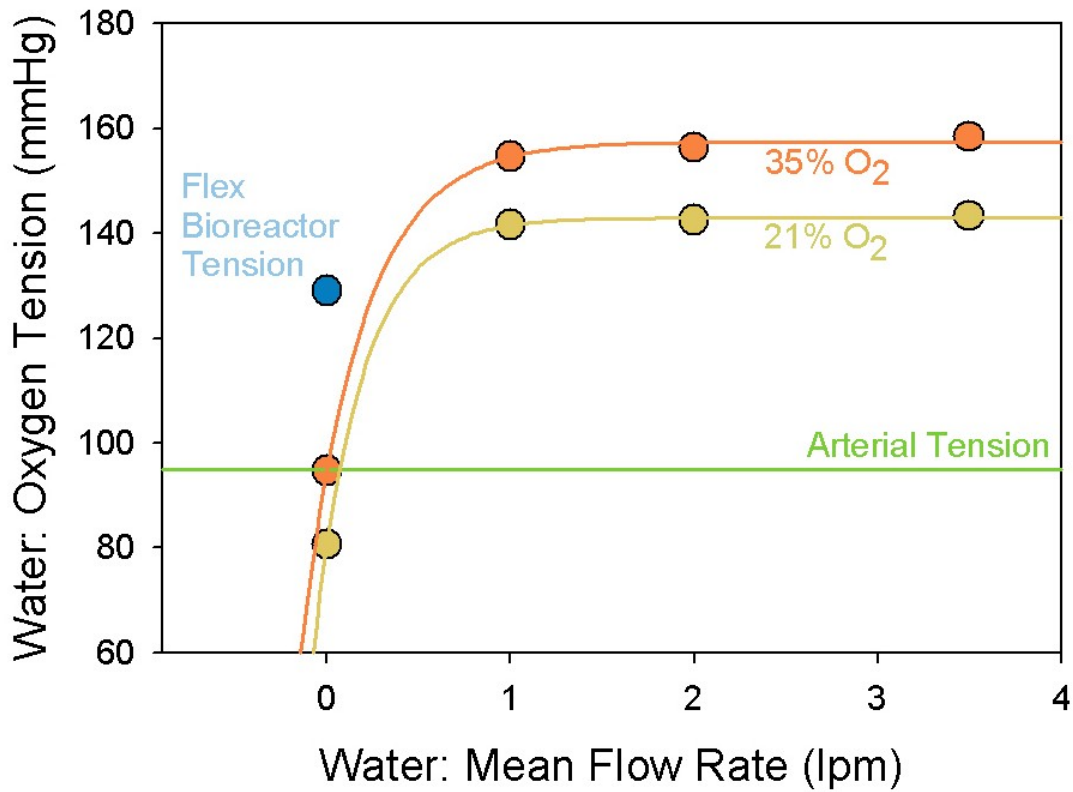


Figure 42 Dissolved oxygen tensions as a function of flow rate and incubator oxygen % in water

For the test using culture media, it was decided to only investigate flow rates below 1 lpm since that was found to be the area of greatest change in oxygen tension in the water experiment. The oxygen tension appeared to decrease fairly linearly from 120 to 40 mmHg from 1 to 0 lpm although with only three measured flow rates, this relationship is at best only a first approximation. The ratio of pH to carbon dioxide tension did not appreciably change and the measured pH was between 7.45 and 7.47 which is only 0.02 pH units above the normal physiologic pH range of 7.35-7.45 [68].

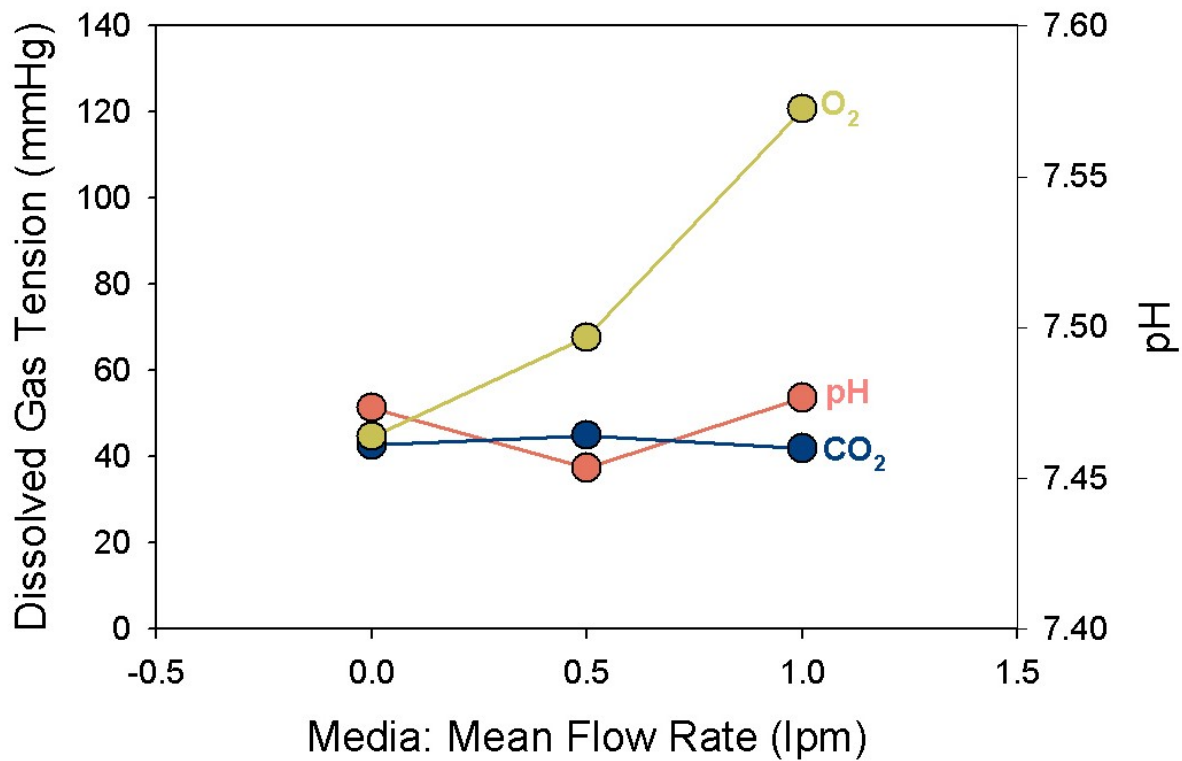


Figure 43 Dissolved gas concentrations and pH as a function of mean flow rate in culture medium. Incubator conditions were standard 37C, 21% O₂, and 5% CO₂

3.2.3 TEHV Ramped Flow Study

3.2.3.1 Pressure and Flow Control The system showed excellent control of pressure and flow, until a leaflet tear, with a narrow distribution of errors shown below. The errors from command were found to be (mean \pm standard deviation) 0.00 \pm 0.08 mmHg and 0.00 \pm 0.03 lpm. The valve, TEHV#2, suffered a leaflet tear along the free edge of one leaflet during the night on day 4, approximately 4.7 days into the test. As with valve TEHV#1, the hemodynamic waveforms became irregular, with regurgitant flow and pressure oscillations. The system attempted to maintain target pressure and flow conditions, but was unable due to the tear which greatly lowered mean pressure and flow rates. This resulted in the system going into standby mode as

expected. Examination of the data indicates that the valve was probably exposed to zero flow conditions for approximately 12 hours. For the remaining hours of the test, the target flow rate was set to 1.0 lpm so as not to further damage the valve and to circulate fluid. After a total of 5 days, the device was removed from the incubator, the media was drained, and the valve and components were examined for signs of contamination such as bacterial or fungal colonies. Every component was disassembled and inspected and no signs of contamination were found as was the case for the valve.

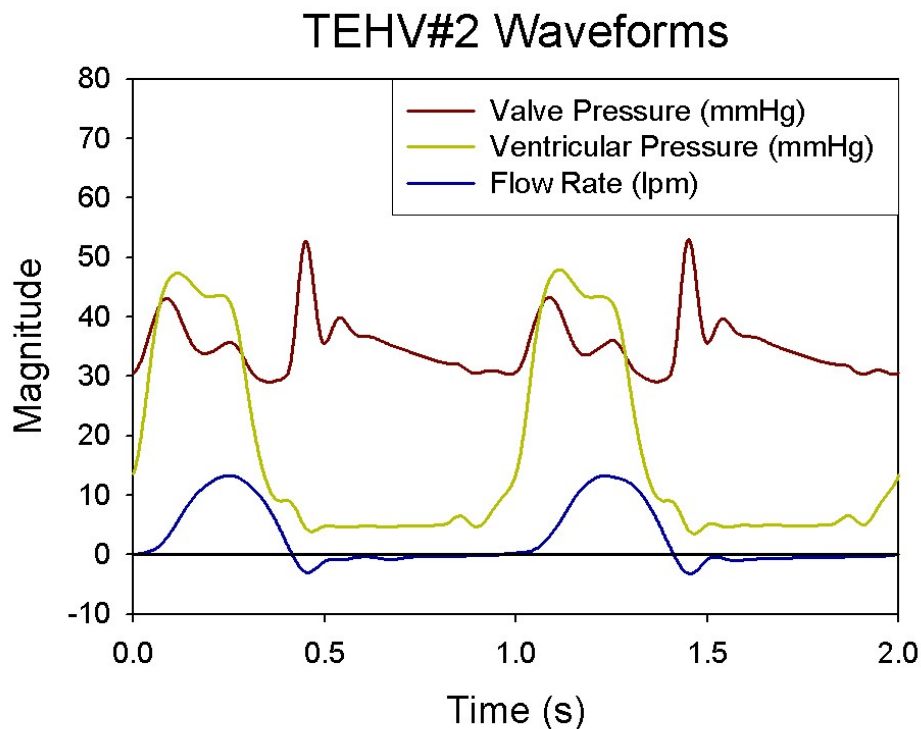


Figure 44 Measured pressure and flow waveforms for TEHV#2

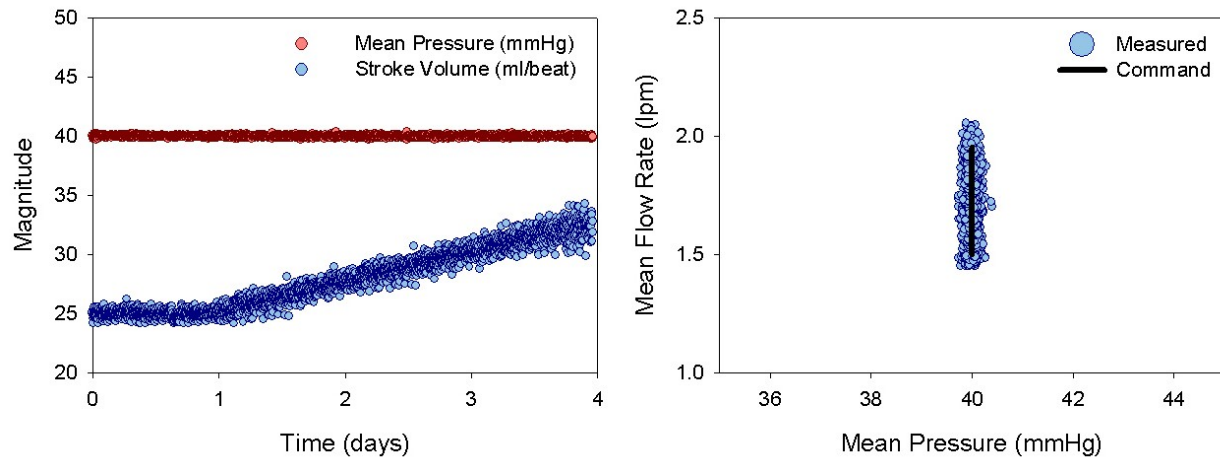


Figure 45 Mean pressure and flow data for the ramped flow TEHV study until system went on standby due to leaflet tear

3.2.3.2 Tissue Analysis Collagen concentration within the leaflets (n=3) was found to be very high overall with average concentrations ranging from the basal stent to free edge of 1200 to 1800 μg collagen/g wet weight as shown below. The collagen concentration in the leaflets appears to be non-homogenous and increases with distance away from the basal stent attachment.

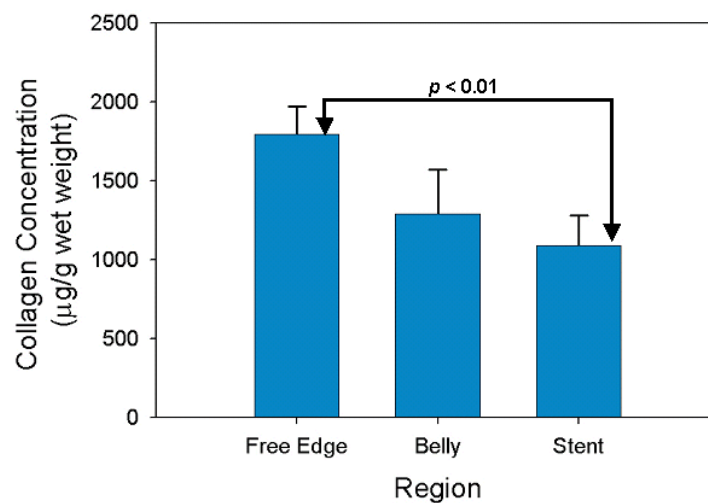


Figure 46 Collagen concentration as a function of location in the leaflet (n=3). There was found to be a significant difference between the amount of collagen within the free edge and at the portion attached to the stent ($p < 0.01$).

Table 3 Summary of tests performed during the evaluation phase of the study

Test Name	Purpose	Valve Design	Fluid	Duration	Qualitative Description of Results
Response	Tune system mean P&Q behavior	Biopros	Tap Water	~ 4 min	System capable of fast & stable mean P and Q control Critically damped mean P response
Stability	Single set pt control	Biopros	Tap Water	15+ hours per test	High long term system stability
Flexibility and Control	Evaluate feedback control scheme	Biopros	Tap Water	~3 hours per test	Excellent accuracy and precision of controller
Waveforms	Produce physiologic P&Q waveforms	Biopros	Tap Water	~ 5 min	Good approximation to physiologic waveforms Strong beat-to-beat similarity Increased upper harmonic content probably due to non-compliant root and sinus
Sterility	Check for gross contamination	TEHV#1	Culture Media	21 days	No evidence of contamination Day 19: Scaffold tear near basal suture attachment on one leaflet leading to probably hypoxic media conditions for ~12 hours
Gasses and pH	Measure gas tensions and pH vs. flow rate	Biopros	Tap Water, Culture Media	At least 2 hours between data pts	O2 tension falls beneath physiologic at low flow rates (<1 lpm) pH (and CO2) remain constant
Ramp Flow w/ Collagen Analyses	Preliminary TEHV test under increasing flow	TEHV#2	Culture Media	5 days	Collagen concentration increases from basal stent to free edge Day 5: Scaffold tear near free edge of one leaflet leading to probably hypoxic media conditions for ~12 hours

4.0 DISCUSSION

4.1 STUDY FINDINGS

4.1.1 Hydrodynamic Performance

The series of studies presented herein were aimed at evaluating the performance of a new pulsatile bioreactor designed for investigating the effects of highly controlled modulations of pulsatile pressure and/or flow on biological tissues. Unique features of the system are a robust control system that utilizes a variable resistance, which can be accurately controlled over a working range of approximately 0.25 to 1.2+ mmHg s ml⁻¹, combined with a pneumatic driver capable of producing well-defined pressure waveforms. The system features a working mean pulsatile pressure range of 15 to 100+ mmHg and a working mean flow rate range of 0-5+ lpm. This produces a system which is capable of running under a wide array of non-physiologic as well as physiologic conditions. The higher than physiologic upper waveform harmonics are most likely due to the use of a rigid sinus rather than an elastic sinus. Whether or not these frequencies have a substantial impact on the hemodynamics is unknown, but previous studies [69, 70] have shown that an elastic sinus can produce a more physiologically accurate valve opening and flow field. The system control and flexibility tests show normally distributed errors with zero means and low standard deviations for both pressure and flow demonstrating the high level of accuracy and precision the control system can achieve. This aspect of the system is critical for studies

where significant differences in cellular function could be dictated by small changes in hemodynamics.

The system has demonstrated a level of hydrodynamic control that exceeds that of all other published pulsatile bioreactors [1, 2]. Unlike these more simplistic bioreactors, this newly created pulsatile bioreactor can control for mean pressure and flow, generate physiologic mean flows (>5 lpm), has an adjustable compliance element, and is capable of generating the pressure and flow waveforms that mimic both the systemic and pulmonary circulations. Our pulsatile bioreactor makes it possible for the first time to perform a controlled study on the effects of dynamically modulating mean pressure and flow during pulsatile culture of biologically active heart valves.

The following parameters are available for automatic control: mean pressure, mean flow rate, beat frequency (HR), stroke volume, and the shape of the driving pressure waveform. Further control of the systolic/diastolic pressure ratio, or pulsatile pressure response, is possible with manual compliance adjustments. Shear stress on the valve can be controlled by adjusting the flow rate and/or by changing the viscosity of the media with the addition of chemicals such as dextrose. Modulating these parameters would in effect modulate the mechanical stress environment the developing valve is exposed to during culture.

4.1.2 Biological Performance

Biologically, the system demonstrated that it could provide suitable, sterile environmental conditions. Carbon dioxide tension and pH were found to be invariant of flow. Using standard incubator settings (5% CO₂), the average pH was found to be 7.45 which is in line with physiologic pH. Proper oxygen tension could be maintained provided the flow rate was kept at or

above 1 lpm. Since the scaffolds tore, forcing the system to go into zero flow standby mode, the oxygen tension presumably dropped to low levels (~ 40 mmHg) during this time. Whether or not this oxygen tension is low enough to cause cell death is unclear. It is important to note that the low oxygen tension is not a result of device failure but it is rather a failure of the scaffold material and/or valve design, which are not related to the completion of the aims of this study. The device functioned exactly as designed throughout the experiments until the TEHV material itself failed. This material failure is probably due to the inelastic nature of the non-woven scaffold materials [71] which exhibit permanent deformation under mechanical loading [32] and can pull away from attachment points (sutures) over time.

With only one valve tested, it is impossible to make meaningful comparisons to the study by the Mayer group [5, 27], but several differences between the study methods can be noted. The scaffold used in their study was a rapidly degrading PGA scaffold whose degradation rate is on the order of 2 weeks. The study reported by the end of 4 weeks, the scaffold was completely absent from the tissue. By the end of their incubation period of 2 weeks, it is very likely that the scaffold was not functional from a structural perspective. Our study used a much slower degrading PGA/PLLA scaffold that retains its structural integrity for at least 8 weeks. The inelastic nature of these scaffolds combined with the non-woven construction results in permanent material deformation under cyclic strains [32]. Until the PGA/PLLA scaffold degrades and the cells have formed an adequate ECM, the construct will continue to largely behave as an inelastic body and continue to deform as dynamic incubation continues which is what probably lead to the tears associated with the TE valves in the study.

Another important difference in their study was the flow magnitude used was initially 0.125 lpm and was increased to 0.75 lpm [5]. The choice of these flows were not given. The final flow

rate that was used by their group is half the initial flow rate used in our studies of 1.5 lpm. As previously discussed, the 1.5 lpm flow rate was chosen because that was the minimum flow rate that produced a physiologically shaped waveform. A lower flow rate would cause pressure and flow oscillations due to improper valve closure. The pressure and flow waveforms were never measured in the Mayer studies, but based on their bioreactor design and the reported driving pressure waveform, it is likely that their pressure and flow waveforms were highly unphysiologic in shape and was thought by our group to be less than ideal for proper development. Whether or not the high flow rate in our study also contributes to early scaffold structural failure is as yet undetermined.

Although the results are only taken from one valve, it is interesting to note that collagen concentration within the leaflets increased from the basal stent attachment towards the free edge. Moreover, measured levels of collagen were higher than those found in a previous study conducted in our lab [37] which utilized dynamic flexure at 1 Hz on rectangular sections of TEHV material seeded at approximately the same cell density. The collagen levels reported in that study, 893 ± 133 $\mu\text{g/g}$ wet weight, are less than the levels found in this study 1392 ± 369 $\mu\text{g/g}$ wet weight. This is promising, indicating that perhaps pulsatile incubation with its complex stress and strain field may better stimulate TEHV tissues mechanically to produce more ECM proteins. As for the regional differences, it is unclear whether or not this is due to the presence of more cells being initially deposited in this area, if cells migrate towards the free edge, or if the cells are stimulated to produce more collagen in these areas. Measuring levels of DNA and testing more valves would help clarify the mechanisms underlying this finding.

4.2 LIMITATIONS

4.2.1 Non-compliant Sinus

The human cardiovascular system has elastic vessels and valve sinuses whereas the pulsatile bioreactor uses rigid tubing which, as previously mentioned, produces waveforms that have enhanced upper frequencies and also as shown in the impedance spectrums of Figure 40 and Figure 41. Having an elastic sinus has proven [69, 70] to reduce this phenomenon and also produces a more physiologically accurate flow field. An elastic sinus may also help to reduce the relatively large backward pressure and flow waveforms shown in Figure 40 and Figure 41. Incorporation of an elastic sinus system, which would also likely entail having to install a compliance chamber around it in order to adjust the elastic response, proved to be a modification which was not feasible at this time since it would further complicate the attachment of the outflow valve.

4.2.2 Manual Atrial Head Pressure Adjustment

The ventricle fills due to the head pressure in the atrium. If the filling rate is too high it will cause ventricular pressure spikes during diastole. In order to easily adjust the filling rate, a clamp can be placed on the tube from the atrium to the ventricle. This is an added level of user adjustment which would ideally liked to be eliminated. More sophisticated atriums have been designed but this would add a great deal of complexity and additional parts. A possible simple solution would be an electronically actuated tubing clamp to adjust the filling rate or an electronically controlled lab jack to automatically control the atrial head pressure.

4.2.3 TEHV Design

As previously discussed, TEHV design was not an aim of this study and any work that was done towards designing a TEHV was to simply serve as a starting point for future work. Native valve tissues have a viscoelastic mechanical response unlike the currently available non-woven polymeric scaffold materials which exhibit an inelastic response which means the scaffolds permanently deform under cyclic mechanical loading. Efforts are underway to develop scaffold materials with elastic properties [71, 72] that could possibly better mimic elastic tissue response and not exhibit the undesirable permanent deformation effects [32] as previously discussed.

4.3 FUTURE MODIFICATIONS AND POTENTIAL APPLICATIONS

The severe problems shown with the clinical use of the Synergraft valves clearly indicates the poor understanding of the biological mechanisms of both the host immune response and tissue remodeling processes in a decellularized valve conduit. The pulsatile bioreactor could potentially explore fundamental questions regarding the interactions between human cell lines seeded on these xenograft scaffolds in a much more highly controlled in vitro setting. This would include the exposure to physiologic pressure and flow waveforms during culture which could be critical for regulation of growth, remodeling, and cellular expression.

The fast system response time makes it possible to perform step changes in mean pulsatile pressure and flow in addition to the gradual changes as shown in the flexibility and control tests. A possible application of this feature would be to investigate changes to intact native valve function such as an “in vitro Ross procedure” where a native pulmonary valve could be switched between being incubated under systemic and pulmonary pressure and flow conditions.

Ideally, it would be convenient for the system to offer automatic compliance adjustments so that one could study the effects of altering this other important hemodynamic feature. This could be done by adding another pneumatic controller to control the volume of air within the compliance chamber. Certain pathological conditions can result in stiffened aortic roots/outflow tracts that have a negative impact on hemodynamic function [9]. Elucidating questions regarding how the native tract remodels due to reduced compliance is another potential application of the pulsatile bioreactor.

Future enhancements to the device could include an integrated non-contacting imaging system to provide information on the time course of leaflet deformation of developing TEHV. Real-time metabolic data and concentrations of dissolved gases could be acquired with the addition of biosensors and compliance changes could be automated by installing another pneumatic system to control the air level within the compliance chamber. Additionally, the system could be easily modified for culturing other cardiovascular structures, such as blood vessels, while providing the same degree of hemodynamic control.

4.4 SUMMARY

This study details the design and evaluation of a pulsatile bioreactor for biologically active heart valves. The study first established the need for the development of such a device by examining current problems with current heart valve replacements and the lack of proper equipment for evaluating novel therapies such as tissue engineered heart valves (decellularized xenograft scaffolds and polymeric scaffolds). A rational set of design requirements were established in order to form a logical basis for creating a design solution. The chosen design solution

incorporated elements of both mock circulatory loop and bioreactor technologies to create a hybrid pulsatile heart valve bioreactor. Both specific design issues such as component design, actuation methods, and their final solutions were discussed in detail. Finally, the process of evaluating a device that has both specific mechanical and biological functions was given attention.

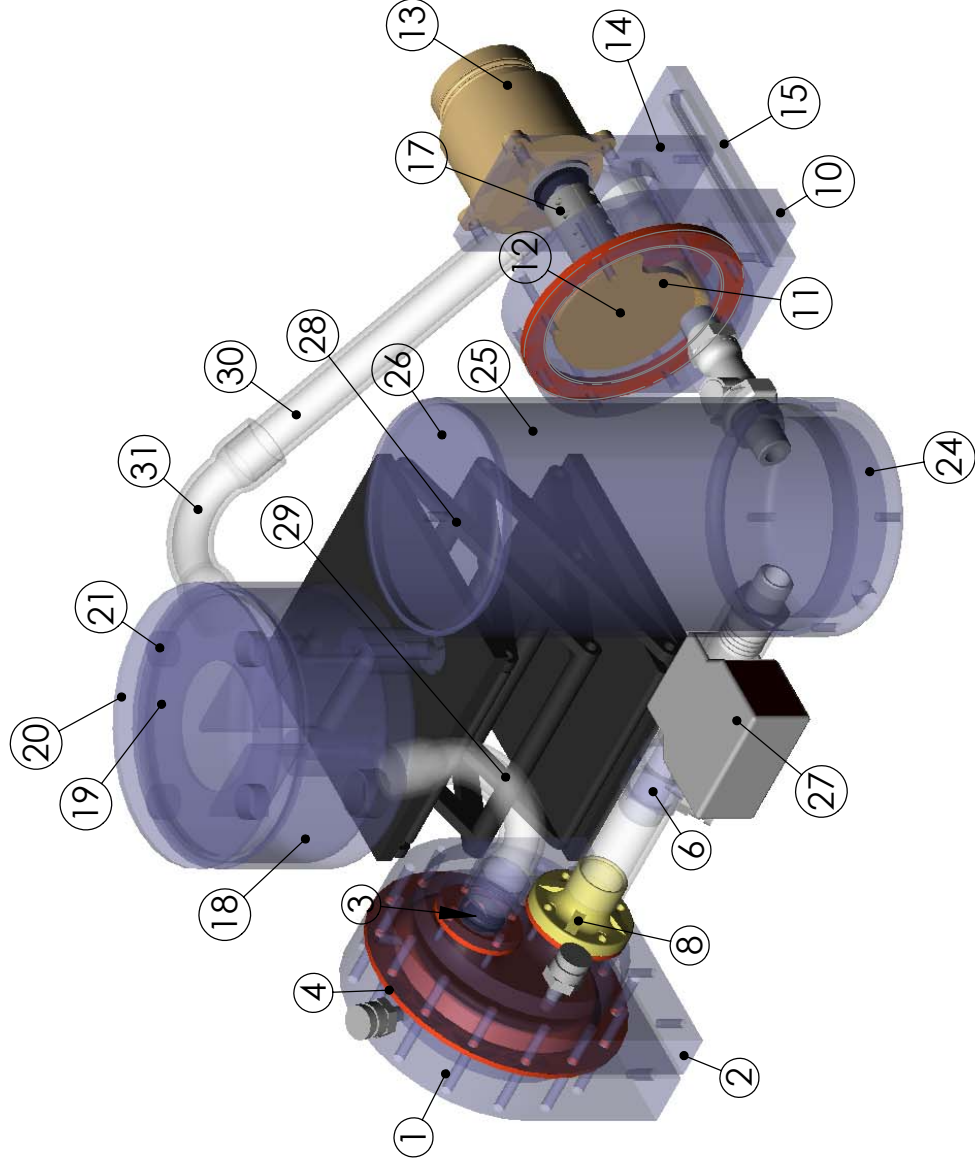
The results of the all the tests indicate that all design requirements have been met and in summary the device has been shown to feature:

1. accurate and precise modulation of pulsatile pressure and flow (normally distributed mean errors from command, zero means with low standard deviations)
2. wide resistance range ($0.25\text{-}1.2\text{+ mmHg s mL}^{-1}$)
3. highly tunable pneumatic waveform
4. good beat-to-beat waveform reproducibility (low mean differences)
5. waveforms can mimic physiologic waveforms (qualitatively and quantitatively by input-impedance spectrum analysis)
6. sterile environment
7. physiologic pH (7.45 without any pCO_2 modulation)
8. oxygen tension can be controlled to provide supra-arterial tensions at flow rates greater than 1 lpm

Also, the preliminary results with the TEHV are promising showing collagen levels that exceed our previous study [37] indicating that pulsatile mechanical stimulation could be enhancing ECM formation. The results when taken together demonstrate that the pulsatile bioreactor can expose a biologically active heart valve to well controlled pulsatile pressures and flows in a biologically relevant environment.

Appendix A

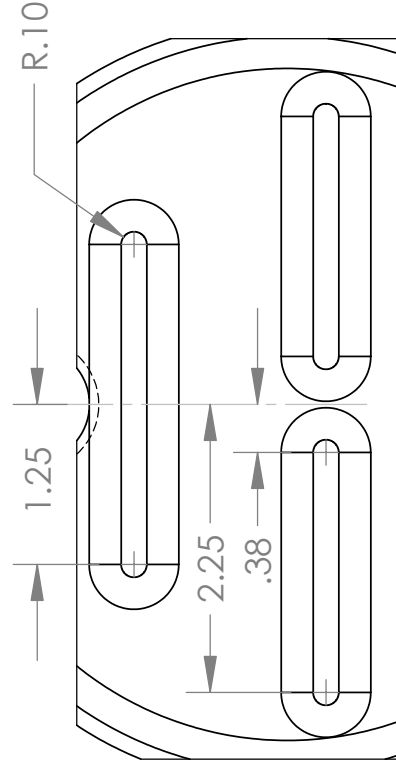
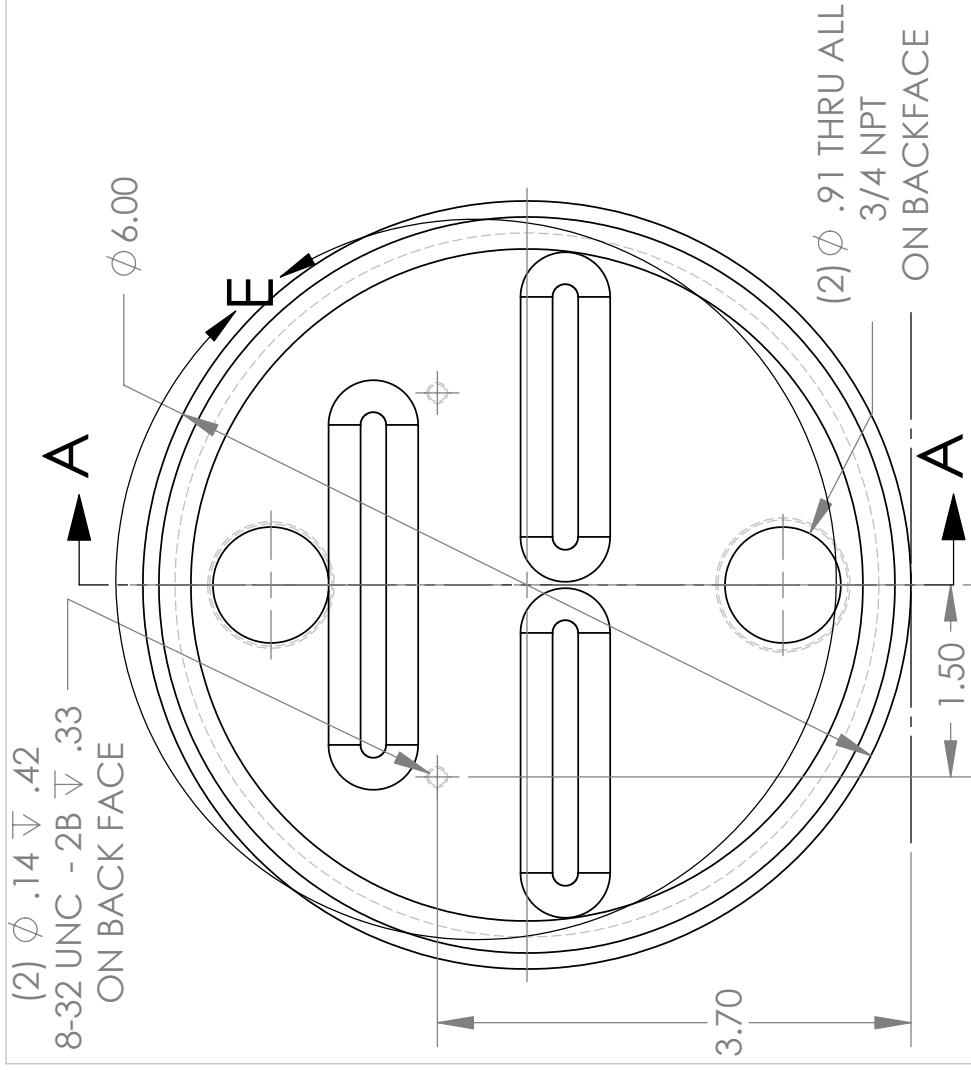
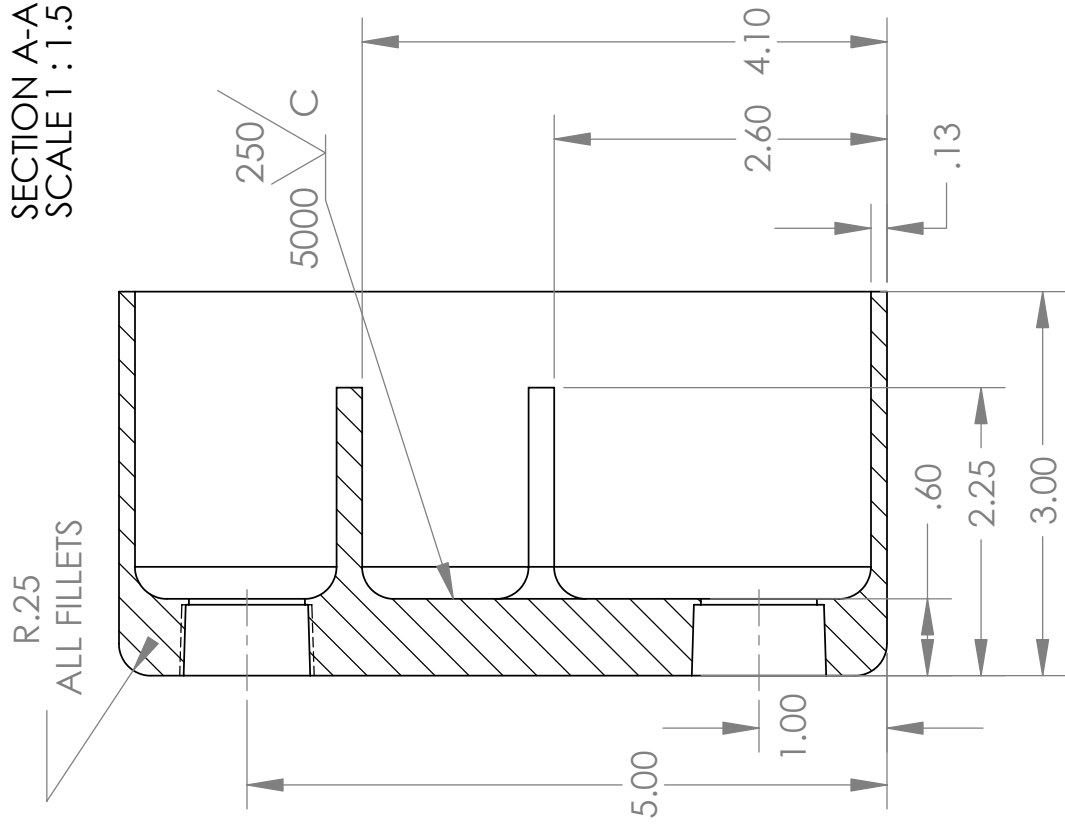
Mechanical Drawings





NO.	PART NO.
1	Vent Chamber -3- Back
2	Vent Chamber -3- Front
3	Wu - mitral valve holder
4	Vent Chamber -3- Bladder
5	Mitral Valve
6	Aortic Pressure - One Piece
7	Pressure Transducer - Package 4
8	Variable Resistor - Outer Tube
9	Variable Resistor - Outflow Nipple
10	Variable Resistor - Stand
11	Variable Resistor - Front Case
12	Variable Resistor - Dial Plate - Loop 2
13	Stepper Motor - Thompson C57
14	Variable Resistor - Base
15	Variable Resistor - Mounting Plate
16	Resistor Tube - One Piece
17	Coupler - 2 Piece
18	Atrial Chamber -3- Base
19	Atrial Chamber -2- Lid Top
20	Atrial Chamber -2- Lid Cover
21	Atrial Chamber -2- Lid Post
22	Atrial Chamber - Stand Post
23	Atrial Chamber -2- Inlet
24	Comp2-Base
25	Comp2-Body
26	Comp2-Lid
27	Transonic Flow Probe - 1-125 Tubing
28	Lab Jack-Link
29	Tubing - U -1.0ID
30	Tubing - Resistor to Atrium
31	Tubing - Ell -1.0ID

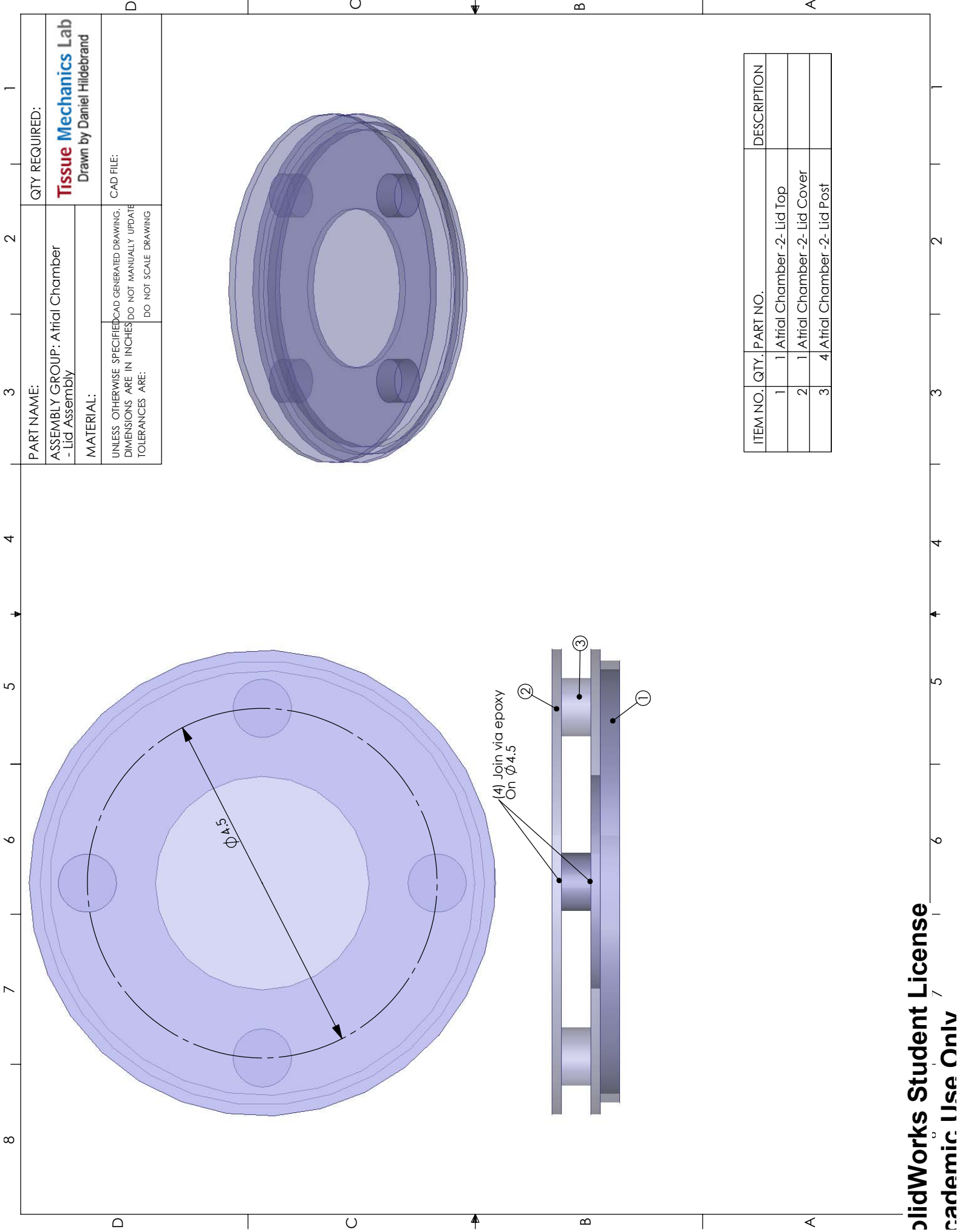
SECTION A-A
SCALE 1:1.5

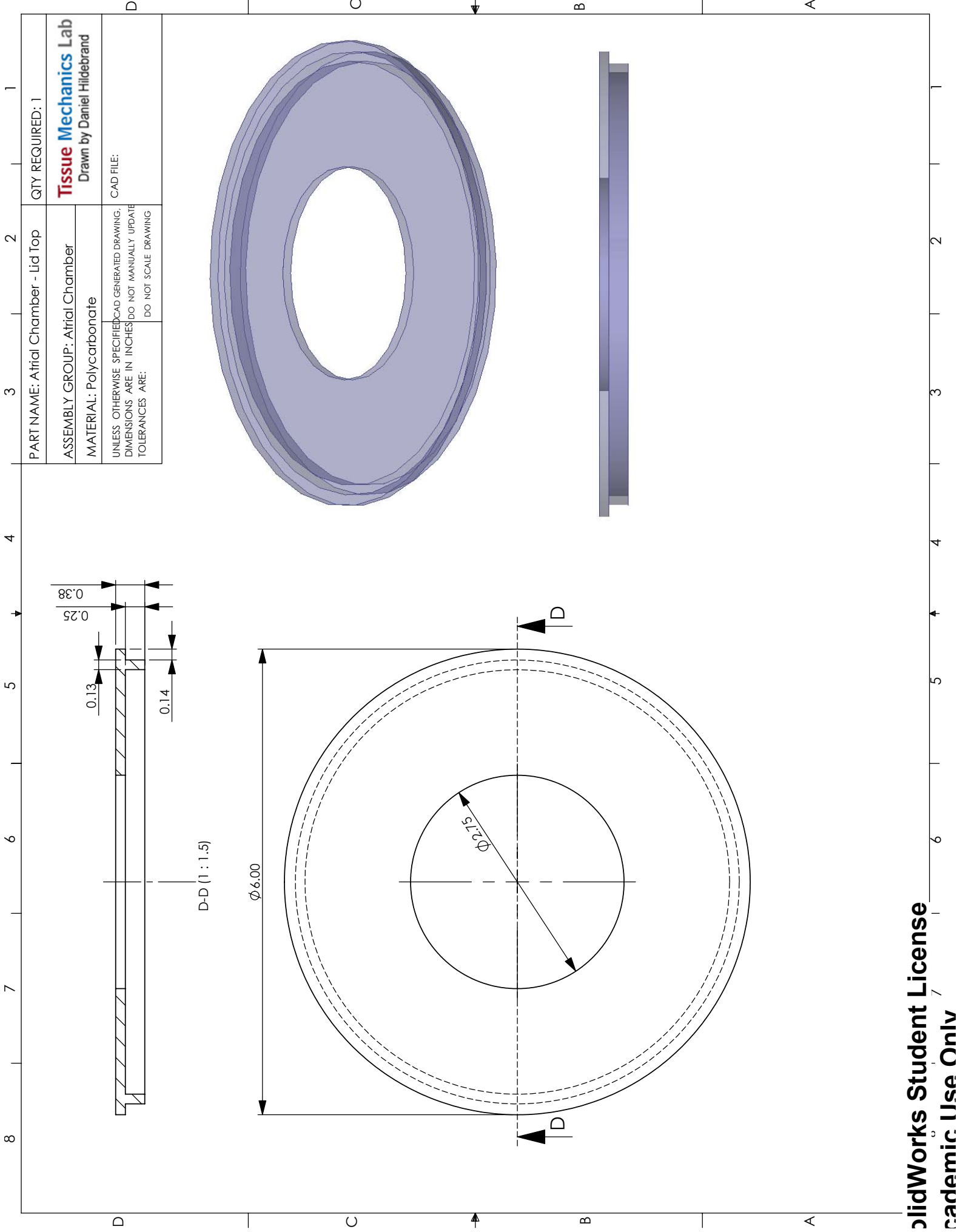
SCALE 1 : 1.5

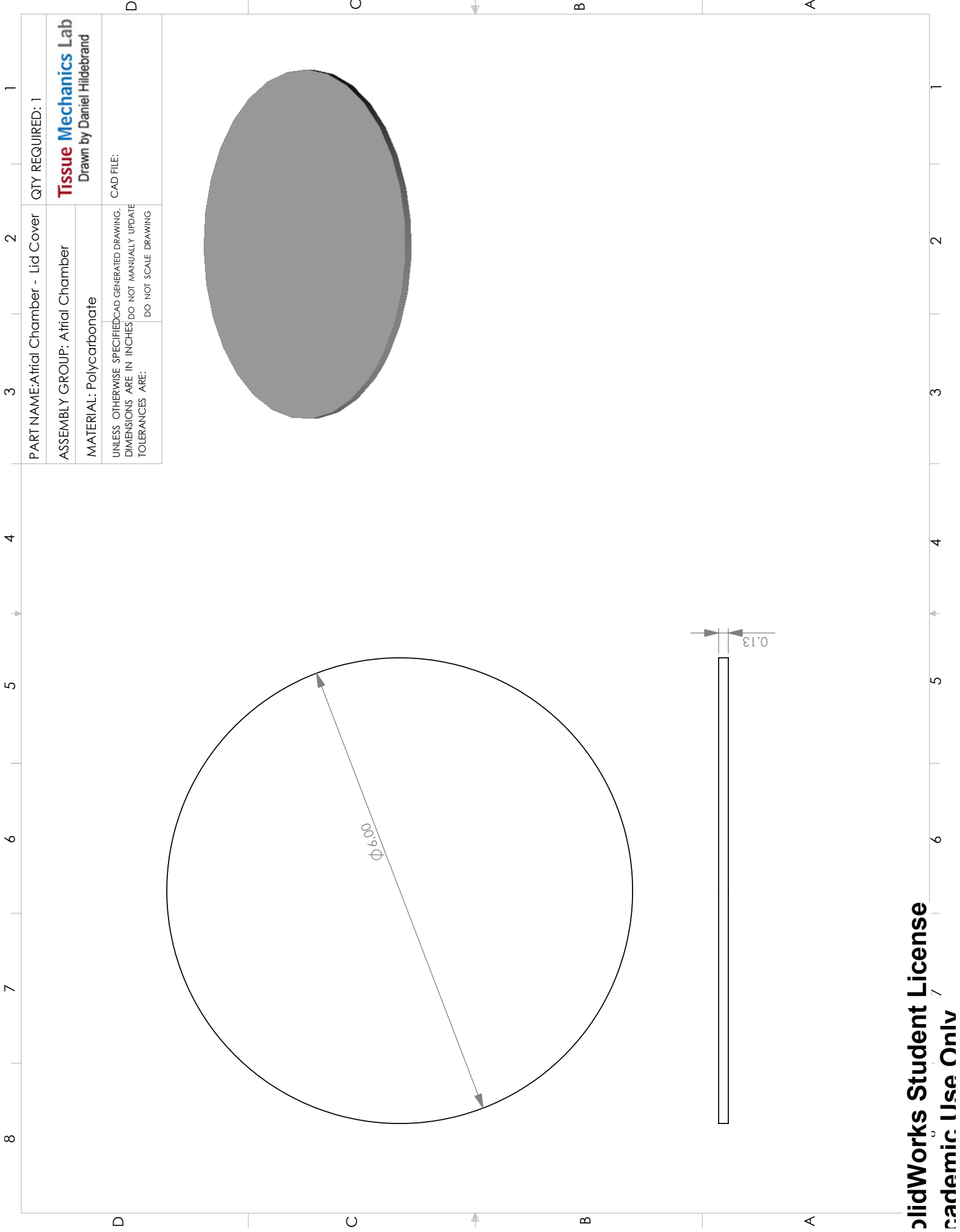


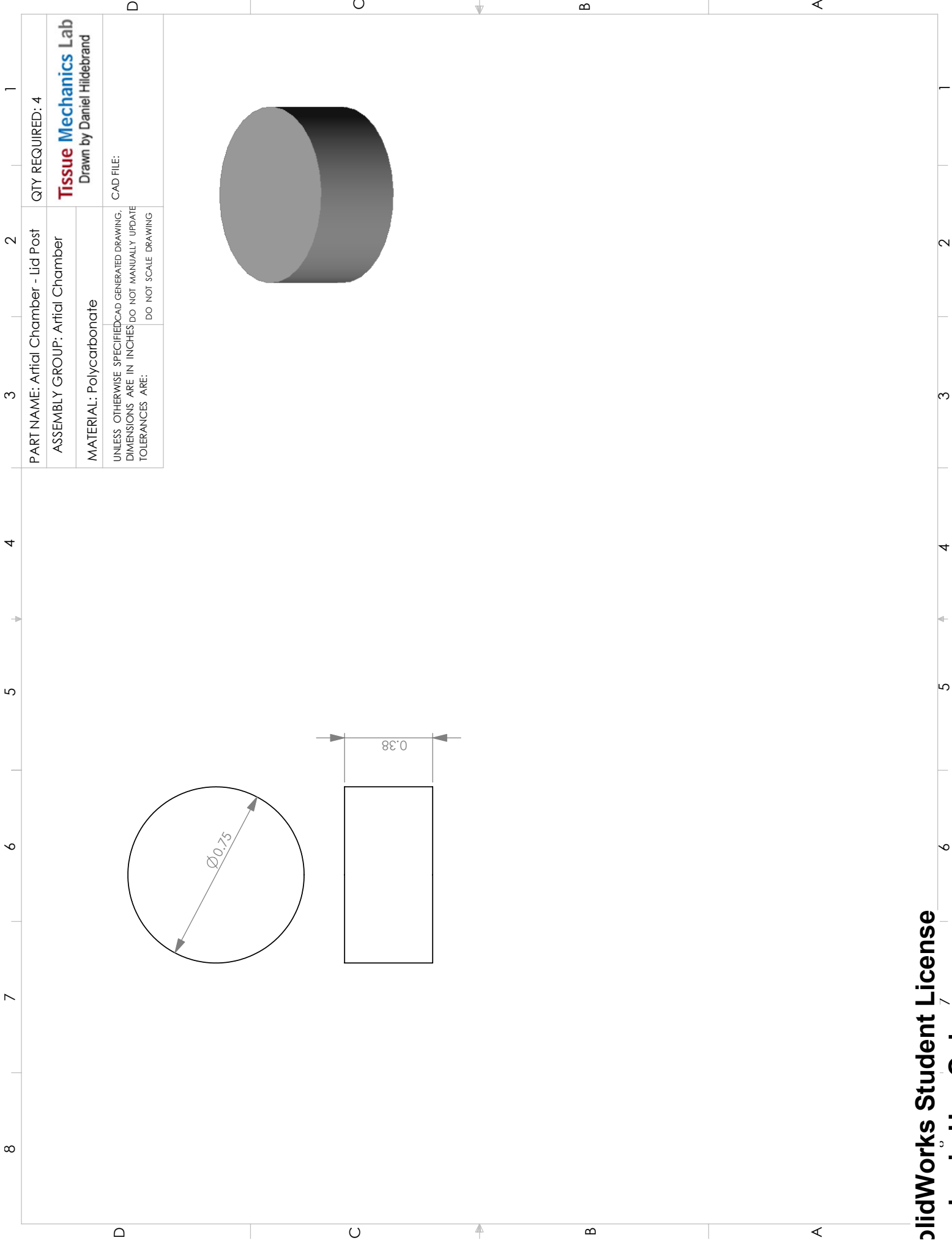
DETAIL E
SCALE 1:1.5

TITLE: ATRIAL-BASE	
UNLESS OTHERWISE SPECIFIED: DIMENSIONS ARE IN INCHES TOLERANCES: FRACTIONAL \pm ANGULAR: MACH \pm BEND \pm TWO PLACE DECIMAL \pm THREE PLACE DECIMAL \pm	
INTERPRET GEOMETRIC TOLERANCING PER:	
MATERIAL POLYCARBONATE	DWG. NO.
FINISH POLISHED	REV
DO NOT SCALE DRAWING	Drawn By: Daniel Hildebrand



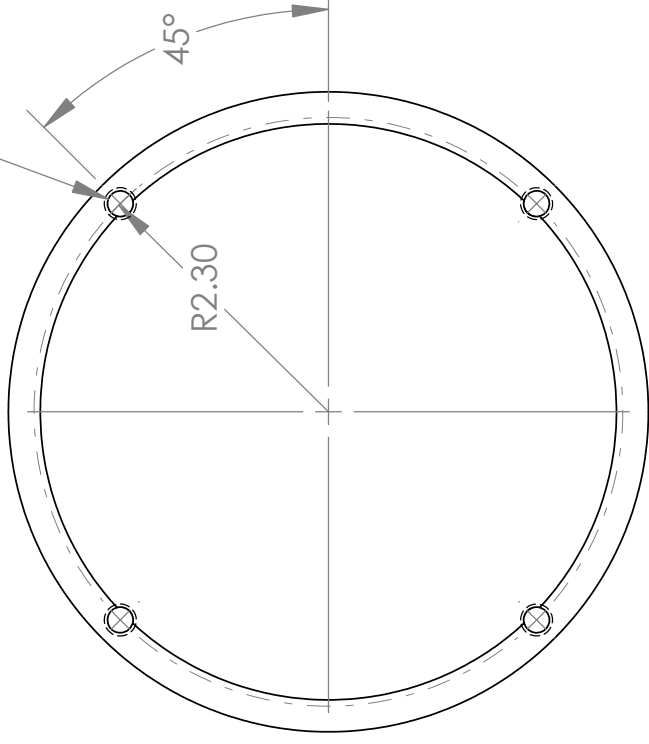
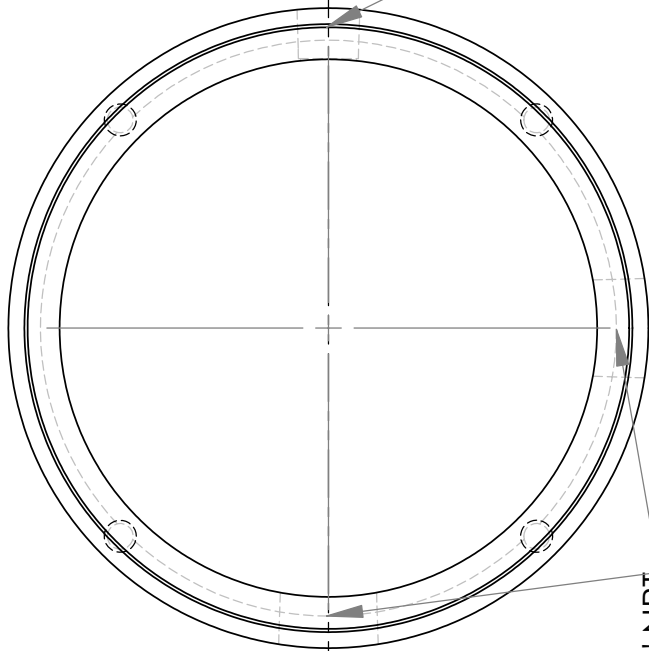
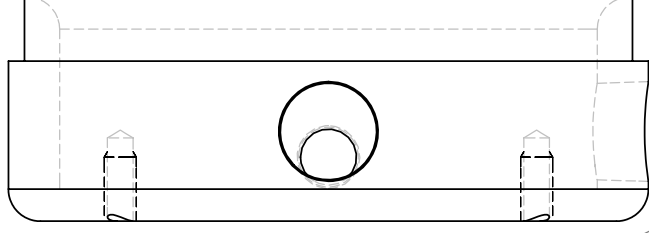




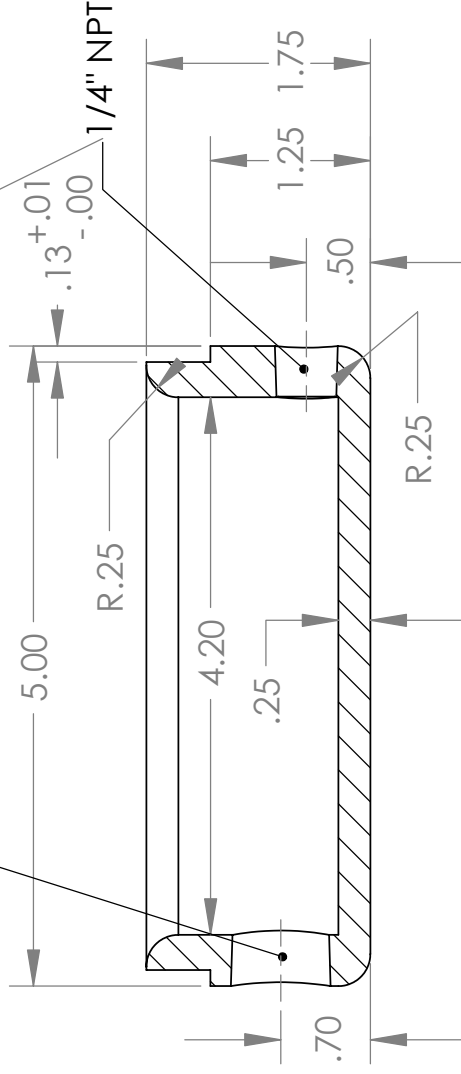


PART NAME: Artial Chamber - Lid Post		QTY REQUIRED: 4
ASSEMBLY GROUP: Artial Chamber		
MATERIAL: Polycarbonate		
UNLESS OTHERWISE SPECIFIED CAD GENERATED DRAWING, DIMENSIONS ARE IN INCHES DO NOT MANUALLY UPDATE TOLERANCES ARE:		CAD FILE:
DO NOT SCALE DRAWING		
Tissue Mechanics Lab Drawn by Daniel Hildebrand		

(4) ϕ .20 ∇ .65
1/4-20 UNC - 2B ∇ .50



(2) 1/2" NPT



SECTION A-A
SCALE 1:1.5

UNLESS OTHERWISE SPECIFIED:

DIMENSIONS ARE IN INCHES

TOLERANCES:

FRACTIONAL \pm

ANGULAR: MACH \pm BEND \pm

TWO PLACE DECIMAL \pm

THREE PLACE DECIMAL \pm

INTERPRET GEOMETRIC

TOLERANCING PER:

MATERIAL

POLYCARBONATE

FINISH

TITLE: **COMP-BASE**

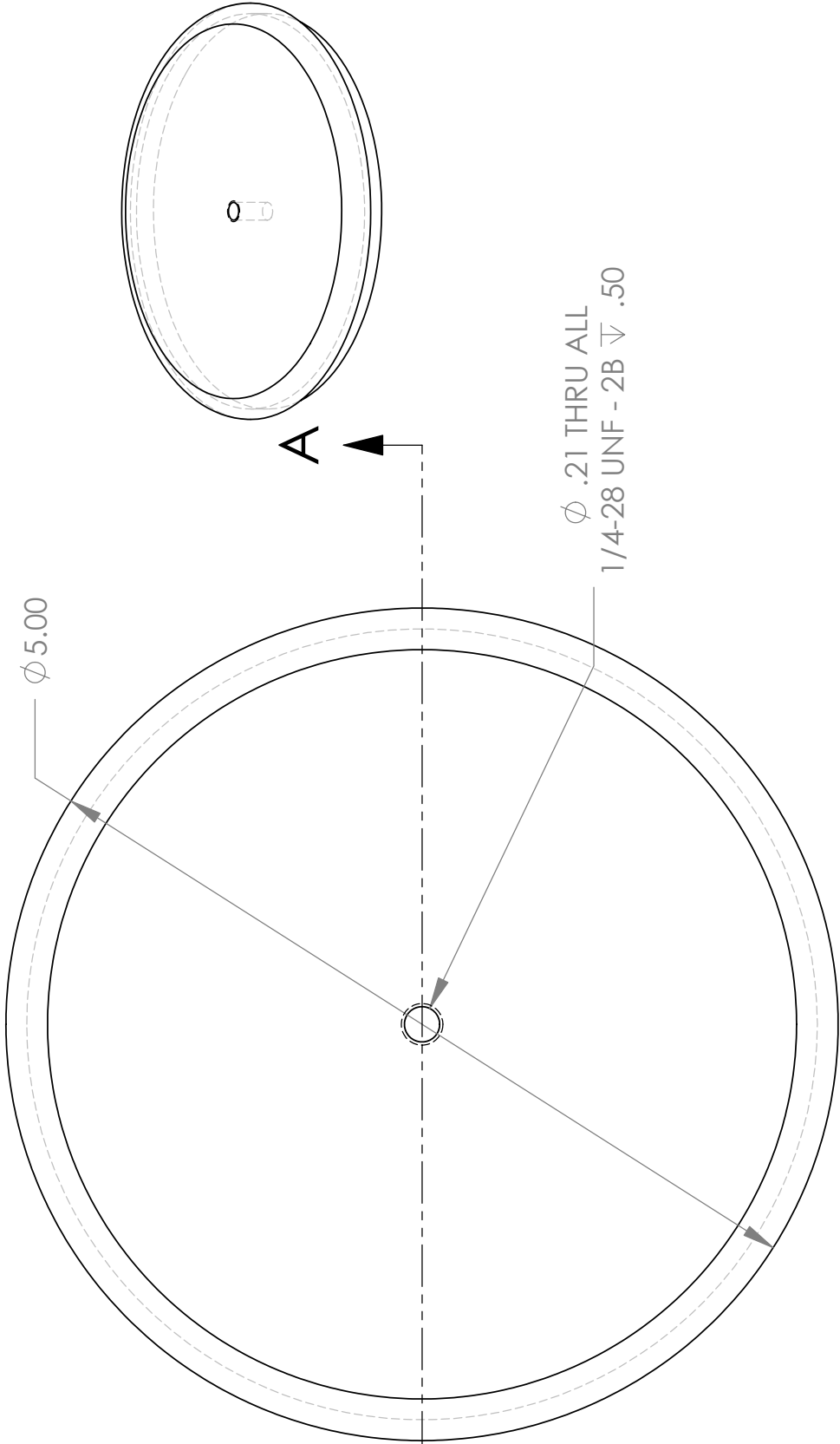


REV

QTY: 2

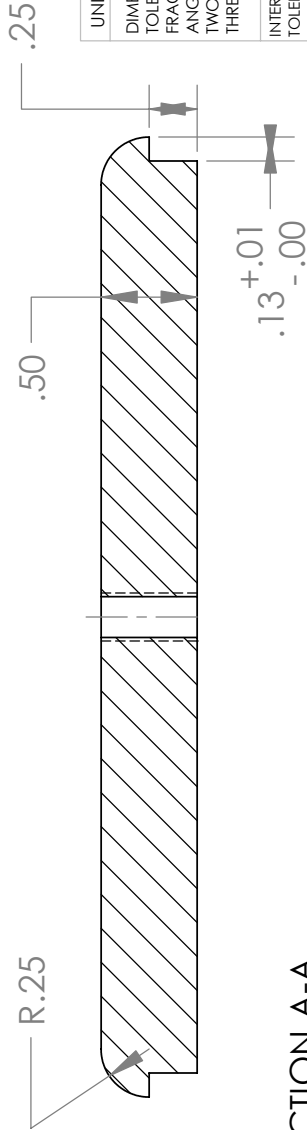
Drawn By: Daniel Hildebrand

DO NOT SCALE DRAWING




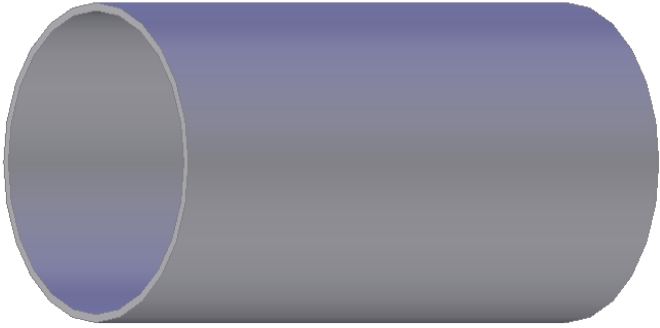
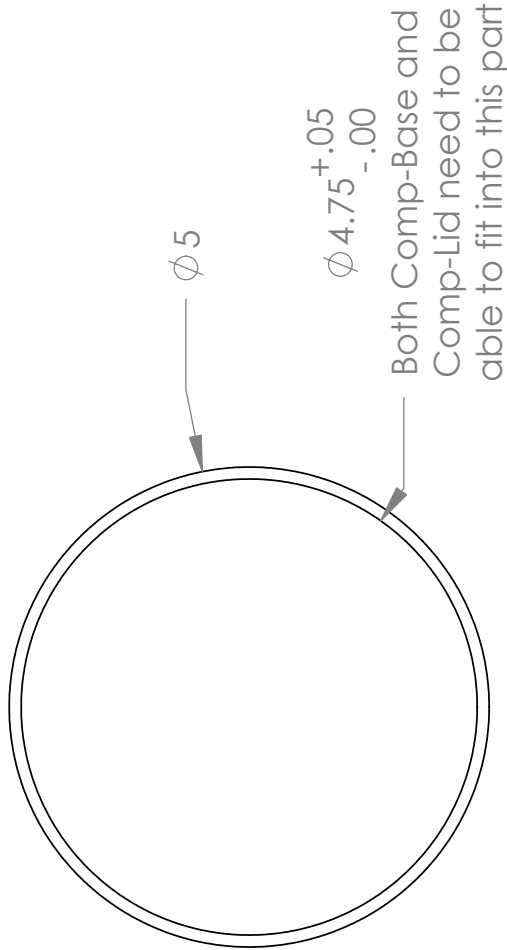
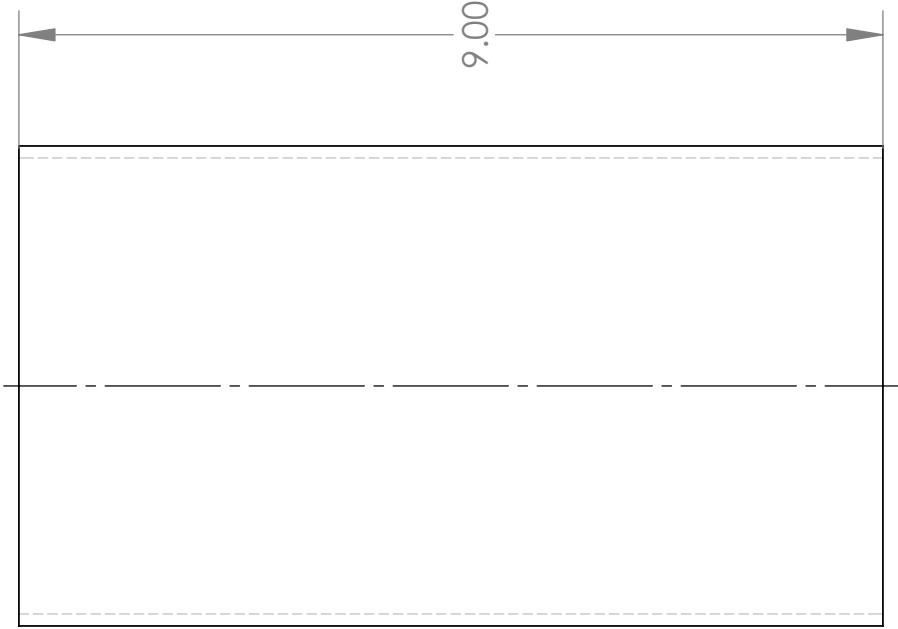
A

A



SECTION A-A
SCALE 1 : 1

UNLESS OTHERWISE SPECIFIED:		TITLE: COMP-LID	
DIMENSIONS ARE IN INCHES			
TOLERANCES:			
FRACTIONAL ±	ANGULAR: MACH ±		
TWO PLACE DECIMAL ±	BEND ±		
THREE PLACE DECIMAL ±			
INTERPRET GEOMETRIC TOLERANCING PER:		QTY: 2	
MATERIAL		REV	
POLYCARBONATE			
FINISH			
DO NOT SCALE DRAWING		Drawn By: Daniel Hildebrand	



UNLESS OTHERWISE SPECIFIED: DIMENSIONS ARE IN INCHES TOLERANCES: FRACTIONAL ± ANGULAR: MACH ± BEND ± TWO PLACE DECIMAL ± THREE PLACE DECIMAL ± INTERPRET GEOMETRIC TOLERANCING PER:	TITLE: COMP-BODY		
	MATERIAL	POLYCARBONATE	REV
	FINISH	POLISHED	QTY: 2
	DO NOT SCALE DRAWING		
Drawn By: Daniel Hildebrand			

BACK FACE

A

$\phi .15 \sqrt{.51}$
10-24 UNC - 2B $\sqrt{.38}$
ON FRONT FACE

1/4-28 THRU

13°

$\phi 4.75$

$\phi .33$ THRU ALL
1/8 NPT
ON FRONT FACE

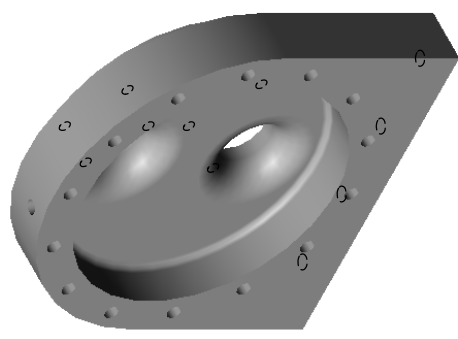
1.25

3.25

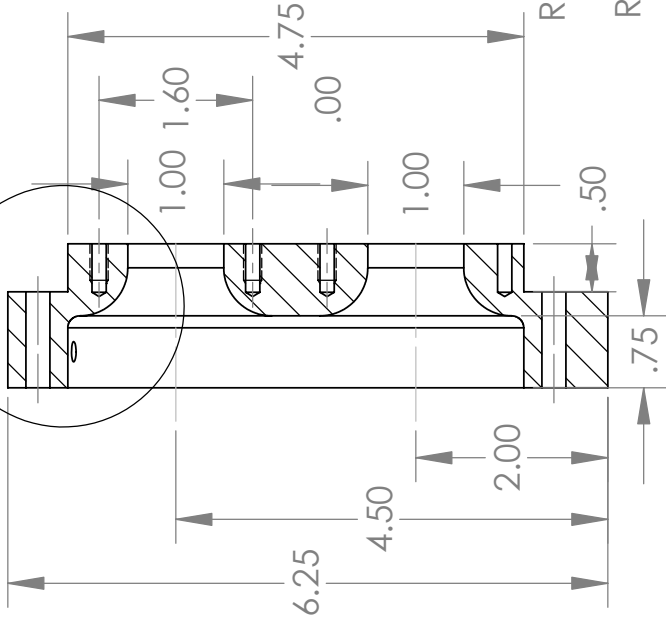
A

$\phi 5.38$

(14) $\phi .25$ THRU ALL

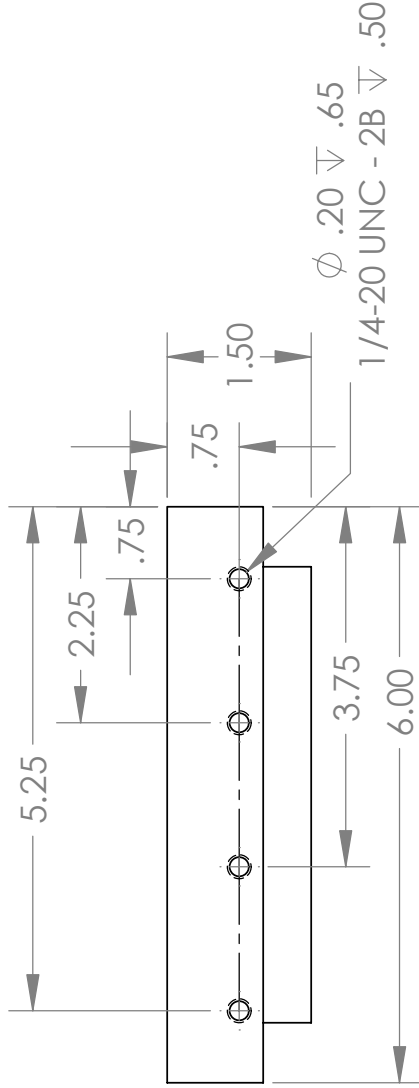


B



SECTION A-A

DETAIL B
SCALE 1 : 1



UNLESS OTHERWISE SPECIFIED:

DIMENSIONS ARE IN INCHES

TOLERANCES:

FRACTIONAL: \pm

ANGULAR: MACH \pm BEND \pm

TWO PLACE DECIMAL \pm

THREE PLACE DECIMAL \pm

INTERPRET GEOMETRIC

TOLERANCING PER:

MATERIAL POLYCARBONATE

FINISH POLISHED

DO NOT SCALE DRAWING

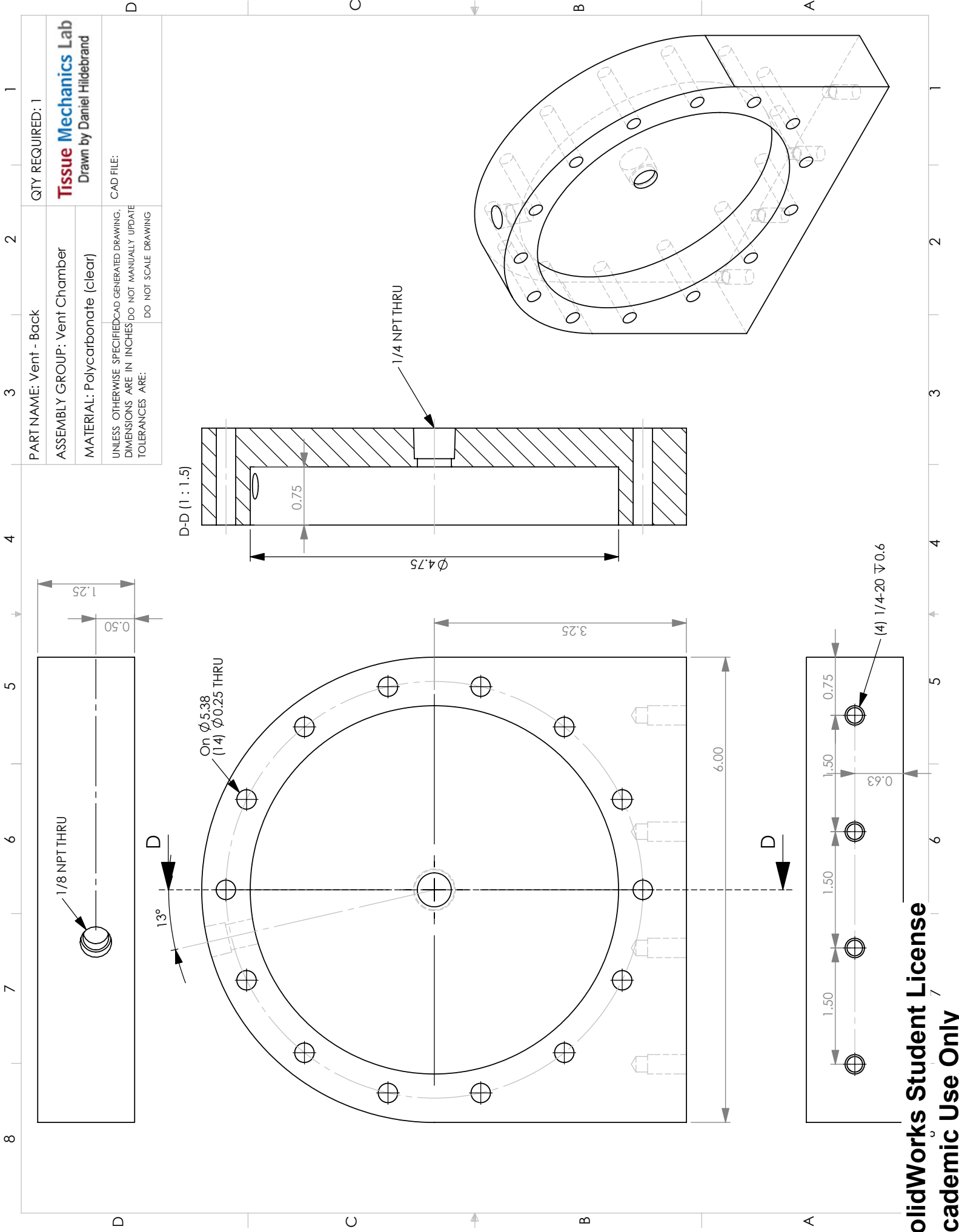
TITLE: VENT - FRONT

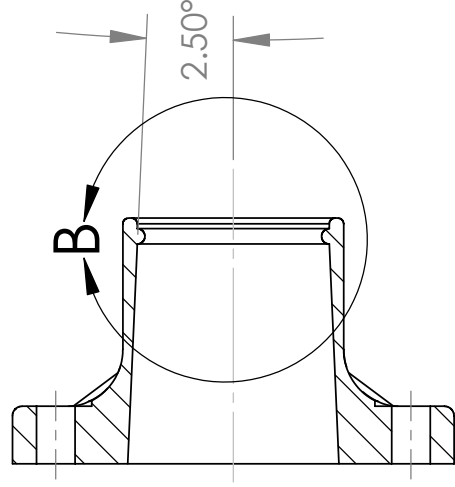
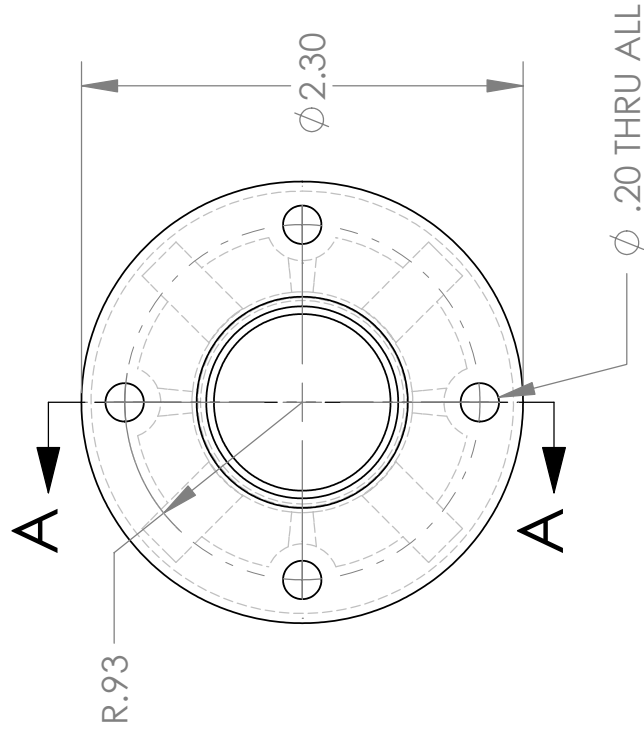


DWG. NO.

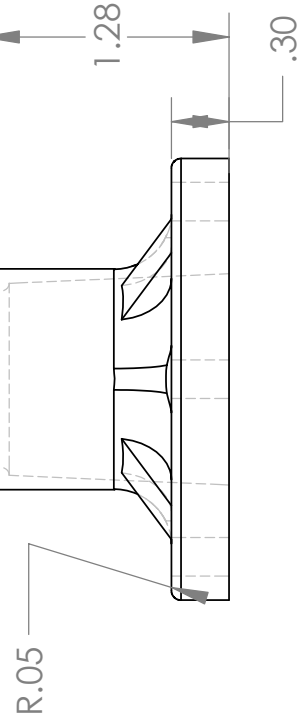
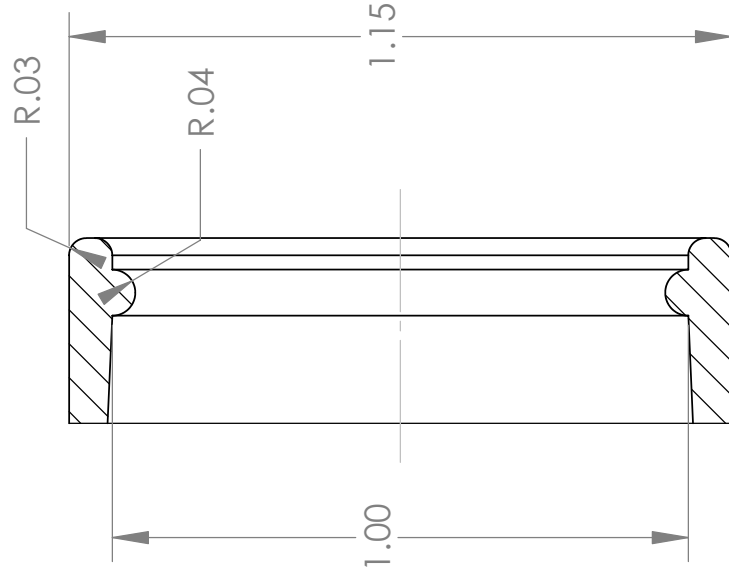
REV

Drawn By: Daniel Hildebrand




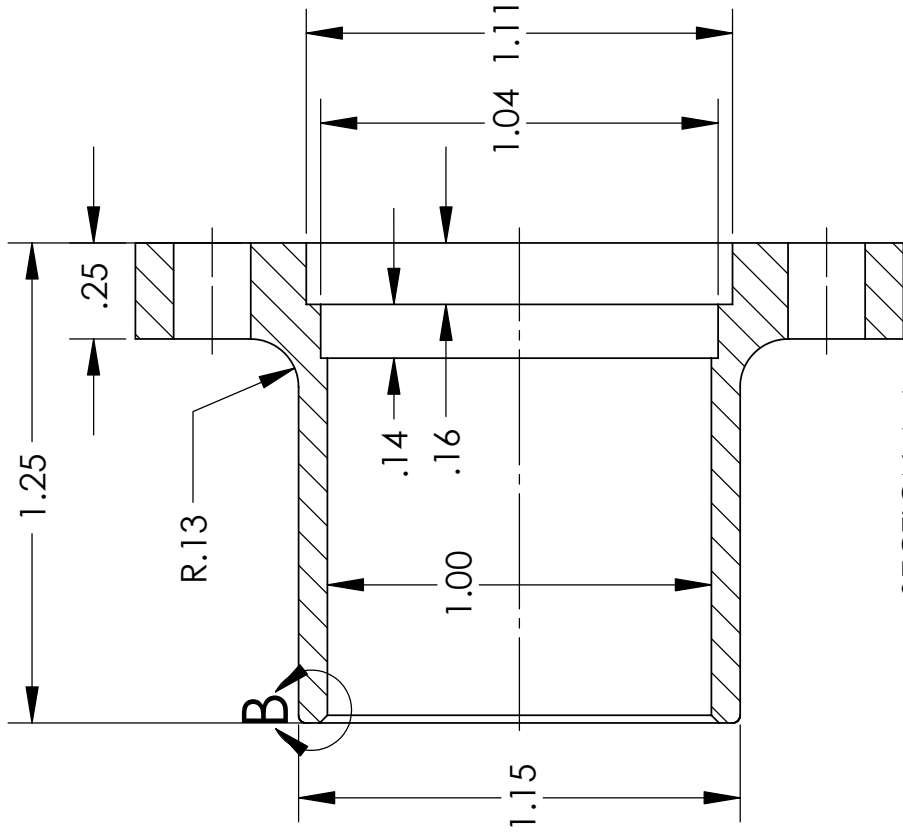
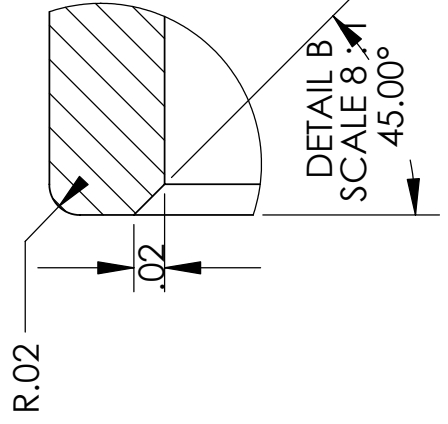
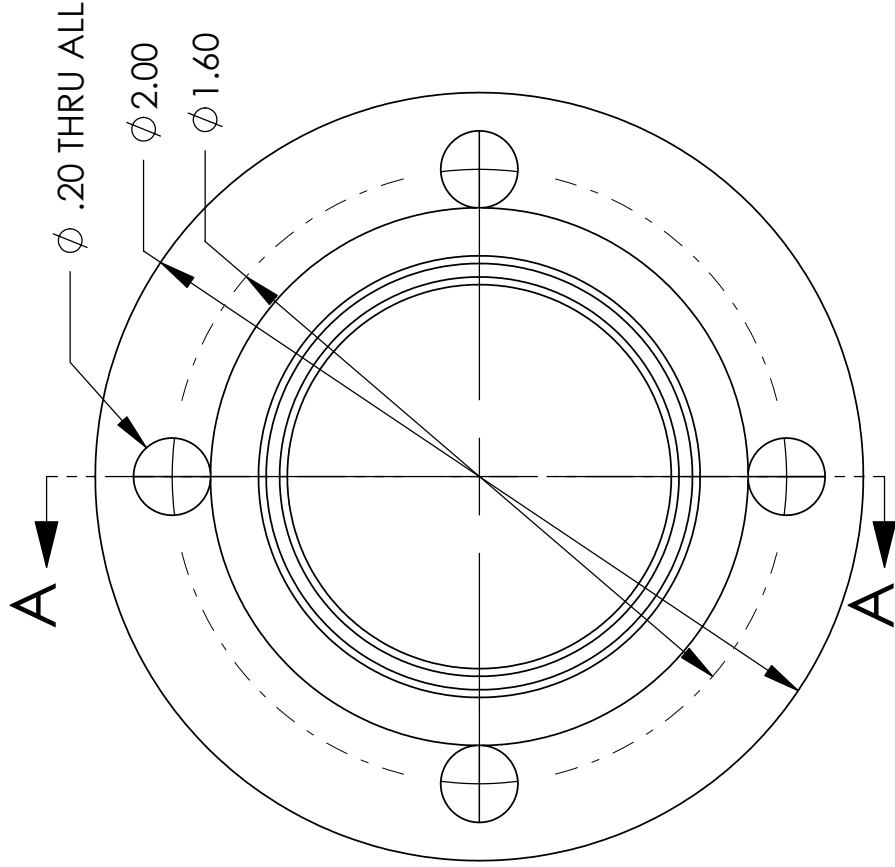


SECTION A-A




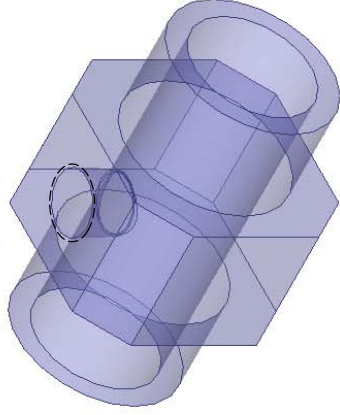
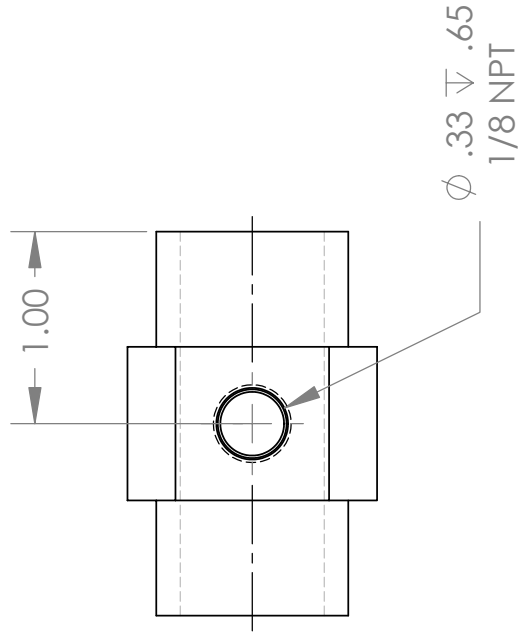
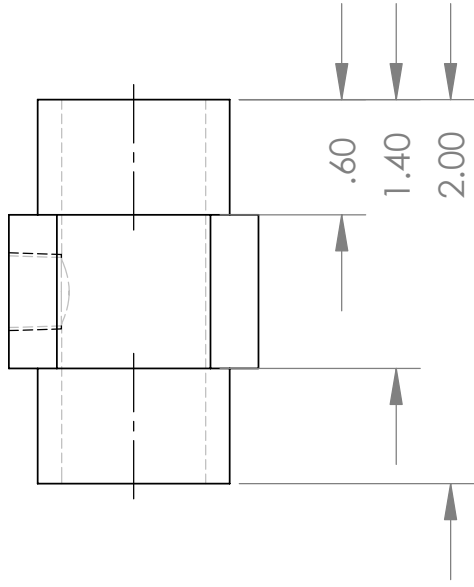
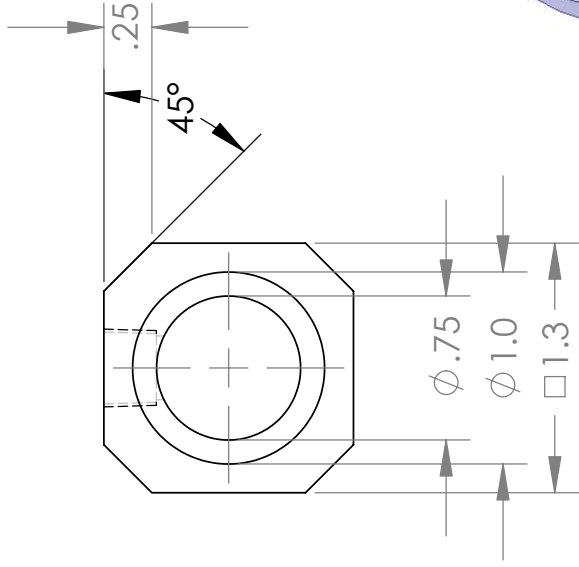
DETAIL B
SCALE 3 : 1


UNLESS OTHERWISE SPECIFIED: DIMENSIONS ARE IN INCHES TOLERANCES: FRACTIONAL ± ANGULAR: MACH ± BEND ± TWO PLACE DECIMAL ± THREE PLACE DECIMAL ± INTERPRET GEOMETRIC TOLERANCING PER:	TITLE: Biopros Holder		
			
	MATERIAL AccuraSi	DWG. NO.	REV
	FINISH		
DO NOT SCALE DRAWING		Drawn By: Daniel Hildebrand	

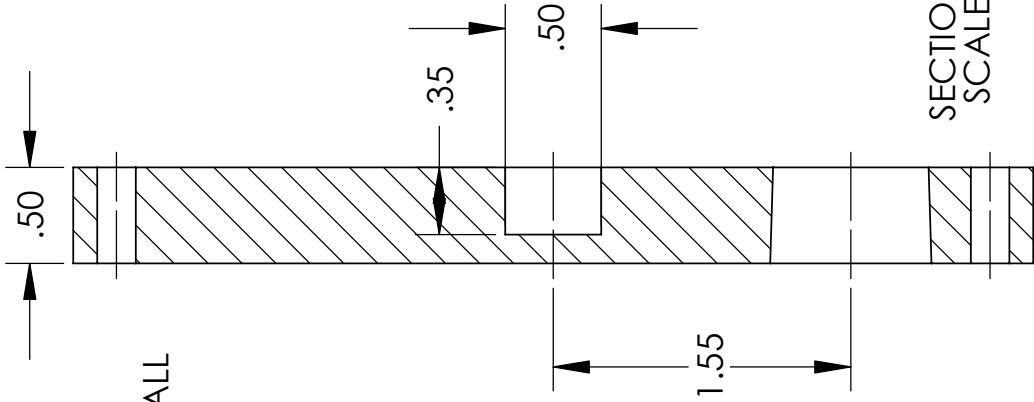
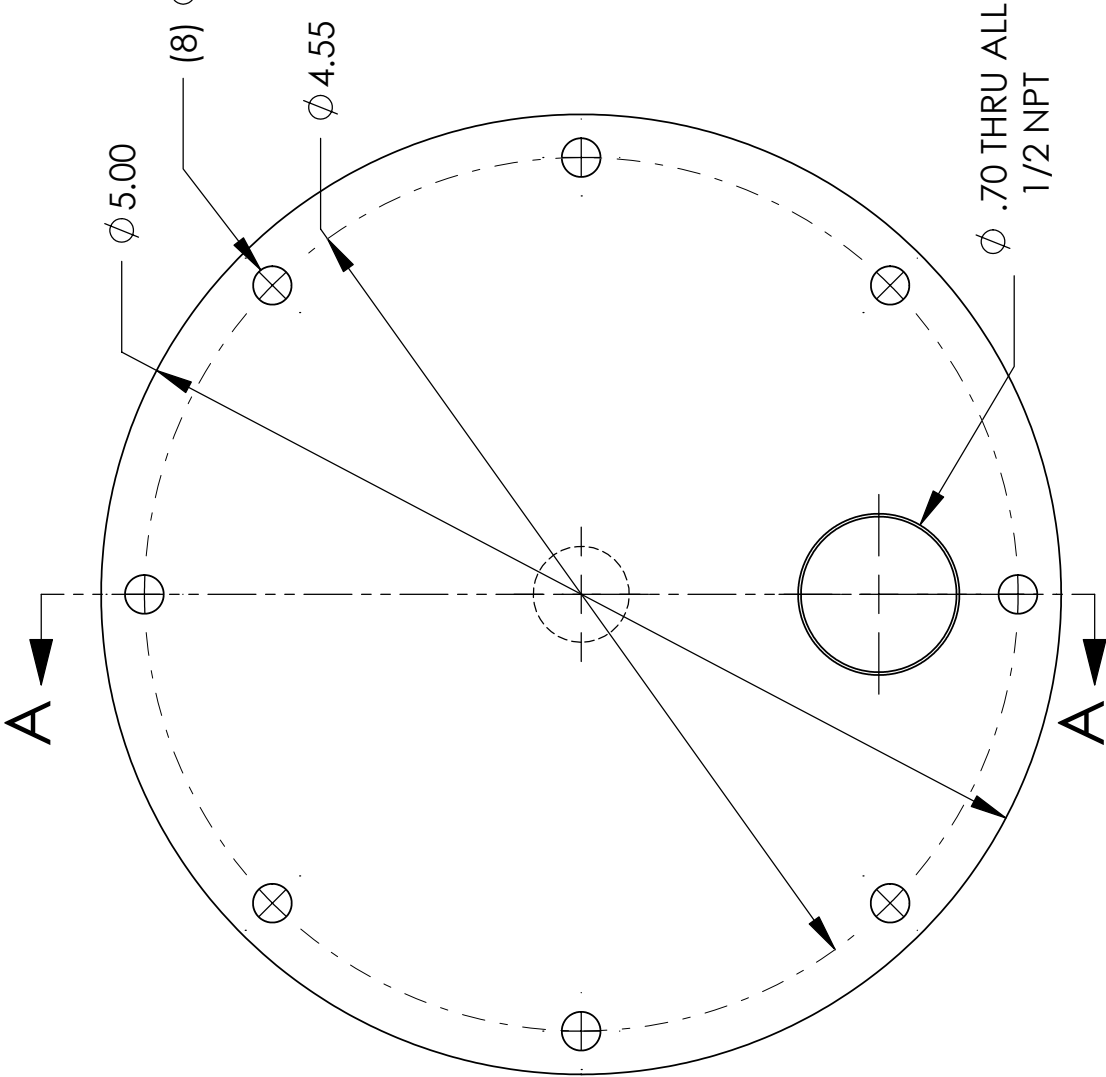


SECTION A-A
SCALE 2:1


UNLESS OTHERWISE SPECIFIED: DIMENSIONS ARE IN INCHES TOLERANCES: FRACTIONAL ± ANGULAR: MACH ± BEND ± TWO PLACE DECIMAL ± THREE PLACE DECIMAL ± INTERPRET GEOMETRIC TOLERANCING PER:	TITLE: MITRAL HOLDER		
			
	MATERIAL POLYCARBONATE	DWG. NO.	REV
	FINISH POLISHED		
DO NOT SCALE DRAWING			
Drawn By: Daniel Hildebrand			

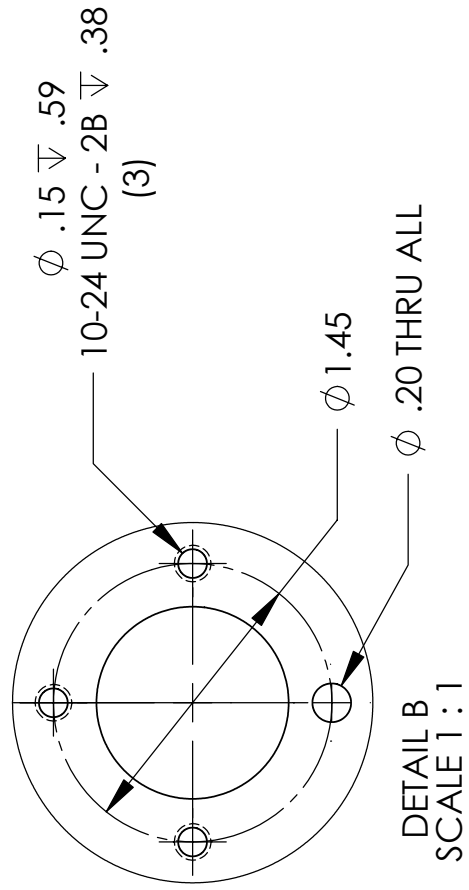
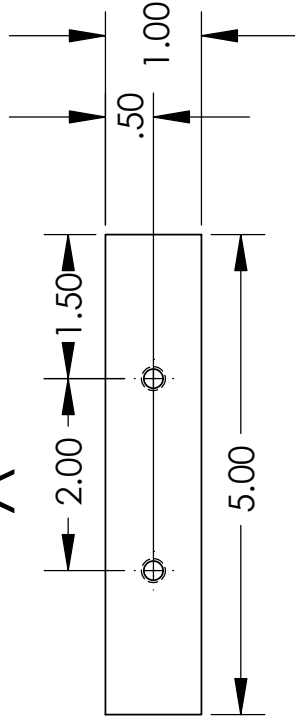
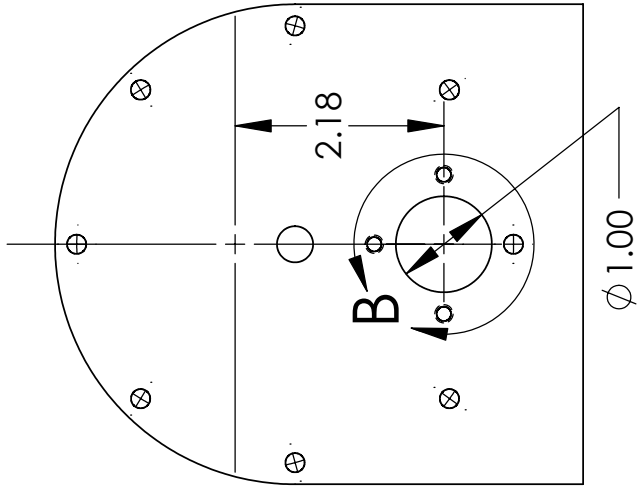
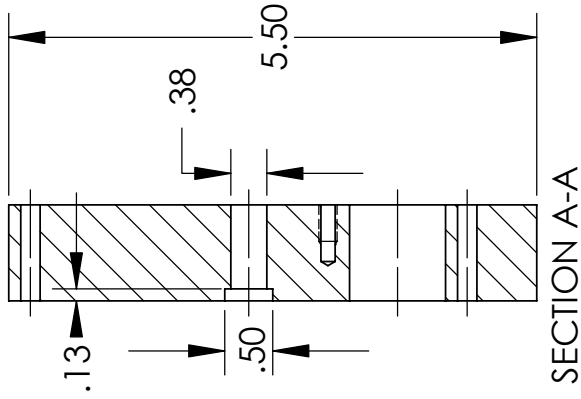
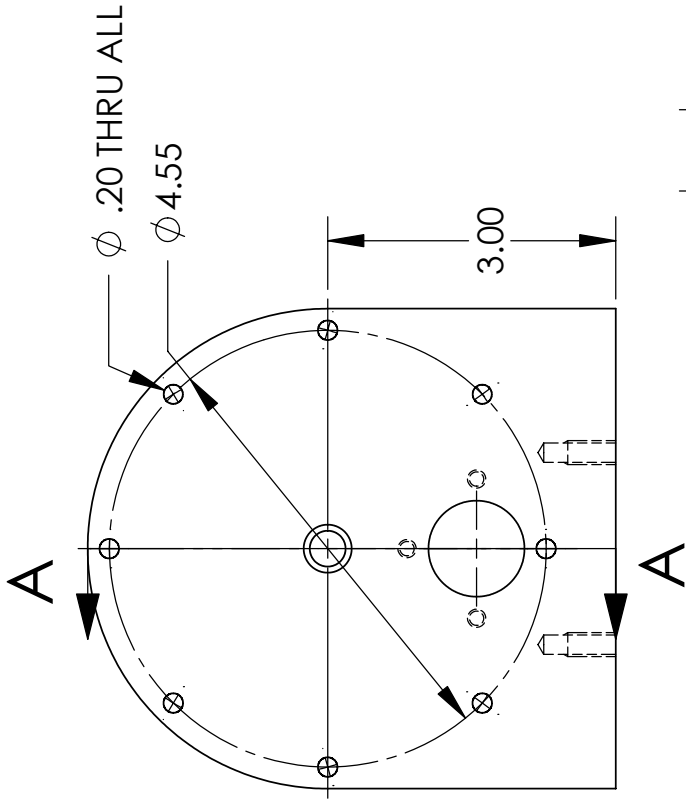



UNLESS OTHERWISE SPECIFIED:		TITLE: Pressure Mount-1	
DIMENSIONS ARE IN INCHES			
TOLERANCES:			
FRACTIONAL: ±			
ANGULAR: MACH ± BEND ±			
TWO PLACE DECIMAL ±			
THREE PLACE DECIMAL ±		QTY: 2	
INTERPRET GEOMETRIC TOLERANCING PER:		REV	
MATERIAL Polycarbonate			
FINISH			
DO NOT SCALE DRAWING		Drawn By: Daniel Hildebrand	

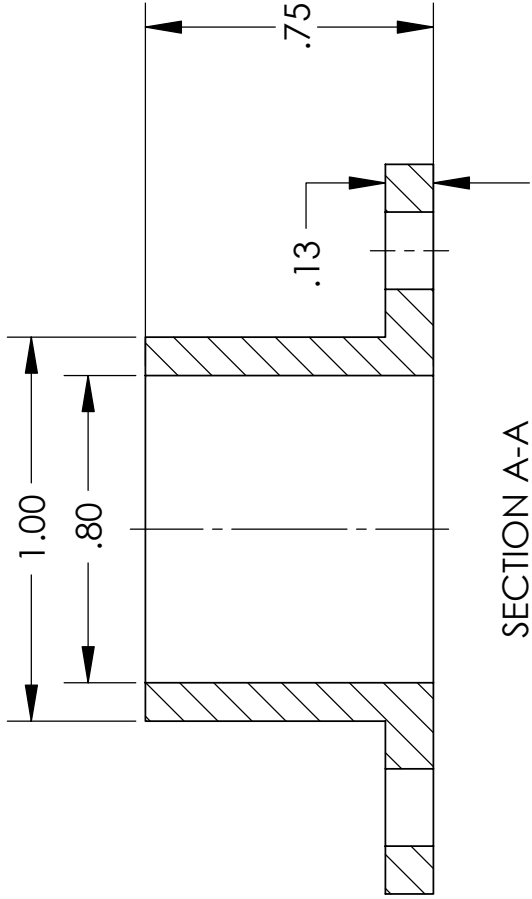
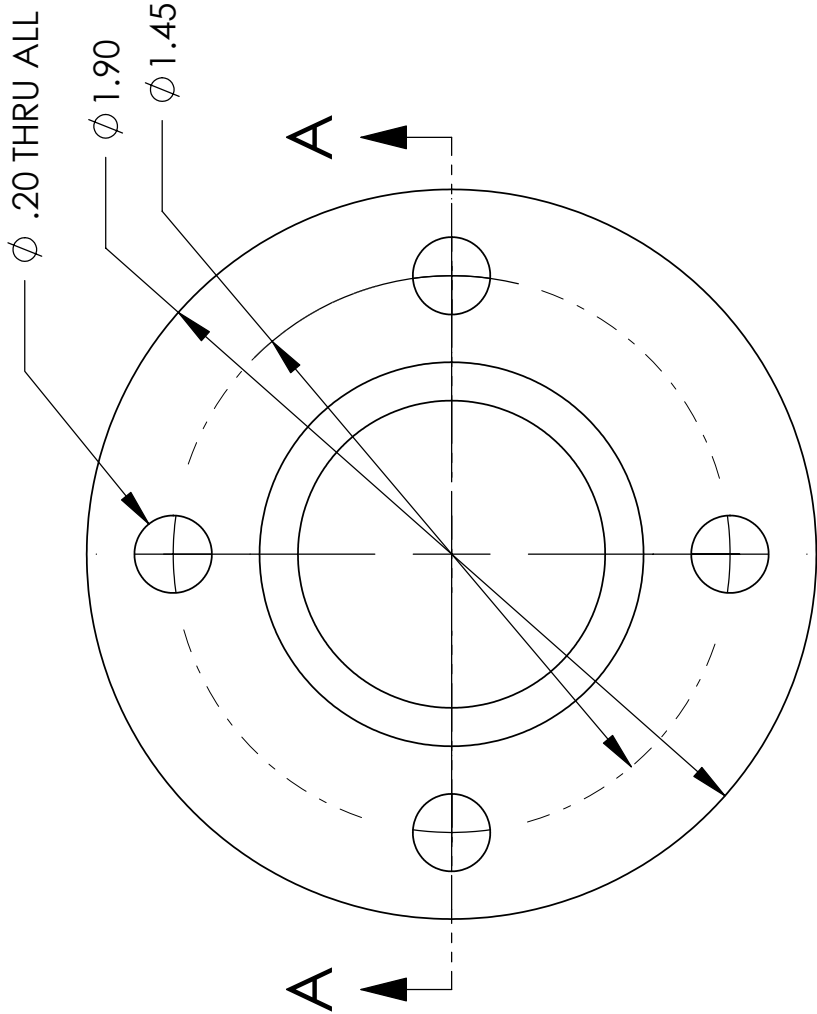


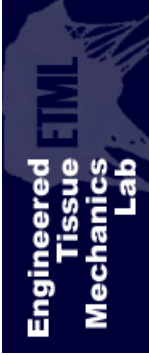
SECTION A-A
SCALE 1 : 1

UNLESS OTHERWISE SPECIFIED:		TITLE: RESISTOR-FRONT	
DIMENSIONS ARE IN INCHES			
TOLERANCES:			
FRACTIONAL ±			
ANGULAR: MACH ± BEND ±			
TWO PLACE DECIMAL ±		DWG. NO.	
THREE PLACE DECIMAL ±			
INTERPRET GEOMETRIC TOLERANCING PER:			
MATERIAL		REV	
POLYCARBONATE			
FINISH			
POLISHED		Drawn By: Daniel Hildebrand	
DO NOT SCALE DRAWING			

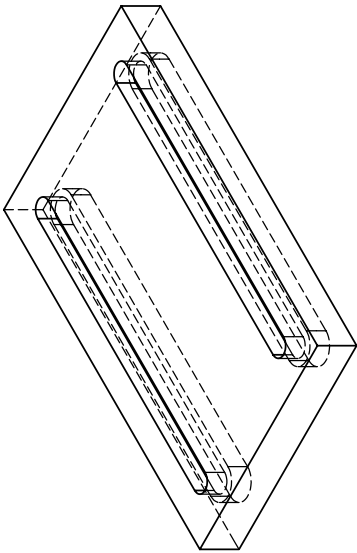
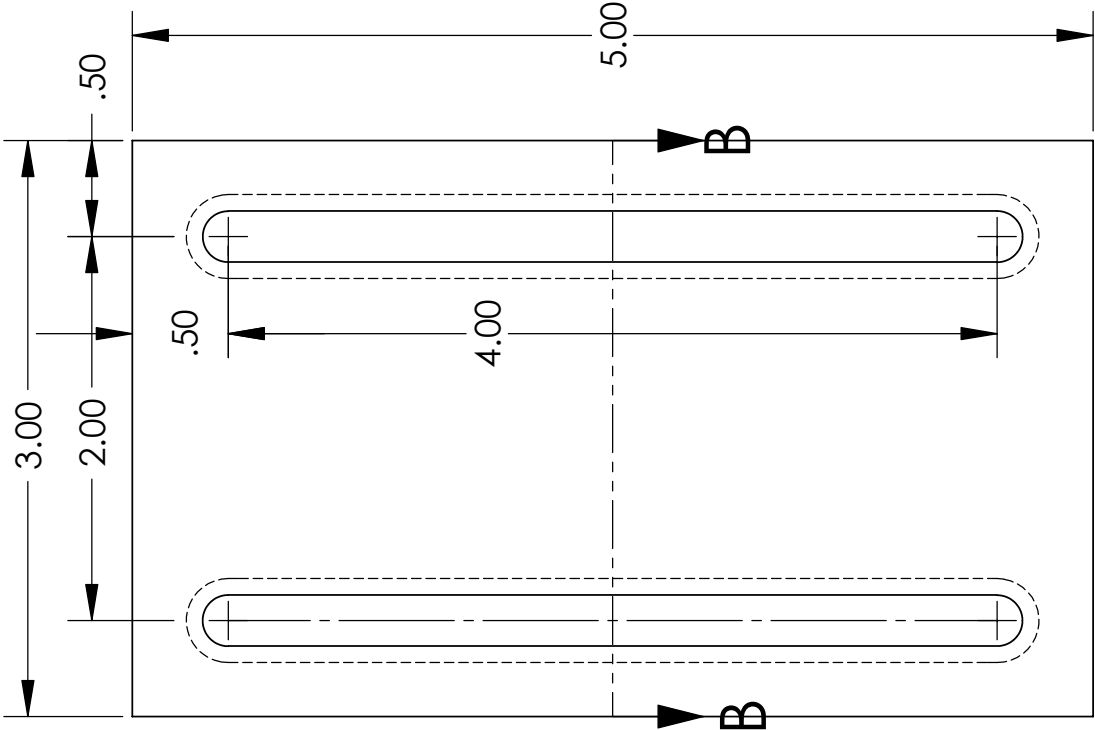
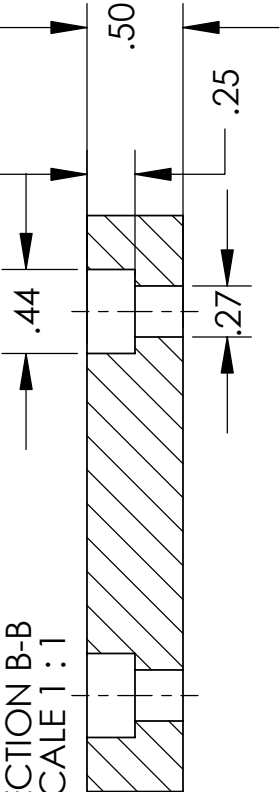


UNLESS OTHERWISE SPECIFIED:		THE RESISTOR-STAND			
DIMENSIONS ARE IN INCHES					
TOLERANCES:					
FRACTIONAL ±					
ANGULAR: MACH ± BEND ±					
TWO PLACE DECIMAL ±		DWG. NO.		REV	
THREE PLACE DECIMAL ±					
INTERPRET GEOMETRIC TOLERANCING PER:					
MATERIAL		POLYCARBONATE		Drawn By: Daniel Hildebrand	
FINISH		POLISHED			
DO NOT SCALE DRAWING					



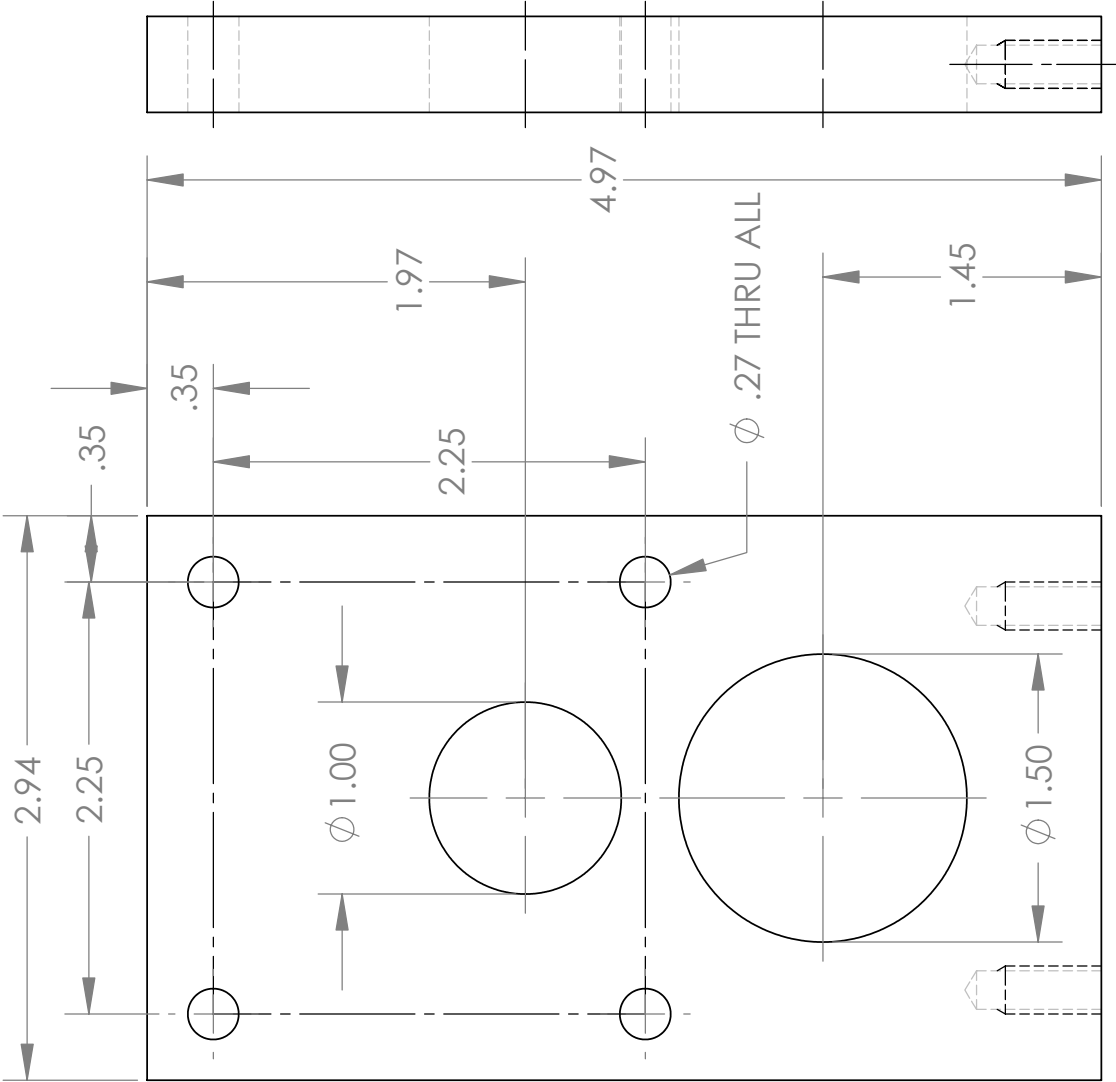
UNLESS OTHERWISE SPECIFIED: DIMENSIONS ARE IN INCHES TOLERANCES: FRACTIONAL ± ANGULAR: MACH ± BEND ± TWO PLACE DECIMAL ± THREE PLACE DECIMAL ± INTERPRET GEOMETRIC TOLERANCING PER:	TITLE: RESISTOR-OUT		
			
	MATERIAL POLYCARBONATE	DWG. NO.	REV
	FINISH POLISHED	Drawn By: Daniel Hildebrand	


SECTION B-B
SCALE 1 : 1



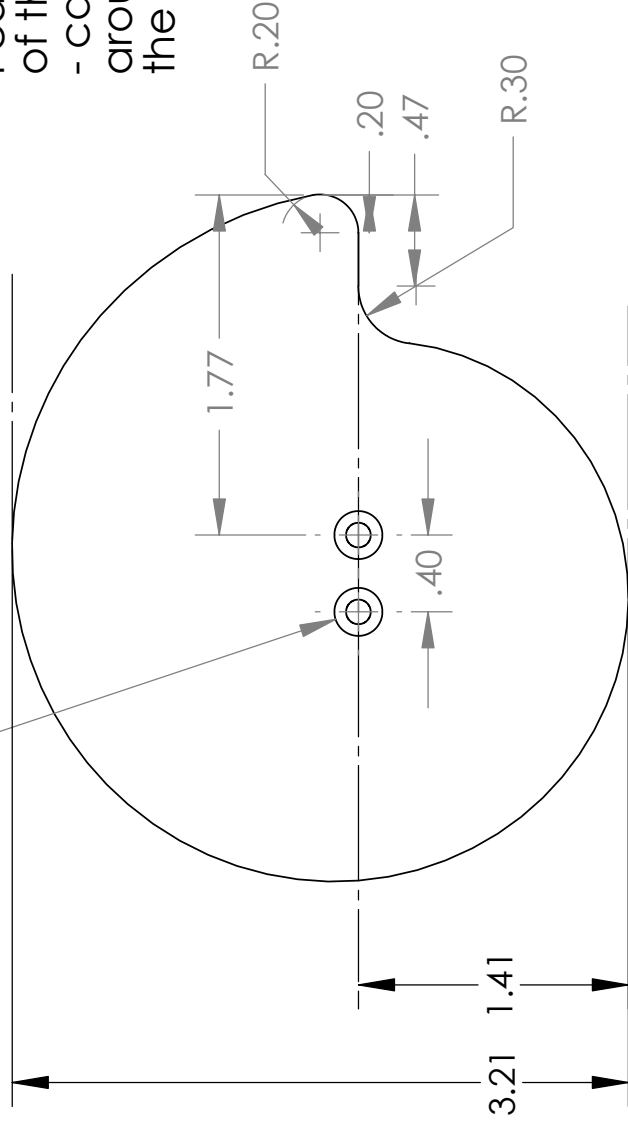
UNLESS OTHERWISE SPECIFIED: DIMENSIONS ARE IN INCHES TOLERANCES: FRACTIONAL ± ANGULAR: MACH ± BEND ± TWO PLACE DECIMAL ± THREE PLACE DECIMAL ± INTERPRET GEOMETRIC TOLERANCING PER:	TITLE: RESISTOR MOUNT		
	<div>Engineered Tissue Mechanics Lab</div>		
	MATERIAL	POLYCARBONATE	DWG. NO.
	FINISH	POLISHED	REV
DO NOT SCALE DRAWING	Drawn By: Daniel Hildebrand		



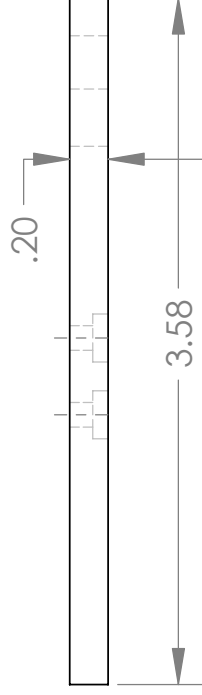


UNLESS OTHERWISE SPECIFIED:		TITLE: MOTOR-BASE	
DIMENSIONS ARE IN INCHES TOLERANCES: FRACTIONAL ± ANGULAR: MACH ± BEND ± TWO PLACE DECIMAL ± THREE PLACE DECIMAL ±			
INTERPRET GEOMETRIC TOLERANCING PER:		DWG. NO.	REV
MATERIAL	POLYCARBONATE		
FINISH	POLISHED		
DO NOT SCALE DRAWING		Drawn By: Daniel Hildebrand	

(2) ϕ .13 THRU ALL
└─┐ ϕ .25 ▽ .08




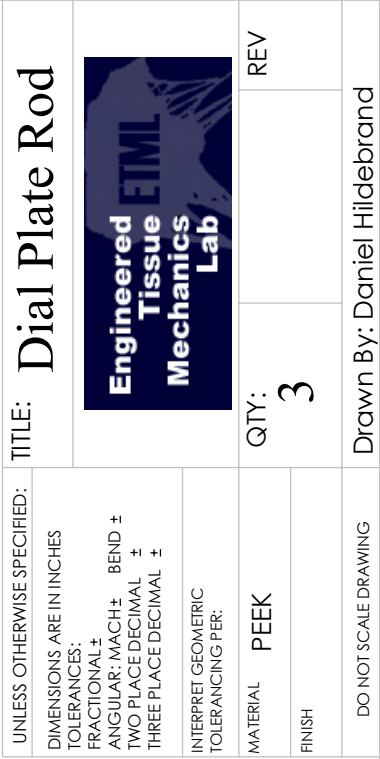
SCALE 1 : 1



Note: The edge makes a spiral pattern.

I can give you a stereolithography copy of the part which we already have
- can you have the CNC machine "scan" around the perimeter in order to make the tooling path?

UNLESS OTHERWISE SPECIFIED: DIMENSIONS ARE IN INCHES TOLERANCES: FRACTIONAL ± ANGULAR: MACH ± BEND ± TWO PLACE DECIMAL ± THREE PLACE DECIMAL ± INTERPRET GEOMETRIC TOLERANCING PER:	TITLE: Resistor Plate	
		
	MATERIAL PEEK	QTY: 3
	FINISH	REV
DO NOT SCALE DRAWING		Drawn By: Daniel Hildebrand



Appendix B

Device Control Code – LabView



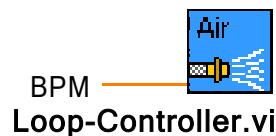
Loop-Controller.vi

C:\Documents and Settings\dan\Desktop\Loop VIs - Loop 1 - 2003-10-17\Loop-Controller.vi

Last modified on 12/2/2003 at 5:12 PM

Printed on 12/2/2003 at 5:13 PM

Connector Pane



ETML Pulsatile Bioreactor control software

- Created by Daniel Hildebrand

Front Panel

Filter

Control Parameters **Command Error**

Main Controls **Protocol**

Automatic Manual 60 BPM

P Target (mmHg) 30.00 Q Target (L/min) 3.00

P Measured 0.00 Q Measured 0.00

P Error 0.00 Q Error 0.00

Initial Air (V) 0.50

Warning: Standby Mode Disabled

Loop in Automatic Mode

Data Log File Name

Command - Air Voltage 0.0000 Beats 0

Command - Stepper 0 - R Restart Counter

START LOGGING

STOP DEVICE

Protocol **Waveform Control** **Beat Analysis**

Flow (L/min) 5 4 3 2 1 0

Pressure (mmHg) 120 110 100 90 80 70 60 50 40 30 20

Time (days) 0 1 2 3

SET PROTOCOL

Flow Pressure

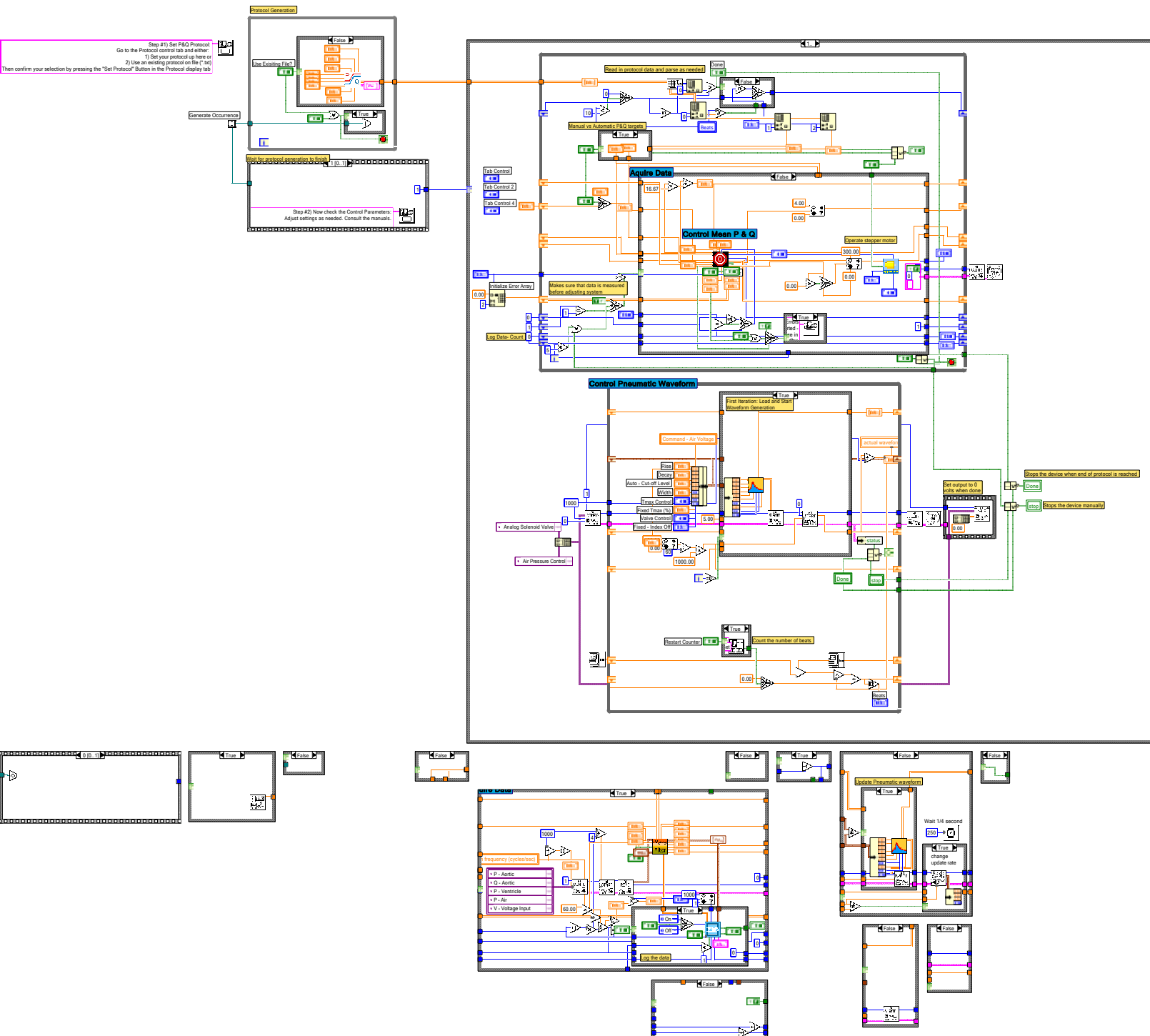
Loop-Controller.vi

C:\Documents and Settings\dan\Desktop\Loop VIs - Loop 1 - 2003-10-17\Loop-Controller.vi

Last modified on 12/2/2003 at 5:12 PM

Printed on 12/2/2003 at 5:13 PM

Block Diagram

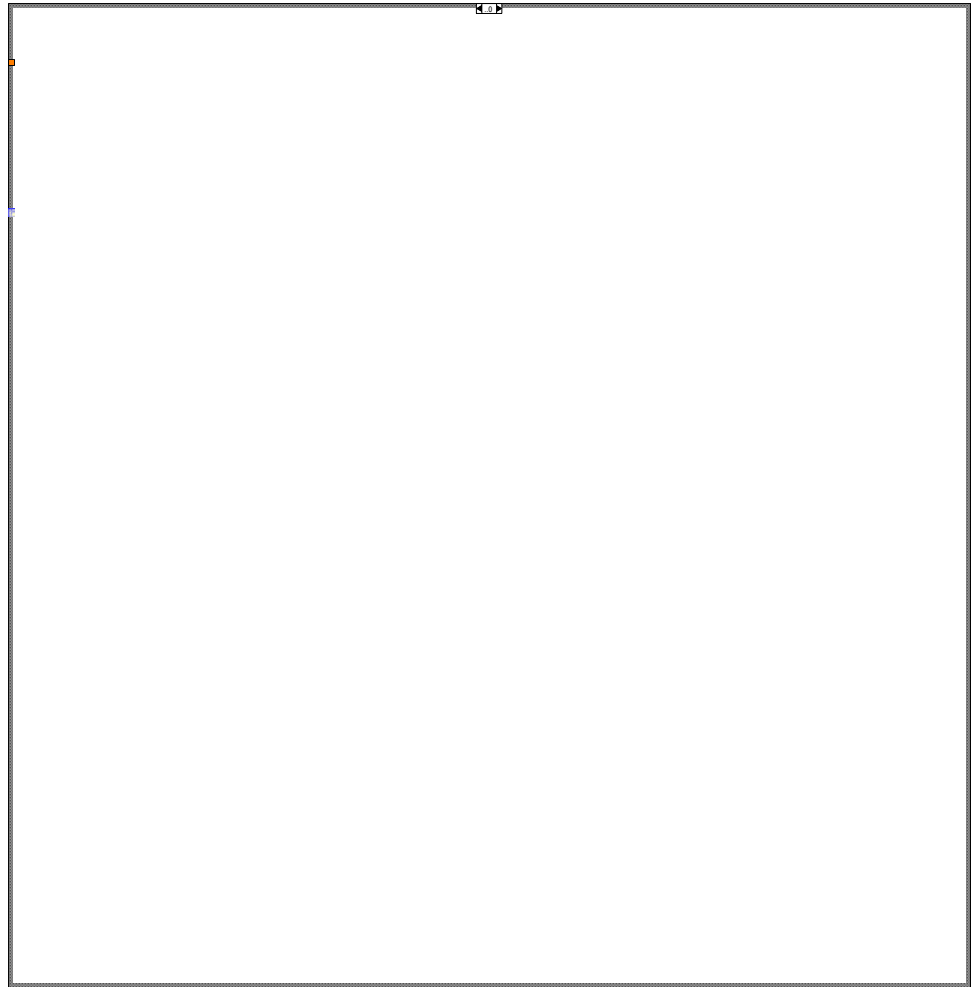


Loop-Controller.vi

C:\Documents and Settings\dan\Desktop\Loop VIs - Loop 1 - 2003-10-17\Loop-Controller.vi

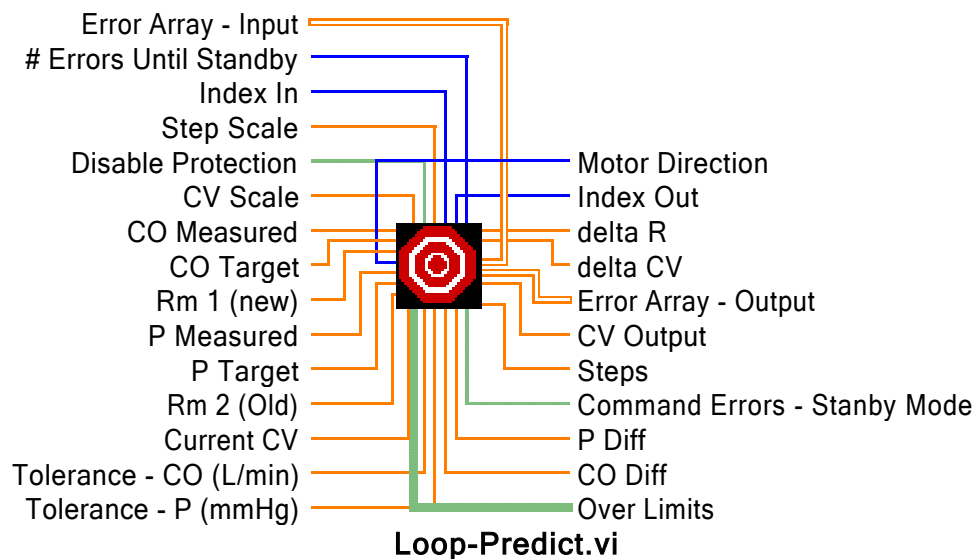
Last modified on 12/2/2003 at 5:12 PM

Printed on 12/2/2003 at 5:14 PM



Loop-Predict.vi
 C:\Documents and Settings\dan\Desktop\Loop VIs - Loop 1 - 2003-10-17\Loop-Predict.vi
 Last modified on 12/2/2003 at 5:22 PM
 Printed on 12/2/2003 at 5:24 PM

Connector Pane





Loop-Predict.vi

C:\Documents and Settings\dan\Desktop\Loop VIs - Loop 1 - 2003-10-17\Loop-Predict.vi

Last modified on 12/2/2003 at 5:22 PM

Printed on 12/2/2003 at 5:24 PM

Front Panel

CO Measured CO Diff Tolerance - CO (L/min)

0.00 0.00 0.10

CO Target

0.00

P Measured P Diff Tolerance - P (mmHg)

0.00 0.00 0.10

P Target

0.00

R Target

0.00

Rm 1 (new) A

0.00 0.00

Rm 2 (Old) B F

0.00 0.00 0.00

delta R Motor Direction

0.0000 - R

Step Scale Steps

0.40 0.00

Current CV delta CV CV Scale CV Output

0.00 0.0000 0.25 0.0000

Disable Protection

Error Array - Input

0	0.00	0.00
0	0.00	0.00
	0.00	0.00
	0.00	0.00
	0.00	0.00

Error Array - Output

0	0.00	0.00
0	0.00	0.00
	0.00	0.00
	0.00	0.00
	0.00	0.00

Over Limits

0 0

P Error Q Error

Command Errors - Standby Mode

Error Limit Array

0	0.00	0.00
0	0.00	0.00
	0.00	0.00
	0.00	0.00
	0.00	0.00

Index In Index Out

0 0

Errors Until Standby

0



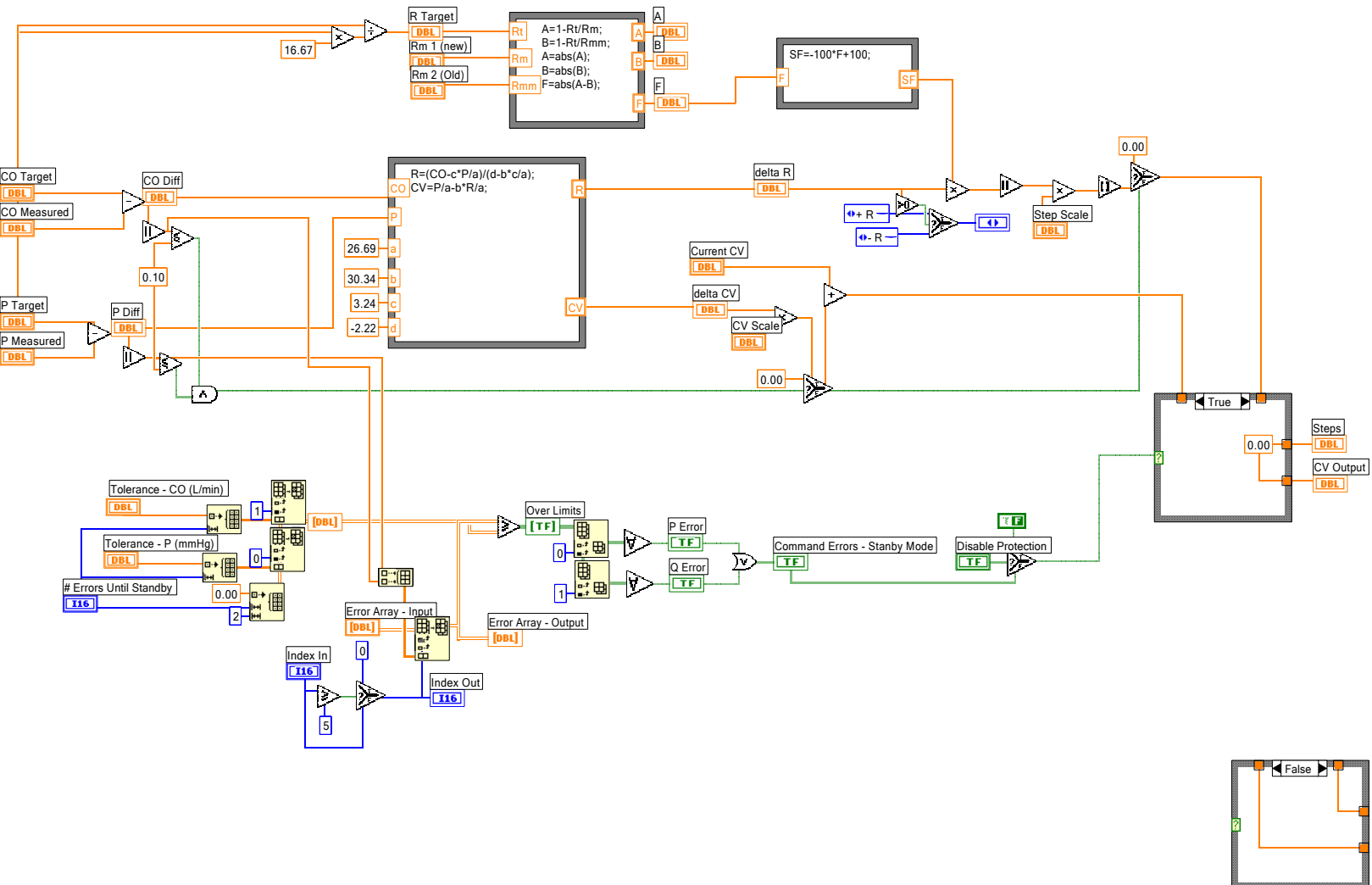
Loop-Predict.vi

C:\Documents and Settings\dan\Desktop\Loop VIs - Loop 1 - 2003-10-17\Loop-Predict.vi

Last modified on 12/2/2003 at 5:22 PM

Printed on 12/2/2003 at 5:24 PM

Block Diagram





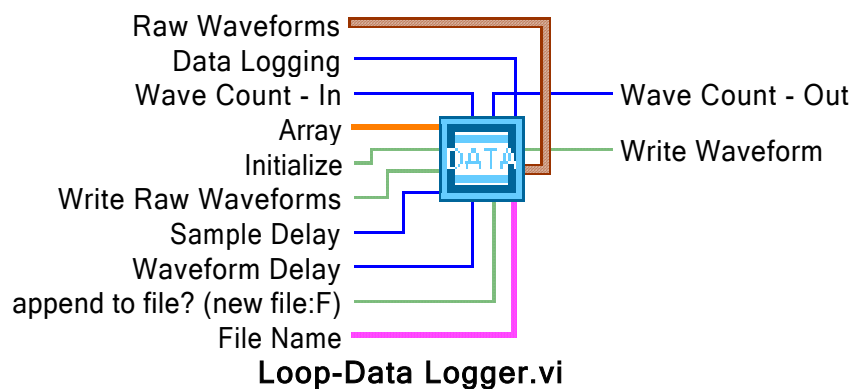
Loop-Data Logger.vi

C:\Documents and Settings\dan\Desktop\Loop VIs - Loop 1 - 2003-10-17\Loop-Data Logger.vi

Last modified on 10/10/2003 at 11:13 PM

Printed on 12/2/2003 at 5:15 PM

Connector Pane



Loop-Data Logger.vi

C:\Documents and Settings\dan\Desktop\Loop VIs - Loop 1 - 2003-10-17\Loop-Data Logger.vi

Last modified on 10/10/2003 at 11:13 PM

Printed on 12/2/2003 at 5:15 PM

Front Panel

Data Logging

On

append to file? (new file:F)

append to file

File Name

Output File Name

Array

0 0.00

Initialize

Output Array

0

Output Array:

- 1) Time
- 2) P Mean
- 3) P Max
- 4) P Min
- 5) Q Mean
- 6) Q Max
- 7) Q Min
- 8) SV Mean
- 9) CO Mean
- 10) HR
- 11) P Error
- 12) Q Error

Raw Waveforms

t0

07:00:00 PM

12/31/1903

dt

0.000000

Y

0

0.00

0.00

0.00

0.00

0.00

Write Raw Waveforms

Write Waveform

Sample Delay

0

Waveform Delay

0

Wave Count - In

0

Wave Count - Out

0

x*y

0

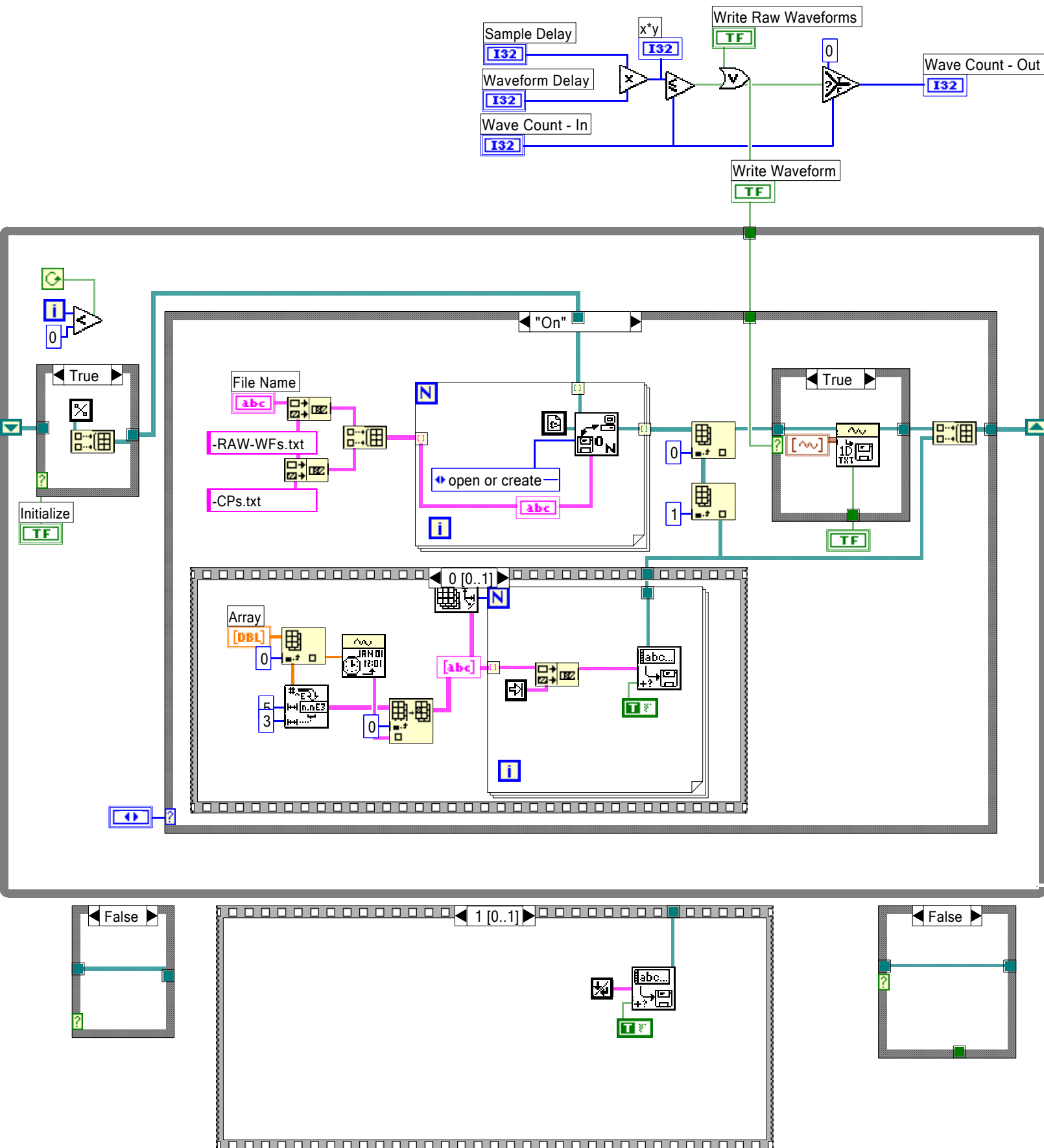
Loop-Data Logger.vi

C:\Documents and Settings\dan\Desktop\Loop VIs - Loop 1 - 2003-10-17\Loop-Data Logger.vi

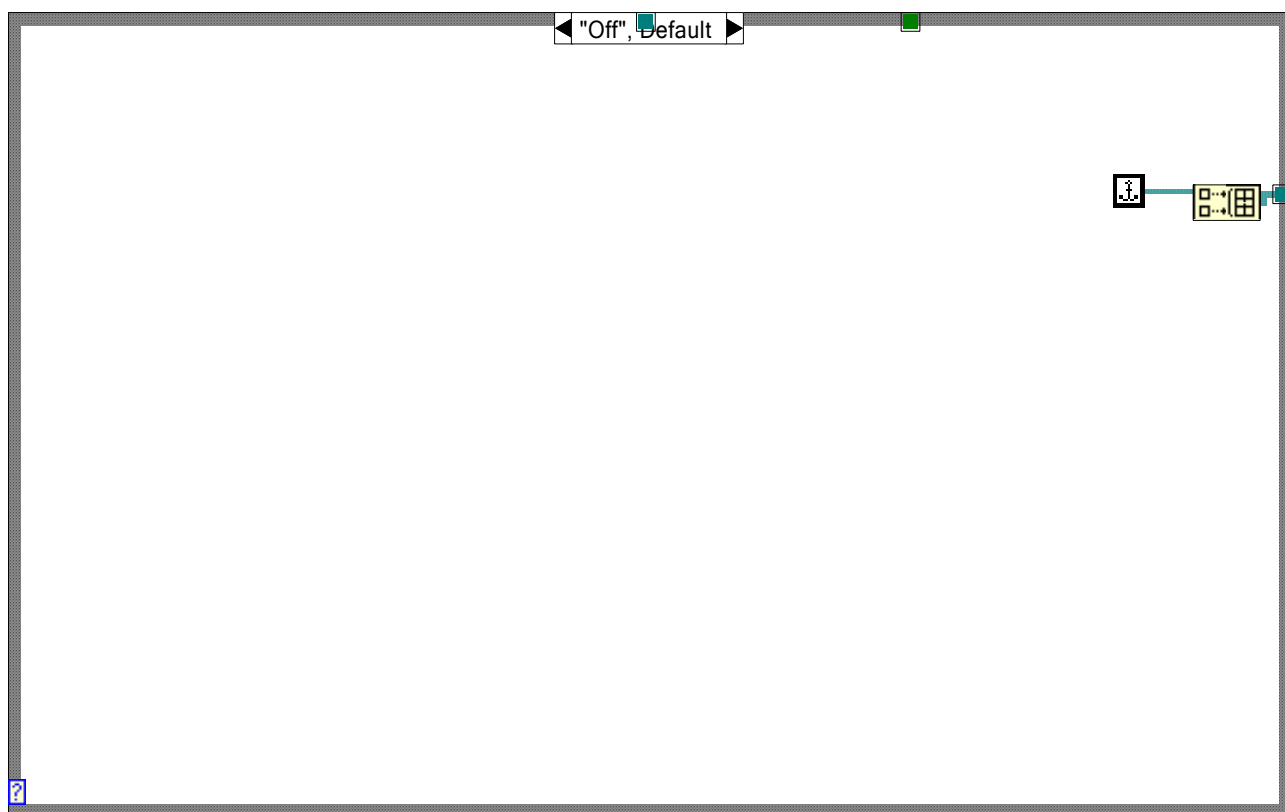
Last modified on 10/10/2003 at 11:13 PM

Printed on 12/2/2003 at 5:15 PM

Block Diagram



Printed on 12/2/2003 at 5:15 PM



Printed on 12/2/2003 at 5:23 PM

The screenshot displays the block diagram of the **Loop-Analyzer.vi**. On the left, the input section includes: **Flow Target**, **Pressure Target**, **Raw Waveforms**, **Heart Rate (Bpm)**, **Filter On**, and **IIR filter specifications**. These inputs feed into a central block labeled **Wave Filter**. On the right, the output section lists: **Output Waveforms**, **(Avg) Pressure - Mean**, **Aortic Pres - Max**, **Aortic Pres - Min**, **(Avg) Flow - Mean**, **Aortic Flow - Max**, **Aortic Flow - Min**, **Data Array**, and **(Avg) Stroke Volume (mL)**. The diagram uses color-coded lines (orange, green, brown) to trace the signal paths between the inputs, the central block, and the outputs.

Pressure & Flow Data

Filter Specs

Pressure Target

0.00

Flow Target

0.00

Heart Rate (Bpm)

0

(Avg) Pressure - Mean

0.00

(Avg) Flow - Mean

0.00

(Avg) Stroke Volume (mL)

0.00

Pressure Error

0.00

Flow Error

0.00

Cardiac Output (L/min)

0.00

Aortic Pres - Max

0.00

Aortic Flow - Max

0.00

Aortic Pres - Min

0.00

Aortic Flow - Min

0.00

Raw Waveforms

0

t0

07:00:00 PM

12/31/1903

dt

0.000000

Y

0

0.0000

0.0000

0.0000

0.0000

0.0000

Output Waveforms

0

t0

07:00:00 PM

12/31/1903

dt

0.000000

Y

0

0.0000

0.0000

0.0000

0.0000

0.0000

Data Array

0

0.00

0.00

0.00

0.00

0.00

0.00

0.00

0.00

0.00

0.00

0.00

0.00

0.00

0.00

Row:

1) Time

2) Mean P

3) Max P

4) Min P

5) Mean Q

6) Max Q

7) Min Q

8) SV

9) HR

10) Command P

11) Command Q

12) Error P

13) Error Q

Tab Control



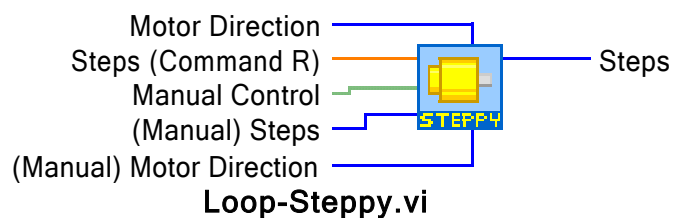
Loop-Steppy.vi

C:\Documents and Settings\dan\Desktop\Loop VIs - Loop 1 - 2003-10-17\Loop-Steppy.vi

Last modified on 8/25/2003 at 11:51 AM

Printed on 12/2/2003 at 5:17 PM

Connector Pane



Front Panel

Diagram of the Front Panel for Loop-Steppy.vi. The panel is a gray rectangle containing several controls:

- Steps (Command R)**: A numeric spinner control with a value of 0.00.
- Motor Direction**: A dropdown menu showing '- R'.
- Steps**: A numeric spinner control with a value of 0.
- Manual Control**: A toggle switch with a green indicator.
- (Manual) Steps**: A numeric spinner control with a value of 0.
- (Manual) Motor Direction**: A dropdown menu showing '- R'.
- Full/Half Step**: A dropdown menu showing 'Full'.
- milliseconds to wait**: A numeric spinner control with a value of 1.

Printed on 12/2/2003 at 5:17 PM



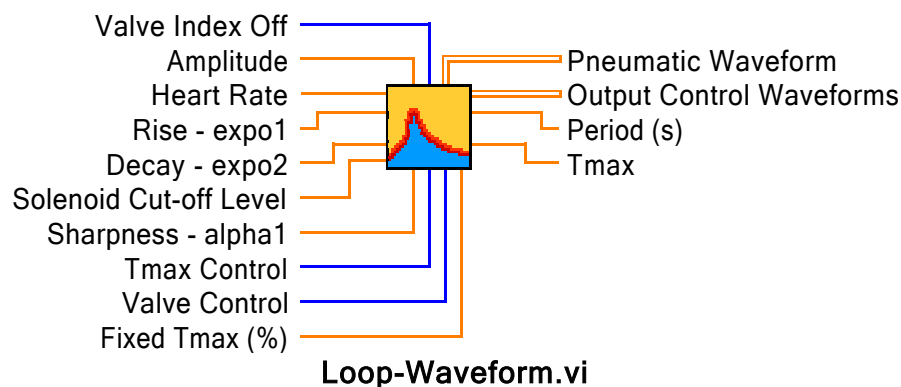
Loop-Waveform.vi

C:\Documents and Settings\dan\Desktop\Loop VIs - Loop 1 - 2003-10-17\Loop-Waveform.vi

Last modified on 8/25/2003 at 11:42 PM

Printed on 12/2/2003 at 5:18 PM

Connector Pane

**Loop-Waveform.vi**

Front Panel

Front Panel of the **Loop-Waveform.vi** showing various controls and plots:

Period (s): 0.00

Tmax: 0.00

Current time: 0.00

time step (s): 0.0000

tn: 0.00

Heart Rate: 68.00

Rise - expo1: 1.90

Decay - expo2: 21.90

Sharpness - alpha1: 0.70

Amplitude: 1.00

time resolution: 0.001

Solenoid Cut-off Level: 0.010

Fixed Tmax (%): 33.00

Valve Index Off: 600

Output Control Waveforms: 0

Tmax Control: Fixed Position

Valve Control: Fixed Position

Activation Function - Look Up Table: (Empty grid)

Pneumatic Waveform: (Plot of Pneumatic CV vs Data Points)

The **Pneumatic Waveform** plot shows the relationship between **Pneumatic CV** (Y-axis, 0.0 to 1.6) and **Data Points** (X-axis, 0 to 1000). The plot area is currently empty.



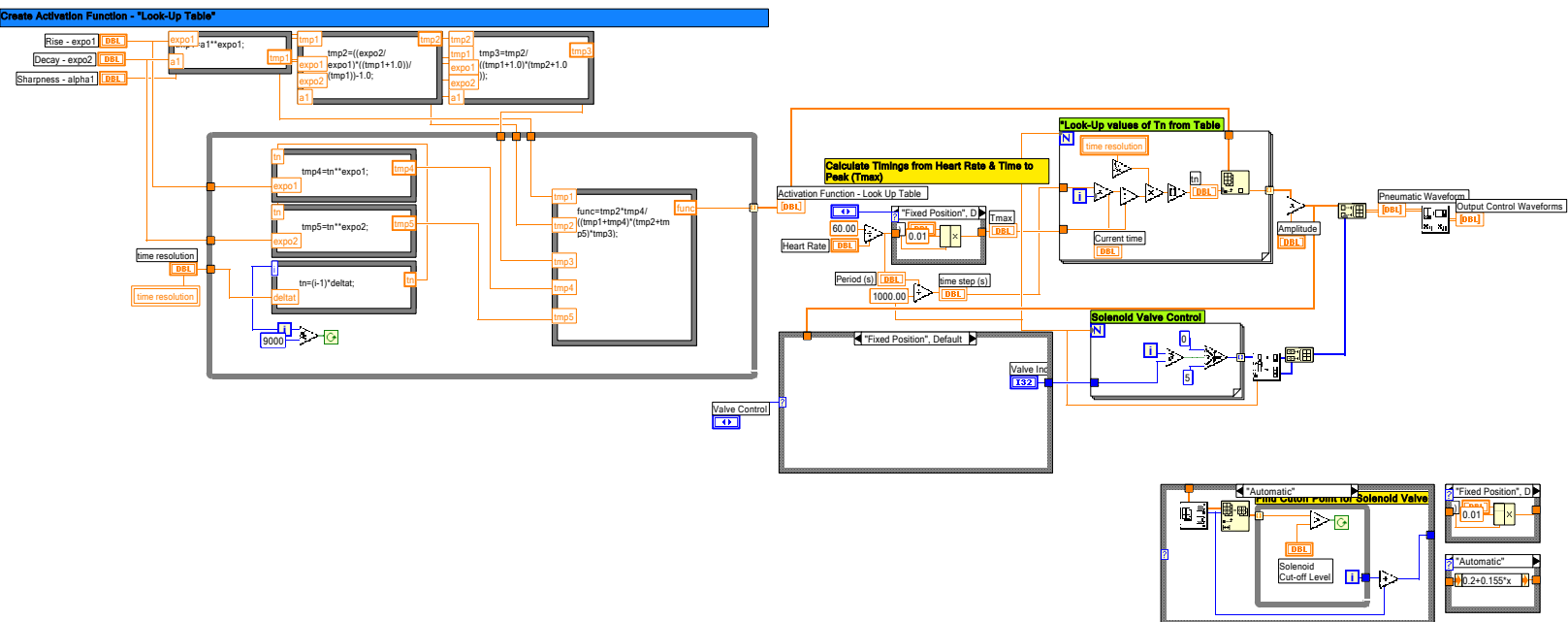
Loop-Waveform.vi

C:\Documents and Settings\dan\Desktop\Loop VIs - Loop 1 - 2003-10-17\Loop-Waveform.vi

Last modified on 8/25/2003 at 11:42 PM

Printed on 12/2/2003 at 5:18 PM

Block Diagram



Appendix C

Input-Impedance Code - MatLab

```
clc
clear
close
```

```
%Read in Data
load tehv2_1.txt
load tehv2_2.txt
load hydro6.txt
load pulmon.txt
load pulmon2.txt
load systemic3.txt
load systemic2.txt
load unfilt.txt
load filt.txt
load shroff.txt
```

```
T21=tehv2_1;
T22=tehv2_2;
H6=hydro6;
PUL=pulmon;
PUL2=pulmon2;
SYS=systemic3;
SYS2=systemic2;
FIL=filt;
UNFIL=unfilt;
SHROFF=shroff;
```

```
data=input('Which data set to analyze? (Ex. ''T21'' for TEHV2_1): ');
```

```
%Number of data points
count=size(data,1)/2; %(divide by 2 usually; divide by 1 for human data from
m shroff- shroff.txt)
```

```
%Assign data
P=data(1:count,1);
Q=data(1:count,2)*16.667; %convert to ml/s;
T=1; % period in seconds (1 for 60bpm; 0.735 for human data from shroff- shroff.txt)
time=(0:(T/((count-1))):T);
```

```
%*****
%           Frequency Domain Data
%*****
```

```
Pfft=fft(P,count);
Pfft=Pfft(1:12);
Pmag=abs(Pfft);
Pang=angle(Pfft)*180/pi;
```

```
Qfft=fft(Q,count);
Qfft=Qfft(1:12);
Qmag=abs(Qfft);
Qang=angle(Qfft)*180/pi;
```

```
Zin=Pfft./Qfft;
Zmag=abs(Zin);
Zang=angle(Zin);
```

```
%*****
%           Calculation of Parameters
%*****
```

```
HR=(60/T);
AOPmean=mean(P);
AOFmean=mean(Q);
SV=cumtrapz(time,Q);
SV=SV(count);
CO=SV*HR;
```

```
%Power terms
convt=1333*10^-7;
Wsteady=AOPmean*AOFmean*convt;
Wtot=P.*Q;
Wtot=mean(Wtot)*convt;
Wosc=Wtot-Wsteady;
Wfrac=abs(Wosc/Wtot)*100;
```

```
%Systemic vascular resistance
R=AOPmean/AOFmean;
```

```
%*****
%           Area Computations
%*****
```

```
%Find Qend_diastolic and Qend_systolic
[Pmax,Pmax_index] = max(P);
[Qmin,Index_post_incisura]=min(Q);
```

```
%Find start of systolic/end of diastolic as the point where flow rate exceeds some threshold value
Qstart_index=min(find(4 < Q));
Pend_dia=P(Qstart_index);
Pend_dia_index=Qstart_index;
[Qmax,Integration_End]=max(Q);
[Pend_sys,Pend_sys_index]=min(P(Pmax_index:Index_post_incisura));
Pend_sys_index=Pend_sys_index+Pmax_index;
[Pmax2,Pmax2_index]=max(P(Pend_sys_index:count));
```

```
Pmax2_index=Pend_sys_index+Pmax2_index;
```

```
%Area of first Diastolic Portion
```

```
Area_dia_1=cumtrapz(time(1:Pend_dia_index),P(1:Pend_dia_index));
```

```
A1_size=size(Area_dia_1);
```

```
Area_dia_1=Area_dia_1(A1_size);
```

```
Area_dia_1=Area_dia_1(1);
```

```
%Area of second Diastolic Portion
```

```
Area_dia_2=cumtrapz(time(Pmax2_index:count),P(Pmax2_index:count));
```

```
A2_size=size(Area_dia_2);
```

```
Area_dia_2=Area_dia_2(A2_size);
```

```
Area_dia_2=Area_dia_2(1);
```

```
%Total Diastolic and Systolic Areas
```

```
Area_dia=Area_dia_1+Area_dia_2;
```

```
Area_total=cumtrapz(time,P);
```

```
Area_total=Area_total(count);
```

```
Area_sys=Area_total-Area_dia;
```

```
%*****  
%           Area Related Calculations, C, RC, RC_T  
%*****
```

```
%Compliance with area method
```

```
K=(Area_sys+Area_dia)/Area_dia;
```

```
C=SV/(K*(Pmax2-Pend_dia));
```

```
%Compute RC & RC/T with area method
```

```
RC=Area_dia/(Pend_sys-Pend_dia);
```

```
RC_T=RC/T;
```

```
%Compute Z0, characteristic impedance using upper harmonics
```

```
Z0=mean(Zmag(4:12));
```

```
%Z0 time domain
```

```
delta_t=time(2)-time(1);
```

```
time_pts=0;
```

```
pts=0;
```

```
while (time_pts<0.05)
```

```
    time_pts=time_pts+delta_t;
```

```
    pts=pts+1;
```

```
end
```

```
end_time=Qstart_index+pts;
```

```
Z0_time=mean(P(Qstart_index:end_time))/mean(Q(Qstart_index:end_time));
```

```
%Forward and backward waveforms
```

```
for i=1:count
Pf(i)=(P(i)+Z0*Q(i))/2;
Pb(i)=(P(i)-Z0*Q(i))/2;
Qf(i)=Pf(i)/Z0;
Qb(i)=-Pb(i)/Z0;
end

%Reflection Coefficient
Reflection_1st=(Zmag(1)-Z0)/(Zmag(1)+Z0);
RI=(max(Pb)-min(Pb))/(max(Pf)-min(Pf));

%*****
%           Results
%*****
S = struct('T',T,'HR',HR,'AOPmean',AOPmean,'AOFmean',AOFmean,'SV',SV,'CO',C,✓
O,'Wtotal',Wtot,'Wsteady',Wsteady,'Wosc',Wosc,'Wfrac',Wfrac,'R',R,'C',C,'Z0'✓
',Z0,'RC',RC,'RCperT',RC_T,'Ref_C',Reflection_1st,'Ref_Index',RI,'Z0_time',✓
Z0_time)

set(gcf,'DefaultLineLineWidth',3)

subplot(221);plot(time,P,time,Pf,time,Pb)
title('Pressure');
xlabel('Time (s)');
ylabel('P (mmHg)');
legend('Pmeas','Pf','Pb');

subplot(222);plot(time,Q,time,Qf,time,Qb)
title('Flow Rate');
xlabel('Time (s)');
ylabel('Q (ml/s)');
legend('Qmeas','Qf','Qb');

subplot(223);plot(Zmag)
title('Impedance');
line([8 12],[Z0 Z0],'Color','k');
xlabel('Freq (Hz)');
ylabel('|Zin| (mmHg s/ml)');

Zang=Zang*180/pi;

subplot(224);plot(Zang)
title('Phase Angle');
line([0 15],[0 0],'Color','k');
xlabel('Freq (Hz)');
ylabel('Phase Angle of Zin (deg)');
```

Appendix D

Device Software Manual

The ETML Pulsatile Bioreactor



Software



V 1.0



Contents

Software: Contents

- Viewing the waveforms
 - **Waveform Analysis**
- Running the loop
 - **Manual Mode**
 - The user can control all aspects of the device
 - **Automatic Mode**
 - The computer controls all aspects of the device
- How mean pressure and flow rate levels vs. time are set up
 - **Protocol**
- The shape of the ventricular waveform
 - **Waveform Shape**
- How the system responds to events
 - **System Control Parameters**
- Data files – saving, format, etc....
 - **Data**
- Removing signal noise
 - **Filtering**

Software: Contents

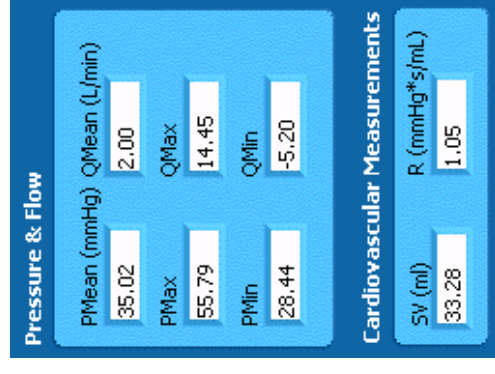
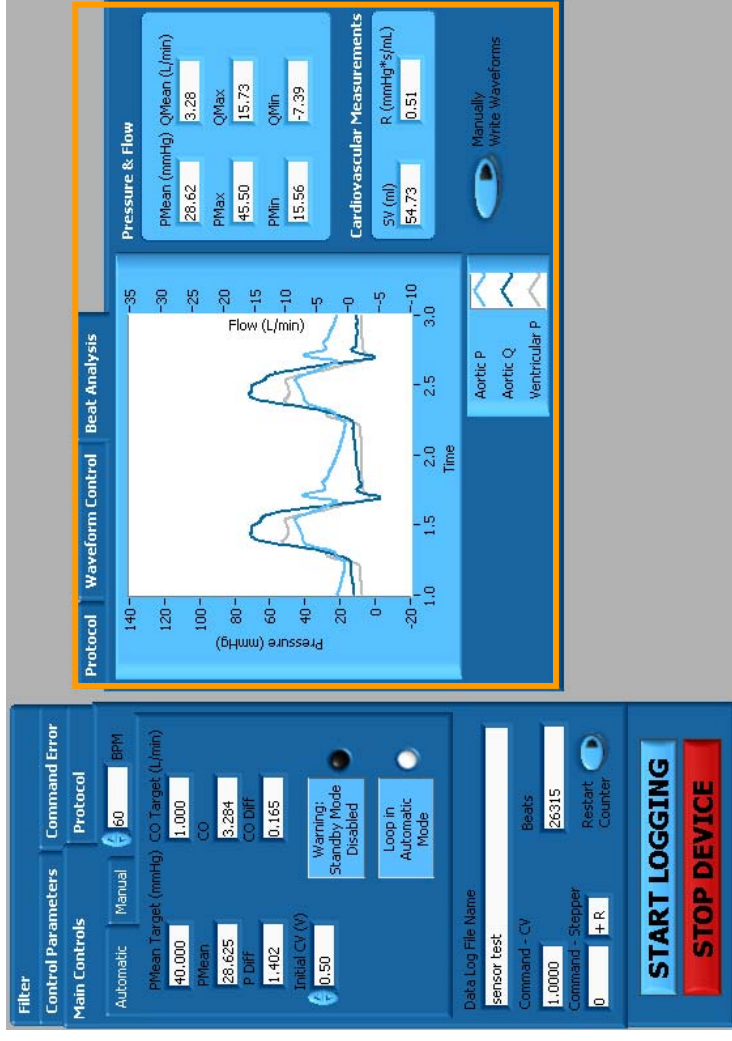
- Performing a Standard Experiment
 - Performing an Experiment
- Miscellaneous
 - Other Stuff



Waveform Analysis

Waveform Analysis

- To view the waveforms while the loop is running, click on the **Beat Analysis** tab
- The following waveforms are displayed:
 - Outflow Pressure (Aortic P)
 - Flow Rate (Aortic Q)
 - Ventricular Pressure
- Common computed parameters are displayed on the right:
 - P & Q: Mean, max, min values
 - Stroke volume (SV)
 - mL ejected per beat
 - Resistance (R)
 - “Peripheral resistance”
 - $R = P_{\text{mean}}/Q_{\text{mean}}$
- Write Waveforms**
 - Saves the waveforms to file
 - See **Saving Data**

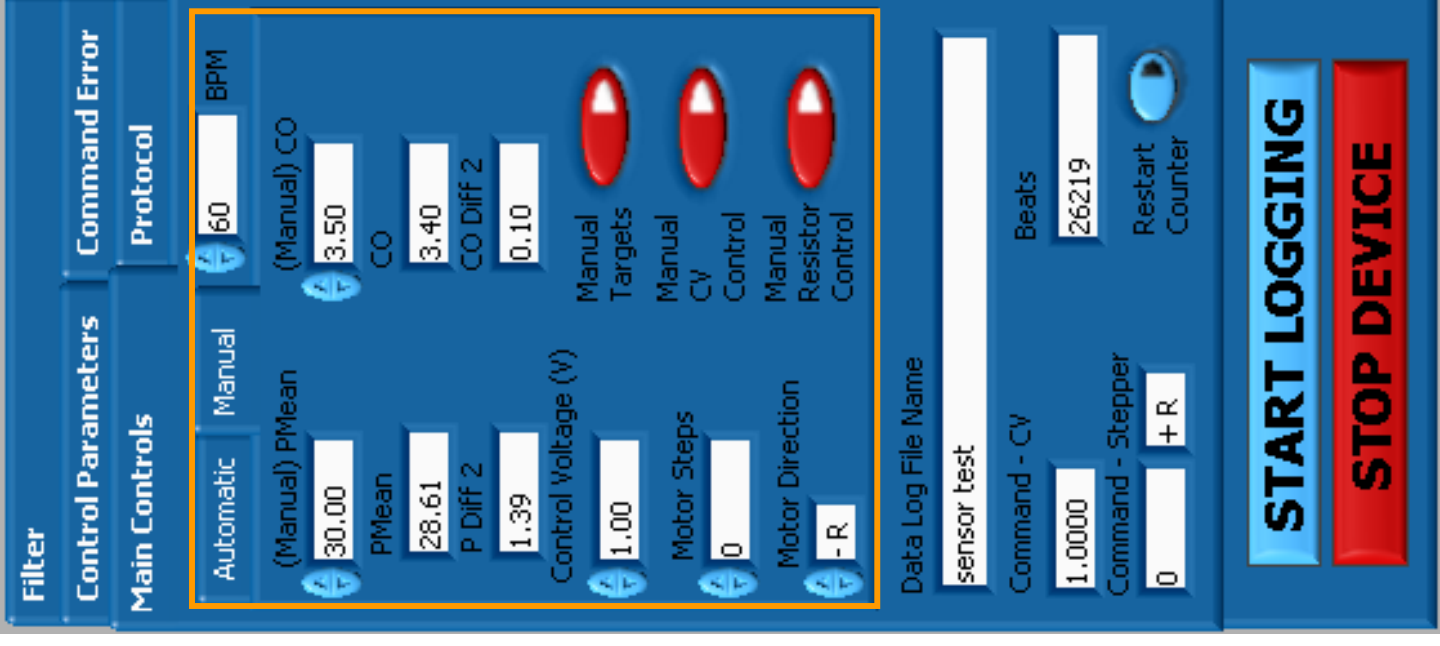




Manual Mode

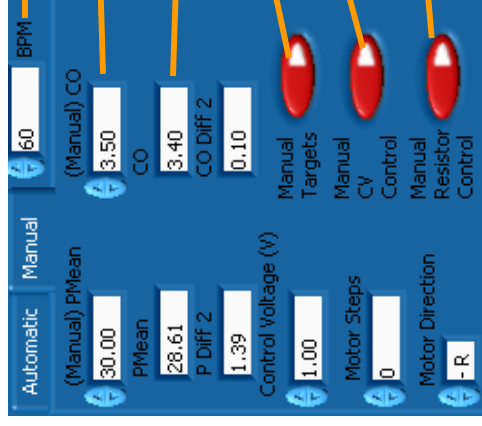
Manual Mode

- Location
 - Main Controls
 - Manual Tab
- Use Manual Mode for:
 - User defined P&Q target levels as opposed to protocol based levels
 - Use: **Manual Targets Mode**
 - Disabling the computer-based or automatic control system
 - Use: **Manual Air (CV) Control**
 - Use: **Manual Resistor Control**
- Putting the Loop into Manual Mode
 - Loop is set up by default to be in manual mode
 - Depends on which features you want to disable (see Use Manual Mode for)

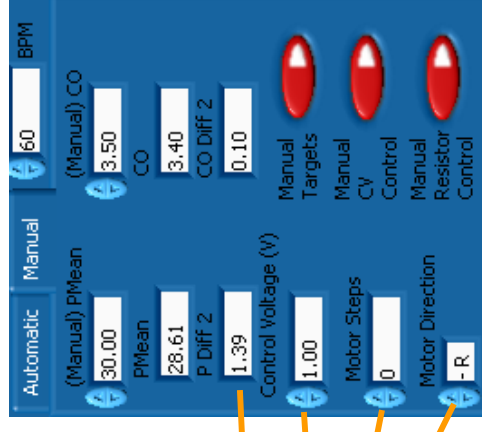


Operating the Loop – Manual Mode

- **Heart Rate**
 - # of beats or cycles per minute
- **Manual P&Q Targets**
 - Only active if **Manual Targets Mode** button is switched
- **P&Q Command Errors**
 - Difference between measured and manual target values
- **Manual Targets Mode**
 - The program will ignore the current protocol based targets and use the values given in **Manual P&Q Targets**
 - This mode is active by default
 - This button does not disable automatic controls by itself
- **Manual Air (CV) Control**
 - Disables automatic air control
 - Uses **Manual Air (CV) Value**
- **Manual Resistor Control**
 - Disables automatic resistor control
 - Uses **Manual Resistor Steps & Resistor Direction** values



- Heart rate
- Manual P&Q Targets
- Measured P&Q
- Manual Targets Mode
- Manual Air (CV) Control
- Manual Resistor Control



- P&Q Command Errors
- Manual Air (CV) Value
- Manual Resistor (Motor) Steps
- Manual Resistor Direction ($\pm R$)

Software



Automatic Mode

Automatic Mode

- Location
 - Main Controls
 - Automatic Tab
- Use Automatic Mode for:
 - Protocol based P&Q levels as opposed to user defined target levels
 - Long-term testing
- Putting the Loop in Automatic Mode
 - Disable the following
 - **Manual Air (CV) Control**
 - **Manual Resistor Control**
 - Also, for protocol based P&Q targets
 - Disable: **Manual Targets Mode**
 - See Manual Mode

Filter Control Parameters Command Error Protocol

Main Controls Manual BPM 60

P Mean Target (mmHg) 40.000 CO Target (L/min) 1.000

P Mean 28.625 CO 3.284

P Diff 1.402 CO Diff 0.165

Initial CV (V) 0.50

Warning: Standby Mode Disabled

Loop in Automatic Mode

Data Log File Name sensor test

Command - CV 1.0000 Beats 26315

Command - Stepper 0 + R Restart Counter

START LOGGING

STOP DEVICE

Operating the Loop – Automatic Mode

- **Heart Rate**
 - # of beats or cycles per minute
- **Current P&Q Targets**
 - Protocol based P&Q target levels
- **P&Q Command Errors**
 - Difference between measured and target values
- **Initial Air (CV) Value**
 - When the loop first runs, this is the air (CV) value that is used
 - This value will not be used after initial loop start-up

The screenshot shows the 'Automatic' mode control panel. It features a 'Manual' button and a 'BPM' display showing '60'. Below this are four rows of controls: 'PMean Target (mmHg)' with a value of '30.00', 'CO Target (L/min)' with a value of '3.00', 'PMea' with a value of '0.00', and 'CO Diff' with a value of '0.00'. At the bottom, there is an 'Initial CV (V)' field with a value of '0.50'. Four orange lines with labels point to specific fields: 'Heart rate' points to the BPM display, 'Current P&Q Targets' points to the CO Target field, 'Measured P&Q' points to the PMea field, and 'P&Q Command Errors' points to the CO Diff field.

Automatic	Manual	BPM
PMean Target (mmHg)	30.00	CO Target (L/min)
CO	3.00	PMea
PMea	0.00	CO Diff
P Diff	0.00	Initial CV (V)
Initial CV (V)	0.50	

The screenshot shows the 'Manual' mode control panel. It features a 'Manual' button and a 'BPM' display showing '60'. Below this are four rows of controls: 'PMean Target (mmHg)' with a value of '30.00', 'CO Target (L/min)' with a value of '3.00', 'PMea' with a value of '0.00', and 'CO Diff' with a value of '0.00'. At the bottom, there is an 'Initial CV (V)' field with a value of '0.50'. An orange line with the label 'Initial Air (CV) Value' points to the 'Initial CV (V)' field.

Automatic	Manual	BPM
PMean Target (mmHg)	30.00	CO Target (L/min)
CO	3.00	PMea
PMea	0.00	CO Diff
P Diff	0.00	Initial CV (V)
Initial CV (V)	0.50	

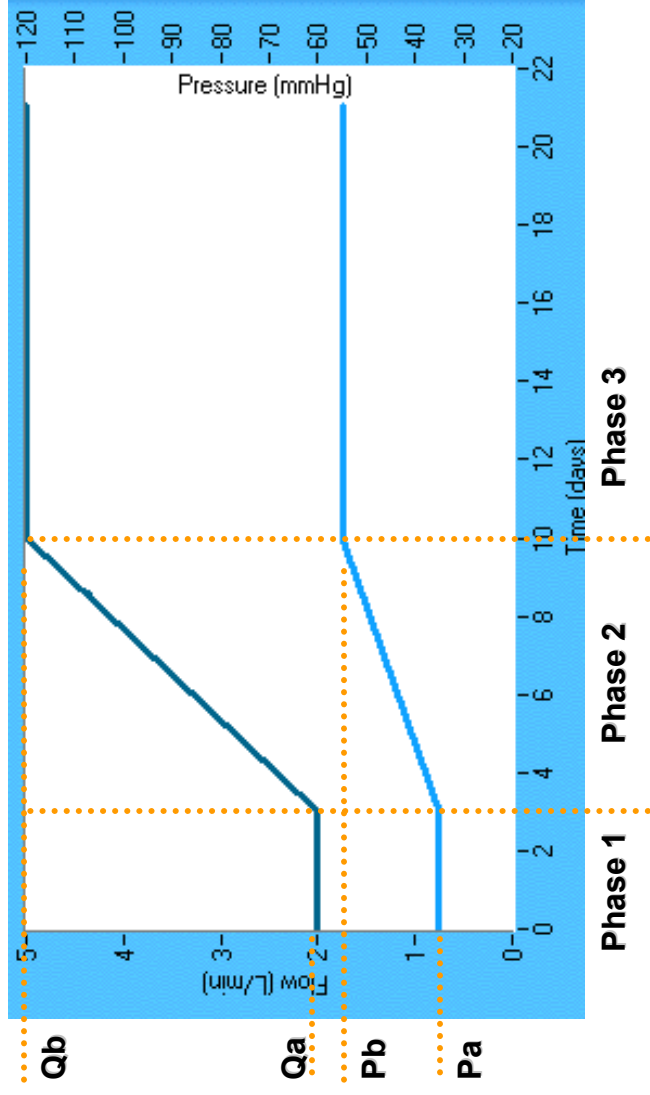
Software



Protocol

P&Q Protocol

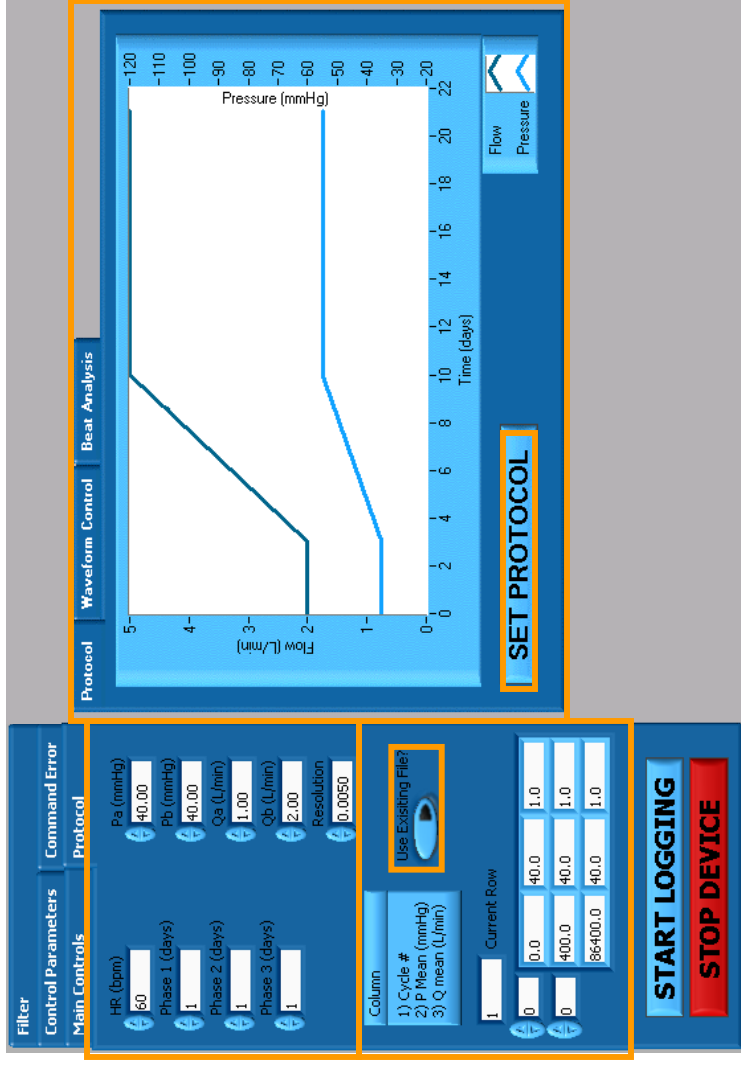
- **P&Q Protocol**
 - The values of mean pressure and flow over the course of the study (aka P,Q vs time)
 - The device will shut down at the end of the protocol (after the last beat # is read)
 - This portion of the program generates an array of pressure and flow values for a given beat #
 - Ex: Beat # - Pressure - Flow Rate
 - 27800 33.125 3.005
 - 28000 33.128 3.010
- The study is divided into 3 phases:
 - **Phase 1** – Initial steady state
 - **Phase 2** – Ramping period
 - **Phase 3** – Final steady state
- The phases are measured in days
- **Levels**
 - Initial levels: **Pa, Qa**
 - Final levels: **Pb, Qb**
- **Resolution**
 - The smallest incremental change in P or Q values during Phase 2
 - The default value is fine for most tests



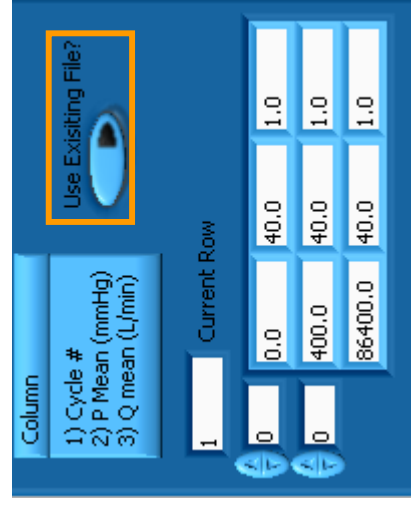
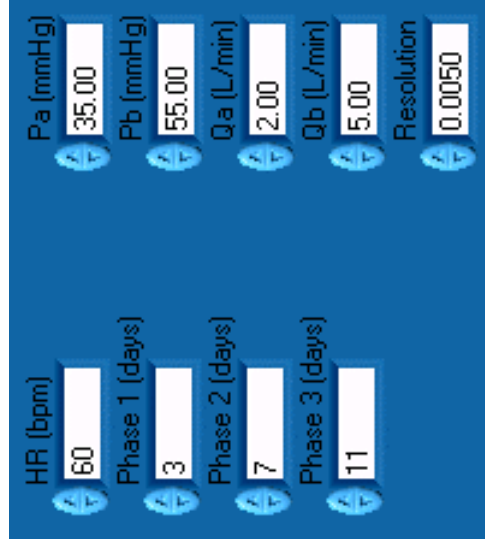
HR (bpm)	<input type="text" value="60"/>	Pa (mmHg)	<input type="text" value="35.00"/>
Phase 1 (days)	<input type="text" value="3"/>	Pb (mmHg)	<input type="text" value="55.00"/>
Phase 2 (days)	<input type="text" value="7"/>	Qa (L/min)	<input type="text" value="2.00"/>
Phase 3 (days)	<input type="text" value="11"/>	Qb (L/min)	<input type="text" value="5.00"/>
		Resolution	<input type="text" value="0.0050"/>

Setting the P&Q Protocol

- **Adjust:**
 - **Use Existing File**
 - Select this if you want to use a protocol already created (*.txt)
 - **Heart Rate**
 - Important – make sure this will be the same HR that is used in running the loop
 - **Phases**
 - **Initial values: Pa, Qa**
 - **Final values: Pb, Qb**
 - **Resolution**
 - Default value is fine for most tests
- **Set the protocol**
 - Press the **Set Protocol** button when finished adjusting values



- **Protocol data will be displayed when protocol is set**
 - The **Current Row** display indicates which row is being used by the program

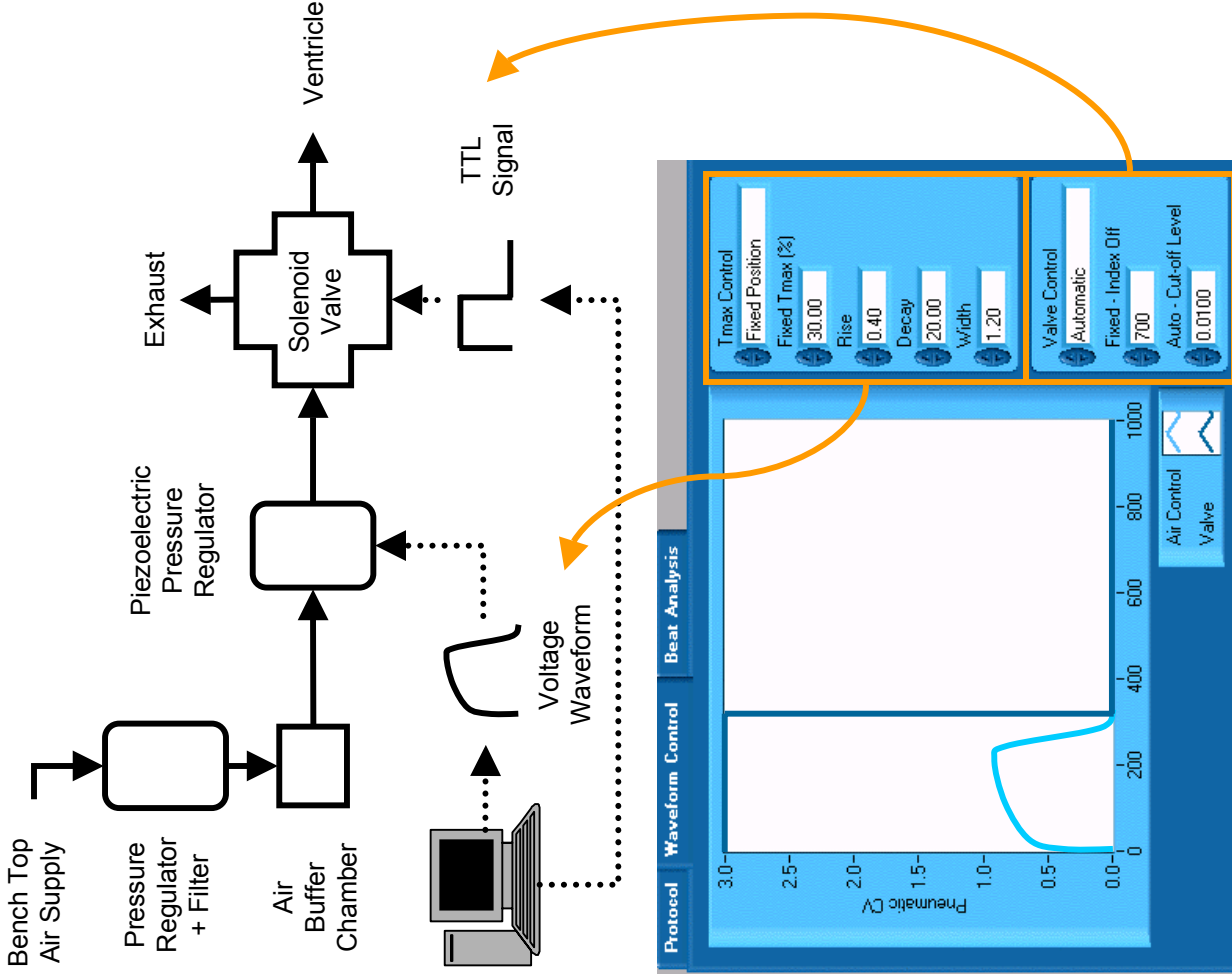




Waveform Shape

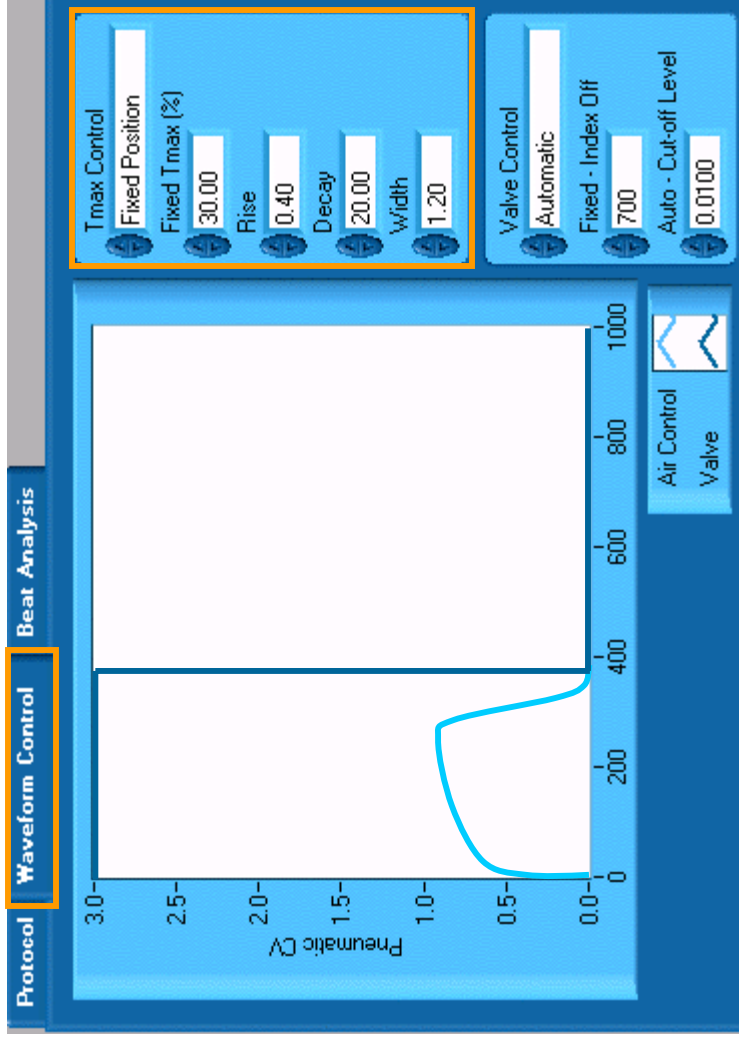
Changing the Shape – Air Pressure Control

- The Waveform Control section is used to control 2 things:
 - The Voltage Waveform
 - The shape of the air pressure waveform
 - Not the magnitude – this produces a normalized function
 - TTL Signal
 - When the air is sent to the bladder for pumping (~systole) and when it is allowed to exhaust (~diastole)
- When might you need to change these settings?
 - When running near the upper limits of flow
 - Filling time becomes CRUCIAL and you may need to change the systolic/diastolic ratio
 - This is done by changing one or more of the following:
 - **Tmax** (Lower value to increase diastole)
 - **Rise** (Decrease value to push the flow “harder”)
 - **Decay** and **Width** as needed
 - Also, the valve controls could be adjusted but this is not recommend until the above options have been tried
 - To achieve a different pressure waveform shape



Air Pressure Control

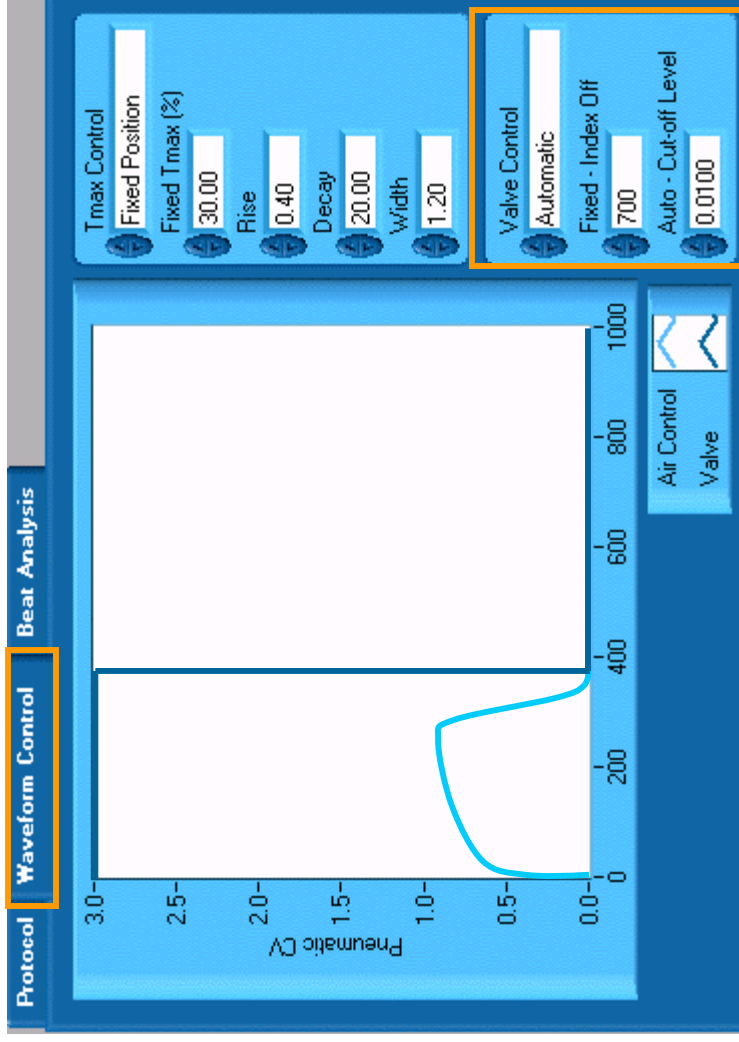
- **Voltage Waveform**
 - **Tmax Control**
 - Location of peak pressure (~peak systole)
 - **Fixed Position**
 - Uses **Fixed Tmax** value
 - **Automatic**
 - Uses the equation: $T_{max} = 0.2 + 0.155 \cdot \text{period}$
- **Rise**
 - The rate of growth of the waveform
- **Decay**
 - The rate of decay of the waveform
- **Width**
 - The distance between rise and decay



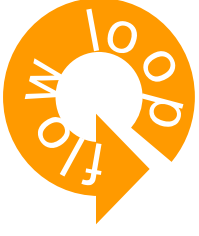
Air Pressure Control

- TTL Signal
 - Valve Control
 - Controls when air can fill / exhaust the air chamber
 - Automatic
 - Valve will exhaust at a fixed time point in the cycle
 - Uses the **Auto Cut-Off Level** value
 - Fixed
 - Valve will exhaust at a fixed time point in the cycle
 - Uses the **Fixed Index Off** value
 - Fixed Index Off
 - Index value (out of 1000)
 - Auto Cut-Off Level
 - Voltage value

TTL Signal  Air to ventricle (systole)
Air to exhaust (diastole)



Software



System Control Parameters

Control Parameters

- **Command Error Tolerances**
 - If something unexpected was to happen to the loop such as:
 - Mechanical failure of the valve(s)
 - Rupture of the air bladder
 - Failure of the resistor
 - Excessive drop in inlet air pressure
 - Excessive leaking
 - The system would generate larger than normal command errors in either or both P & Q
 - The **P Tolerance** and **Q Tolerance** are the thresholds for the levels at which the program will know there is “something wrong”
 - **# of Errors Until Standby** is just how many of these errors in a row are needed before the system goes into **Standby Mode**
- **Example: With the settings shown:**
 - A P error would be a **P Command Error** that is greater than or equal to 2.00
 - A **Q Command Error** would be one that is greater than or equal to 0.60
 - It will take at least 5 of these values in a row (in either P OR Q) to cause the device to go into **Standby Mode**
- **Warning Off** turns of the text warning that the device is in **Standby Mode**

The screenshot shows a control interface with three main tabs: Main Controls, Filter, and Protocol. The 'Main Controls' tab is active, displaying 'Control Parameters' and 'Command Error' sections.

Command Error Tolerances:

- P Tolerance: 5.00
- Q Tolerance: 1.00
- # Errors Until Standby: 5
- Warning Off: (toggle switch)
- Disable Standby Mode: (button)

Data Logging:

- Sample Delay: 4
- Waveform Delay: 30
- ~Min/Sample: 0.33
- ~Min/Waveform: 10.00
- ~Min/Waveform = Min/Sample * Waveform Delay

Response Tuning:

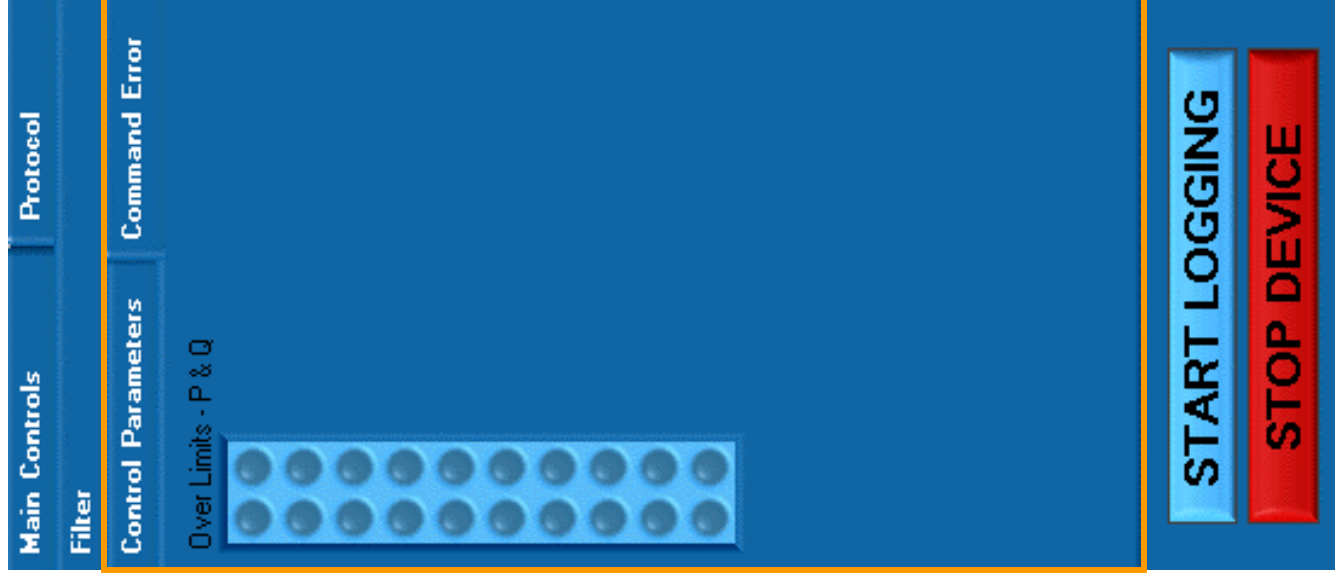
- Resistor Tuning: 4.80
- Voltage Tuning: 0.30

Buttons:

- START LOGGING
- STOP DEVICE

Control Parameters

- Command Error Tolerances
 - Command Error Tab
 - Displays errors in a boolean (true/false) array where:
 - Column 1 = P Error
 - Column 2 = Q Error



Control Parameters

- Data Logging
 - **Sample Delay** controls the rate at which data is saved to the files
 - The value to the right of the control shows the current value of the delay
 - Use larger levels (30+) for most long-term tests
 - Use smaller levels (0) during the initial or starting portion of the test
 - **~ Min/Sample** is roughly how many minutes will pass between storing samples
 - **Waveform Delay** controls the rate at which the waveforms are saved to the files
 - **~ Min/Waveform** is roughly how many minutes will pass between storing waveforms
 - $\text{min/waveform} = \text{Sample Delay} * \text{Waveform Delay} = (\text{min/sample}) * (\text{sample/waveform})$

The screenshot displays a control interface with three main sections: Command Error Tolerances, Data Logging, and Response Tuning. Each section contains several adjustable parameters with up/down arrows and a 'Disable Standby Mode' button.

Command Error Tolerances

- P Tolerance: 5.00
- CO Tolerance: 1.00
- # Errors Until Standby: 5
- Warning Off: (toggle switch)
- Disable Standby Mode: (button)

Data Logging

- Sample Delay: 4 (range 3-5)
- ~ Min/Sample: 0.33
- Waveform Delay: 30 (range 55-100)
- ~ Min/Waveform: 10.00
- ~Min/Waveform = Min/Sample * Waveform Delay

Response Tuning

- Resistor Tuning: 4.80
- Voltage Tuning: 0.30

START LOGGING (button)

STOP DEVICE (button)

Control Parameters

- Response Tuning
 - These are the **R Tuning** and **CV (Air)** **Tuning** parameters used in the Control System
 - They adjust how much or how fast the system responds to changes in P and Q
 - These parameters should only be adjusted if:
 - System performance is unstable (large or under-damped oscillations about the target levels)
 - Running very different types of tests than what the system is designed for such as a step tests (square wave)
 - See Control System

Main Controls

Protocol

Filter

Control Parameters

Command Error

Command Error Tolerances

P Tolerance

5.00

CO Tolerance

1.00

Errors Until Standby

5

Warning Off

Disable Standby Mode

Data Logging

Sample Delay

4

3

~ Min/Sample

0.33

Waveform Delay

30

55

~ Min/Waveform

10.00

~Min/Waveform =
Min/Sample * Waveform Delay

Response Tuning

Resistor Tuning

4.80

Voltage Tuning

0.30

START LOGGING

STOP DEVICE

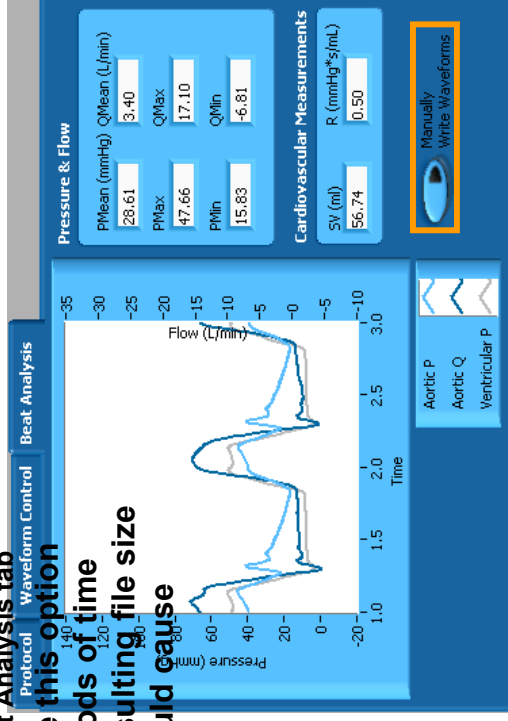
Software



Data Files

Saving Data

- **Saving P&Q Data**
 - Enter the desired file name in the **Data Log File Name** box
 - Do not include *.txt
 - Press the Start Logging button
 - A dialogue will appear when it is time to log data – Press OK
 - See **System Control Parameters** for Data Logging info
- **Manually writing P&Q Waveforms**
 - The above must be completed first
 - Then leave the **Manually Write Waveforms** button pressed for as many data logging cycles as desired
 - See **System Control Parameters** for Data Logging info
 - The **Manually Write Waveforms** button is located on the Beat Analysis tab
- **Important:** Do not leave this option turned on for long periods of time (over an hour) – the resulting file size will be very big and could cause memory problems



The screenshot shows the 'System Control Parameters' dialog box with several tabs: Filter, Control Parameters, Command Error, Main Controls, Automatic, Manual, and Protocol. The 'Main Controls' tab is active, showing various parameters for manual and automatic control. The 'Data Log File Name' field is highlighted with an orange box and contains the text 'sensor test'. Other fields include 'Command - CV' (1.0000), 'Command - Stepper' (0), 'Beats' (26267), and 'Restart Counter' (0). The 'Manual' tab shows 'P Mean' (30.00), 'P Diff 2' (28.56), 'P Diff 2' (1.44), 'Control Voltage (V)' (1.00), 'Motor Steps' (0), and 'Motor Direction' (-R). The 'Protocol' tab shows 'CO' (3.50), 'CO Diff 2' (3.33), and 'CO Diff 2' (0.17). The 'Command Error' tab shows 'Manual Targets', 'Manual CV Control', and 'Manual Resistor Control'.

START LOGGING

STOP DEVICE

Data Format

- General P&Q data
 - File name will be:
 - “InputFileName”-CPs.txt
 - Can be imported into any spreadsheet program
 - Format as shown below:

date & time	P mean	P max	P min	Q mean	Q max	Q min	SV	HR	P command	Q command	P error	Q error
	mmHg	mmHg	mmHg	L/min	L/min	L/min	mL/beat	BPM	mmHg	L/min	mmHg	L/min

- P&Q waveform data
 - File name will be:
 - “InputFileName”-CPs.txt
 - Can be imported into any spreadsheet program
 - Format as shown below:

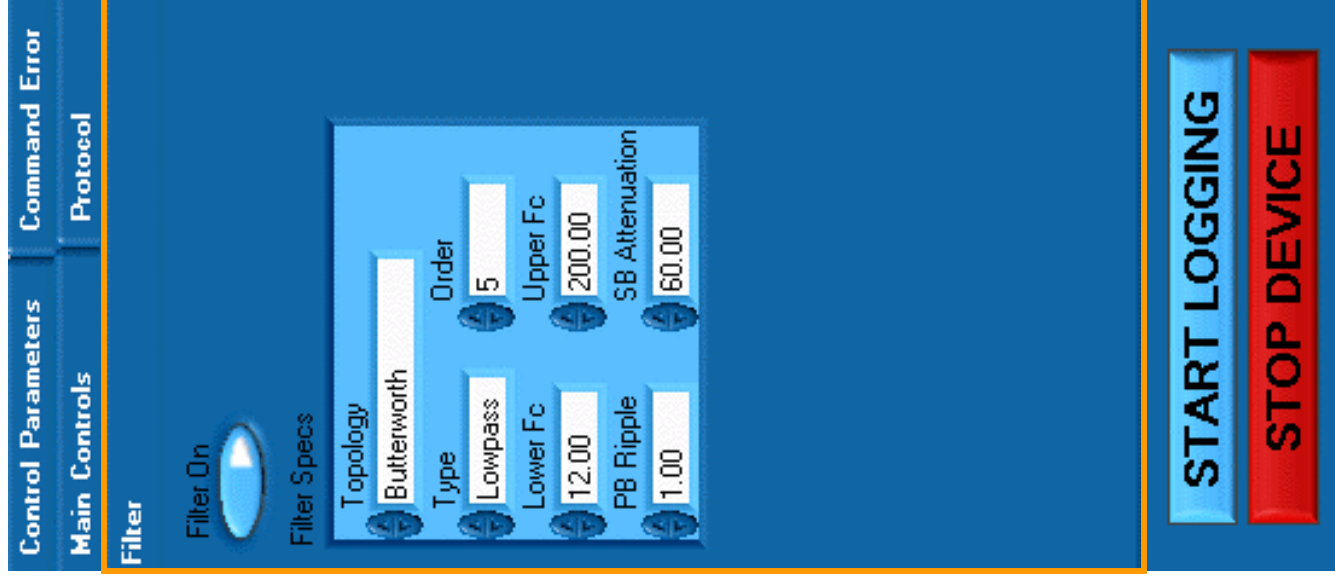
date & time	Aortic P	Aortic Q	Vent P	Air P	Pneumatic Voltage
	mmHg	L/min	mmHg	mmHg	V



Filtering

Filter

- The filter is used to remove high frequency noise from the signal
- Usually these settings will not need to be adjusted
- For information on settings see LabVIEW IIR Filter



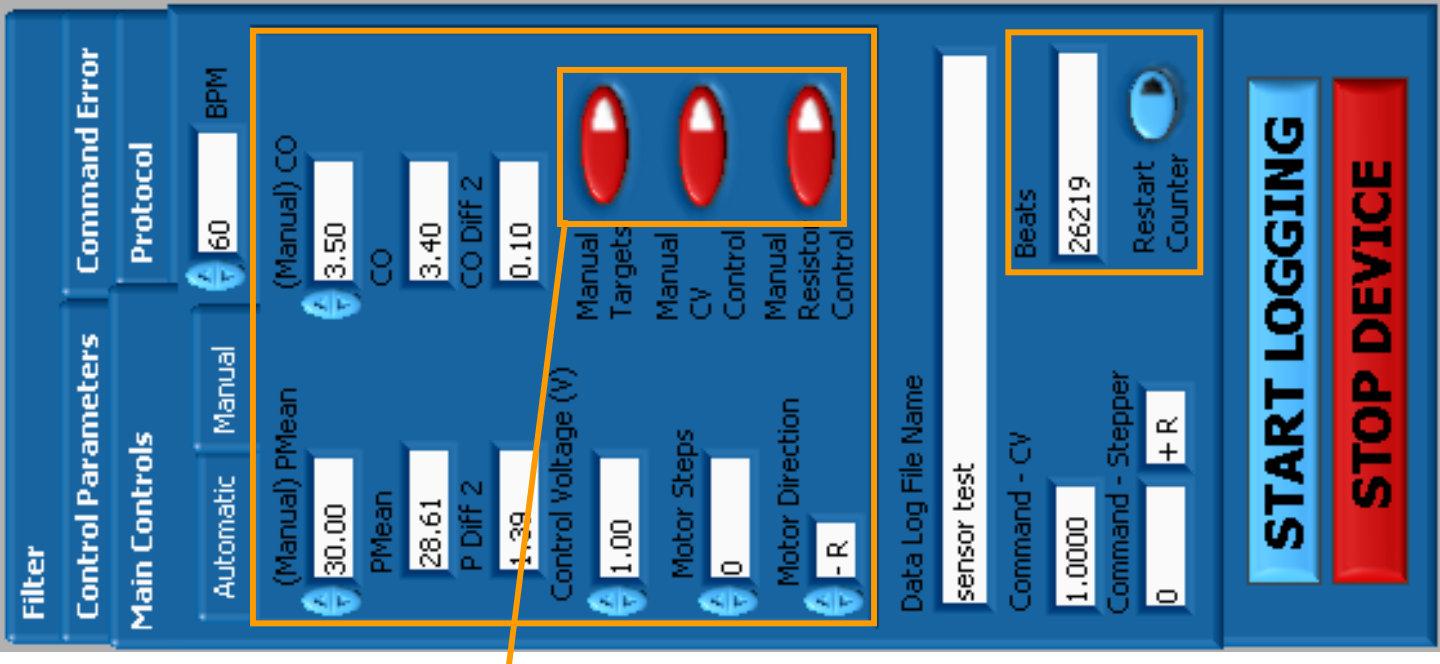
Software



Performing an Experiment

Performing an Experiment

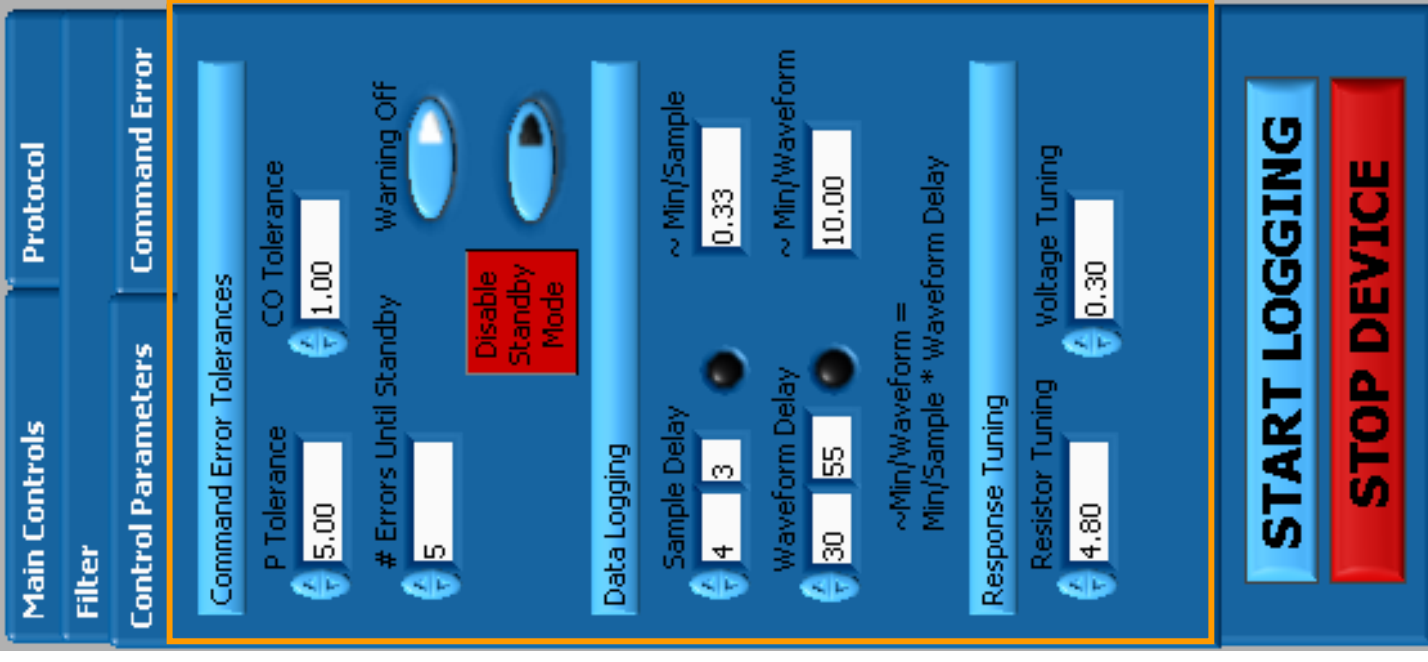
- Completely set up system
 - See **Device Set Up**
- Run/start program
- Set up **Protocol**
- Restart **Beat Counter** to zero
 - Found in both manual and automatic control tabs
- In **FULLY Manual Mode**
 - Slowly increase **CV** until beating starts
 - Allow waveforms to be acquired
 - Set **Manual Targets** to be near those measured (aka minimize P&Q differences)
 - Resume **Automatic Control** of both the CV and Resistor; leave **Manual Targets On**
 - Set the **Manual Q Target** to ~1 L/min (or slightly less if that is the **Qa** level)
 - Verify the resistor function by setting the **Manual P Target** to be ~ ± 5 mmHg
 - If the resistor is functioning properly it should attain this new set point while holding the flow rate quite steady
 - Input **Data Log File Name** & start **Data Logging**
 - Restart **Beat Counter** to zero



Performing an Experiment

- Resume **FULLY Automatic Control**
- **Write Waveforms** to file for at least one cycle
- Increase **Sample Delay** in **Control Parameters** to 30+
- Verify **P&Q Tolerances** in **Control Parameters**

- That's it – the device should be running now under total computer control and will not stop until the **Protocol** is finished!!



BIBLIOGRAPHY

1. Hoerstrup, S.P., R. Sodian, J.S. Sperling, J.P. Vacanti, and J.E. Mayer, Jr., *New pulsatile bioreactor for in vitro formation of tissue engineered heart valves*. *Tissue Eng*, 2000. **6**(1): p. 75-9.
2. Dumont, K., J. Yperman, E. Verbeken, P. Segers, B. Meuris, S. Vandenberghe, W. Flameng, and P.R. Verdonck, *Design of a new pulsatile bioreactor for tissue engineered aortic heart valve formation*. *Artif Organs*, 2002. **26**(8): p. 710-4.
3. Nishimura, R.A., *Cardiology patient pages. Aortic valve disease*. *Circulation*, 2002. **106**(7): p. 770-2.
4. Shinoka, T., C.K. Breuer, R.E. Tanel, G. Zund, T. Miura, P.X. Ma, R. Langer, J.P. Vacanti, and J.E. Mayer, Jr., *Tissue engineering heart valves: valve leaflet replacement study in a lamb model*. *Ann Thorac Surg*, 1995. **60**(6 Suppl): p. S513-6.
5. Hoerstrup, S.P., R. Sodian, S. Daebritz, J. Wang, E.A. Bacha, D.P. Martin, A.M. Moran, K.J. Guleserian, J.S. Sperling, S. Kaushal, J.P. Vacanti, F.J. Schoen, and J.E. Mayer, Jr., *Functional living trileaflet heart valves grown In vitro*. *Circulation*, 2000. **102**(19 Suppl 3): p. III44-9.
6. Sodian, R., S.P. Hoerstrup, J.S. Sperling, S.H. Daebritz, D.P. Martin, F.J. Schoen, J.P. Vacanti, and J.E. Mayer, Jr., *Tissue engineering of heart valves: in vitro experiences*. *Ann Thorac Surg*, 2000. **70**(1): p. 140-4.
7. Schoen, F. and R. Levy, *Tissue heart valves: Current challenges and future research perspectives*. *Journal of Biomedical Materials Research*, 1999. **47**: p. 439-465.
8. FDA, *Replacement Heart Valve Guidance*. 1994, United States Food and Drug Administration: Rockville.

9. Robicsek, F., M.J. Thubrikar, and A.A. Fokin, *Cause of degenerative disease of the trileaflet aortic valve: review of subject and presentation of a new theory*. Ann Thorac Surg, 2002. **73**(4): p. 1346-54.
10. Vesely, I., N. Macris, P.J. Dunmore, and D. Boughner, *The distribution and morphology of aortic valve cusp lipids*. J Heart Valve Dis, 1994. **3**(4): p. 451-6.
11. Sugimoto, H., K. Shimada, and M.S. Sacks, *Dynamic Geometry of the native aortic heart valve leaflet*. Journal of Biomechanics, submitted.
12. Iyengar, A.K.S., H. Sugimoto, D.B. Smith, and M.S. Sacks, *Dynamic in vitro quantification of bioprosthetic heart valve leaflet motion using structured light projection*. Ann Biomed Eng, 2001. **29**(11): p. 963-73.
13. Deck, J.D., M.J. Thubrikar, P.J. Schneider, and S.P. Nolan, *Structure, stress, and tissue repair in aortic valve leaflets*. Cardiovasc Res, 1988. **22**(1): p. 7-16.
14. Schoen, F.J., *Aortic valve structure-function correlations: role of elastic fibers no longer a stretch of the imagination [editorial]*. J Heart Valve Dis, 1997. **6**(1): p. 1-6.
15. AHA, *Heart Disease and Stroke Statistics - 2003 Update*. 2002, American Heart Association: Dallas, Tx.
16. Starr, A., C.L. Fessler, G. Grunkemeier, and G.W. He, *Heart valve replacement surgery: past, present and future*. Clin Exp Pharmacol Physiol, 2002. **29**(8): p. 735-8.
17. Butterfield, M., J. Fisher, K.J. Lockie, G.A. Davies, and K. Watterson, *Frame-mounted porcine valve bioprostheses: preparation during aortic-root dilation. Biomechanics and design considerations*. J Thorac Cardiovasc Surg, 1993. **106**(6): p. 1181-8.
18. Hampl, H., C. Sternberg, S. Berweck, D. Lange, F. Lorenz, C. Pohle, E. Riedel, L. Gogoll, and L. Hennig, *Regression of left ventricular hypertrophy in hemodialysis patients is possible*. Clinical Nephrology, 2002. **58 Suppl 1**: p. S73-96.
19. Ross, D., *Aortic root replacement with a pulmonary autograft: current trends*. Journal of heart valve disease, 1994. **3**: p. 358-360.

20. Dohmen, P.M., A. Lembcke, H. Hotz, D. Kivelitz, and W.F. Konertz, *Ross operation with a tissue-engineered heart valve*. Ann Thorac Surg, 2002. **74**(5): p. 1438-42.
21. Hutmacher, D.W., *Scaffold design and fabrication technologies for engineering tissues--state of the art and future perspectives*. J Biomater Sci Polym Ed, 2001. **12**(1): p. 107-24.
22. Simon, P., M.T. Kasimir, G. Seebacher, G. Weigel, R. Ullrich, U. Salzer-Muhar, E. Rieder, and E. Wolner, *Early failure of the tissue engineered porcine heart valve SYNERGRAFT in pediatric patients*. Eur J Cardiothorac Surg, 2003. **23**(6): p. 1002-6; discussion 1006.
23. Coppin, C., M. Torrianni, Y. Ueda, Y. Sawa, and S. Iwai. *The Biomechanics Of Revitalized Vascular Xenografts*. in *BMES 2003 Annual Fall Conference*. 2003. Nashville, TN.
24. Stock, U.A., J.P. Vacanti, J.E. Mayer Jr, and T. Wahlers, *Tissue engineering of heart valves -- current aspects*. Thorac Cardiovasc Surg, 2002. **50**(3): p. 184-93.
25. Shinoka, T., D. Shum-Tim, P.X. Ma, R.E. Tanel, N. Isogai, R. Langer, J.P. Vacanti, and J.E. Mayer, Jr., *Creation of viable pulmonary artery autografts through tissue engineering*. J Thorac Cardiovasc Surg, 1998. **115**(3): p. 536-45; discussion 545-6.
26. Zilla, P.P. and H.P. Greisler, *Tissue engineering of vascular prosthetic grafts*. Tissue engineering intelligence unit. 1999, Austin: R.G. Landes Co. 621.
27. Sodian, R., S.P. Hoerstrup, J.S. Sperling, D.P. Martin, S. Daebritz, J.E. Mayer, Jr., and J.P. Vacanti, *Evaluation of biodegradable, three-dimensional matrices for tissue engineering of heart valves*. Asaio J, 2000. **46**(1): p. 107-10.
28. Sodian, R., J.S. Sperling, D.P. Martin, A. Egozy, U. Stock, J.E. Mayer, Jr., and J.P. Vacanti, *Fabrication of a trileaflet heart valve scaffold from a polyhydroxyalkanoate biopolyester for use in tissue engineering*. Tissue Eng, 2000. **6**(2): p. 183-8.
29. Sodian, R., J.S. Sperling, D.P. Martin, U. Stock, J.E. Mayer, Jr., and J.P. Vacanti, *Tissue engineering of a trileaflet heart valve-early in vitro experiences with a combined polymer*. Tissue Eng, 1999. **5**(5): p. 489-94.
30. Weston, M.W. and A.P. Yoganathan, *Biosynthetic activity in heart valve leaflets in response to in vitro flow environments*. Ann Biomed Eng, 2001. **29**(9): p. 752-63.

31. Stock, U.A. and J.P. Vacanti, *Cardiovascular physiology during fetal development and implications for tissue engineering*. Tissue Eng, 2001. **7**(1): p. 1-7.
32. Mol, A., C.V. Bouten, G. Zund, C.I. Gunter, J.F. Visjager, M.I. Turina, F.P. Baaijens, and S.P. Hoerstrup, *The relevance of large strains in functional tissue engineering of heart valves*. Thorac Cardiovasc Surg, 2003. **51**(2): p. 78-83.
33. Altman, G.H., H.H. Lu, R.L. Horan, T. Calabro, D. Ryder, D.L. Kaplan, P. Stark, I. Martin, J.C. Richmond, and G. Vunjak-Novakovic, *Advanced bioreactor with controlled application of multi-dimensional strain for tissue engineering*. J Biomech Eng, 2002. **124**(6): p. 742-9.
34. Mitchell, S.B., J.E. Sanders, J.L. Garbini, and P.K. Schuessler, *A device to apply user-specified strains to biomaterials in culture*. IEEE Trans Biomed Eng, 2001. **48**(2): p. 268-73.
35. Kim, B.S. and D.J. Mooney, *Scaffolds for engineering smooth muscle under cyclic mechanical strain conditions*. J Biomech Eng, 2000. **122**(3): p. 210-5.
36. Engelmayr, G.C., D.K. Hildebrand, F.W. Sutherland, J.E. Mayer, and M.S. Sacks, *A novel bioreactor for the dynamic flexural stimulation of tissue engineered heart valve biomaterials*. Biomaterials, 2003. **24**(14): p. 2523-32.
37. Engelmayr, G., E. Rabkin, F. Sutherland, F. Schoen, J. Mayer, and M.S. Sacks, *Functional tissue engineering of heart valves: The role of cyclic flexure in early tissue development*. Submitted to Biomaterials, 2003.
38. Hoerstrup, S.P., G. Zund, Q. Ye, A. Schoeberlein, A.C. Schmid, and M.I. Turina, *Tissue engineering of a bioprosthetic heart valve: stimulation of extracellular matrix assessed by hydroxyproline assay*. Asaio J, 1999. **45**(5): p. 397-402.
39. Hoerstrup, S.P., A. Kadner, S. Melnitchouk, A. Trojan, K. Eid, J. Tracy, R. Sodian, J.F. Visjager, S.A. Kolb, J. Grunenfelder, G. Zund, and M.I. Turina, *Tissue engineering of functional trileaflet heart valves from human marrow stromal cells*. Circulation, 2002. **106**(12 Suppl 1): p. I143-50.
40. Sodian, R., S.P. Hoerstrup, J.S. Sperling, S. Daebritz, D.P. Martin, A.M. Moran, B.S. Kim, F.J. Schoen, J.P. Vacanti, and J.E. Mayer, Jr., *Early In vivo experience with tissue-engineered trileaflet heart valves [In Process Citation]*. Circulation, 2000. **102**(19 Suppl 3): p. III22-9.

41. Ferrari, G., C. De Lazzari, R. Mimmo, G. Tosti, D. Ambrosi, and K. Gorczynska, *A computer controlled mock circulatory system for mono- and biventricular assist device testing*. Int J Artif Organs, 1998. **21**(1): p. 26-36.
42. Weston, M.W., D.V. LaBorde, and A.P. Yoganathan, *Estimation of the shear stress on the surface of an aortic valve leaflet*. Ann Biomed Eng, 1999. **27**(4): p. 572-9.
43. Jin, W. and C. Clark, *Pressure development within a sac-type pneumatically driven ventricular assist device*. J Biomech, 1994. **27**(11): p. 1319-29.
44. Toy, S.M., J. Melbin, and A. Noordergraaf, *Reduced models of arterial systems*. IEEE Trans Biomed Eng, 1985. **32**(2): p. 174-6.
45. Hales, S., *Statical Essays: Containing Haemostaticks*. Vol. II. 1733, London, England: Innys and Manby.
46. McDonald, D.A., *Blood flow in arteries: theoretical, experimental and clinical principles*, ed. M.F. O'Rourke. Vol. 3. 1990, London: Edward Arnold.
47. Liu, Z., K.P. Brin, and F.C. Yin, *Estimation of total arterial compliance: an improved method and evaluation of current methods*. Am J Physiol, 1986. **251**(3 Pt 2): p. H588-600.
48. Li, J.K.J., *The arterial circulation : physical principles and clinical applications*. 2000, Totowa, N.J.: Humana Press. xi, 271.
49. Ferrari, G., C. De Lazzari, M. Kozarski, F. Clemente, K. Gorczynska, R. Mimmo, E. Monnanni, G. Tosti, and M. Guaragno, *A hybrid mock circulatory system: testing a prototype under physiologic and pathological conditions*. Asaio J, 2002. **48**(5): p. 487-94.
50. Vandenberghe, S., P. Segers, B. Meyns, and P. Verdonck, *Hydrodynamic characterisation of ventricular assist devices*. Int J Artif Organs, 2001. **24**(7): p. 470-7.
51. Lim, W.L., Y.T. Chew, T.C. Chew, and H.T. Low, *Pulsatile flow studies of a porcine bioprosthetic aortic valve in vitro: PIV measurements and shear-induced blood damage*. J Biomech, 2001. **34**(11): p. 1417-27.

52. Knierbein, B., H. Reul, R. Eilers, M. Lange, R. Kaufmann, and G. Rau, *Compact mock loops of the systemic and pulmonary circulation for blood pump testing*. Int J Artif Organs, 1992. **15**(1): p. 40-8.
53. Verdonck, P., A. Kleven, R. Verhoeven, B. Angelsen, and J. Vandenbogaerde, *Computer-controlled in vitro model of the human left heart*. Med Biol Eng Comput, 1992. **30**(6): p. 656-9.
54. Donovan, F.M., Jr., *Design of a hydraulic analog of the circulatory system for evaluating artificial hearts*. Biomater Med Devices Artif Organs, 1975. **3**(4): p. 439-49.
55. Jensen, M.O., J.D. Lemmon, V.C. Gessaghi, C.P. Conrad, R.A. Levine, and A.P. Yoganathan, *Harvested porcine mitral xenograft fixation: impact on fluid dynamic performance*. J Heart Valve Dis, 2001. **10**(1): p. 111-24.
56. Ferrari, G., C. De Lazzari, R. Mimmo, D. Ambrosi, and G. Tosti, *Mock circulatory system for in vitro reproduction of the left ventricle, the arterial tree and their interaction with a left ventricular assist device*. J Med Eng Technol, 1994. **18**(3): p. 87-95.
57. Kitamura, T., K. Affeld, and A. Mohnhaupt, *Design of a new pulse duplicator system for prosthetic heart valves*. J Biomech Eng, 1987. **109**(1): p. 43-7.
58. D'Souza, S.S., M. Butterfield, and J. Fisher, *Kinematics of synthetic flexible leaflet heart valves during accelerated testing*. J Heart Valve Dis, 2003. **12**(1): p. 110-9; discussion 119-20.
59. Brant, A.M., J.F. Chmielewski, T.K. Hung, and H.S. Borovetz, *Simulation in vitro of pulsatile vascular hemodynamics using a CAD/CAM-designed cam disc and roller follower*. Artif Organs, 1986. **10**(5): p. 419-21.
60. Jin, W. and C. Clark, *Experimental investigation of the motions of the pumping diaphragm within a sac-type pneumatically driven ventricular assist device*. J Biomech, 1994. **27**(1): p. 43-55.
61. Sodian, R., T. Lemke, M. Loebe, S.P. Hoerstrup, E.V. Potapov, H. Hausmann, R. Meyer, and R. Hetzer, *New pulsatile bioreactor for fabrication of tissue-engineered patches*. J Biomed Mater Res, 2001. **58**(4): p. 401-5.

62. Sodian, R., T. Lemke, C. Fritsche, S.P. Hoerstrup, P. Fu, E.V. Potapov, H. Hausmann, and R. Hetzer, *Tissue-engineering bioreactors: a new combined cell-seeding and perfusion system for vascular tissue engineering*. Tissue Eng, 2002. **8**(5): p. 863-70.
63. Hoerstrup, S.P., G. Zund, R. Sodian, A.M. Schnell, J. Grunenfelder, and M.I. Turina, *Tissue engineering of small caliber vascular grafts*. Eur J Cardiothorac Surg, 2001. **20**(1): p. 164-9.
64. Sutherland, F.W., T.E. Perry, B.A. Nasser, J. Wang, S. Kaushal, K.J. Guleserian, D.P. Martin, J.P. Vacanti, and J.E. Mayer, Jr., *Advances in the mechanisms of cell delivery to cardiovascular scaffolds: comparison of two rotating cell culture systems*. Asaio J, 2002. **48**(4): p. 346-9.
65. Nasser, B.A., I. Pomerantseva, M.R. Kaazempur-Mofrad, F.W. Sutherland, T. Perry, E. Ochoa, C.A. Thompson, J.E. Mayer, Jr., S.N. Oesterle, and J.P. Vacanti, *Dynamic rotational seeding and cell culture system for vascular tube formation*. Tissue Eng, 2003. **9**(2): p. 291-9.
66. Brown, A.N., B.S. Kim, E. Alsberg, and D.J. Mooney, *Combining chondrocytes and smooth muscle cells to engineer hybrid soft tissue constructs*. Tissue Eng, 2000. **6**(4): p. 297-305.
67. Chakravarti, Laha, and Roy, *Handbook of Methods of Applied Statistics*. Vol. Volume I. 1967: John Wiley and Sons.
68. Seeley, R., T. Stephens, and P. Tate, *Anatomy & Physiology*. 4th ed. 1998: McGraw-Hill.
69. Robicsek, F. and M.J. Thubrikar, *Loss of sinus compliance, cause of degenerative aortic valve disease, and early failure of biological valves*. Z Kardiol, 2000. **89** Suppl 7: p. 104-6.
70. Robicsek, F. and M.J. Thubrikar, *Role of sinus wall compliance in aortic leaflet function*. Am J Cardiol, 1999. **84**(8): p. 944-6, A7.
71. Guan, J., M.S. Sacks, E.J. Beckman, and W.R. Wagner, *Synthesis, characterization, and cytocompatibility of elastomeric, biodegradable poly(ester-urethane)ureas based on poly(caprolactone) and putrescine*. J Biomed Mater Res, 2002. **61**(3): p. 493-503.

72. Kwon, I.K., K.D. Park, S.W. Choi, S.H. Lee, E.B. Lee, J.S. Na, S.H. Kim, and Y.H. Kim, *Fibroblast culture on surface-modified poly(glycolide-co-epsilon-caprolactone) scaffold for soft tissue regeneration*. J Biomater Sci Polym Ed, 2001. **12**(10): p. 1147-60.